Cosmogenic ^{36}Cl Dating of Geomorphic Surfaces

by

Marek G. Zreda

Fred M. Phillips

Stewart S. Smith

Hydrology Report # H90-1

Hydrology Program

New Mexico Institute of Mining and Technology

Socorro, NM 87801

May, 1990

Acknowledgements

This research was supported by the National Science Foundation (grants EAR–8603440, SES–8901437, PHY–8515908, and PHY–8818281) and by the National Geographic Society (grant 3687–87).

Table of content

List of figures

List of tables

Abstract

Geomorphic surfaces consist of redistributed material and are therefore not amenable to the standard dating techniques. The last decade has seen development of several new surface exposure dating techniques that give numerical ages. Although for many of them the production rates have already been obtained, no successful field application has been reported to date. In this work, calibration of the cosmogenic ^{36}Cl method and its applications to dating of geomorphic surfaces at different locations are presented.

Cosmogenic ^{36}Cl is produced in rocks exposed to cosmic rays through thermal neutron activation of ^{35}Cl, spallation of ^{39}K and ^{40}Ca, and negative muon capture by ^{40}Ca. The ^{36}Cl content of ^{14}C–dated glacial boulders from the White Mountains in eastern California and in a ^{14}C–dated basalt flow from Utah was measured by using Accelerator Mass Spectrometry. Effective, time–integrated production parameters were calculated by simultaneous solution of the ^{36}Cl production equations. The production rates due to spallation are $3{,}560 \pm 465$ and $2{,}740 \pm 245$ atoms ^{36}Cl per year per mole ^{39}K and ^{40}Ca, respectively and the thermal neutron stopping rate is $(2.64 \pm 0.42) \times 10^5$ neutrons per kg of rock per year. The reported values are normalized to sea level and high geomagnetic latitudes. Production rates at different latitudes and latitudes can be estimated by scaling of the sea level rates. The appropriate scaling factors were chosen from previously published formulations. The production parameters and the correction factors were verified experimentally by dating rocks of known ages from different elevations and geomagnetic latitudes. The calculated ages are in excellent agreement with those obtained using independent techniques.

The calibrated cosmogenic ^{36}Cl method was used to obtain a chronology for glacial deposits at Bloody Canyon, California, and to calculate the age of Meteor Crater, Arizona. The accumulation of cosmogenic ^{36}Cl in boulders exposed on moraine crests indicates episodes of glaciation at about 21, 24, 65, 115, 145, and 200 thousands years ago (ka). This chronology supports synchroneity of glacial events in the Sierra Nevada with both the global glacial indications of the marine ^{18}O record and with minima in summer insolation. However, an inverse relationship between the glacial magnitudes indicated by the marine ^{18}O and glacial ^{36}Cl records was found. The marine record shows progressive buildup of continental ice sheets from the previous interglacials through the last glacial maximum, whereas at Bloody Canyon the earlier mountain glaciers were the most extensive. In addition, the ^{36}Cl show a rapid transition from full interglacial to full glacial conditions which is in conflict with much slower changes in the marine ^{18}O record. This discrepancy may indicate that small mountain glaciers responded more rapidly than continental ice sheets to abrupt changes of mode in the global ocean and atmosphere circulation.

Five Meteor Crater samples yielded the mean age of 50.8 ± 6.5 ka which is in excellent agreement with the age of 49.0 ± 3.0 ka obtained from thermoluminescence studies of shock–metamorphosed minerals. Varnish–^{14}C studies of the same material yielded "dead radiocarbon" which supports the ^{36}Cl results. The ^{36}Cl data are very consistent. Four out of five samples yielded almost identical ages, with standard deviation smaller than analytical uncertainty of the individual AMS measurements. This suite of samples indicates that given favorable geological conditions, such as low erosion rates in arid environments, the cosmogenic ^{36}Cl buildup method gives reliable and accurate exposure ages.

1. Introduction

For many years Quaternary geologists have struggled to assign numerical ages to geomorphic surfaces. They have lacked tools that would directly date the formation time of morphological surfaces. Conventional radiometric techniques are inadequate because they measure the age of the mineral formation rather than the age of geomorphic rejuvenation. Cosmogenic nuclide accumulation methods have the potential to be very useful tools for measuring the exposure time of landforms and thus for estimating their time of formation; the buildup of cosmogenic isotopes starts with the exposure of a given structure to the cosmic rays and is an exponential function of time.

Cosmogenic nuclide accumulation is a function of exposure time, geographic location, and the abundance of target elements in a sample. Possible applications of cosmogenic nuclide methods in earth sciences were first suggested over 30 years ago (eg., Davis and Schaeffer, 1955). However, their geochronological potential could not be fully realized due to the lack of sufficiently sensitive analytical techniques. This limitation has lately been overcome for ^{36}Cl by rapid developments in accelerator mass spectrometry (Elmore and Phillips, 1987). However, despite the spectacular analytical achievements of the last decade, cosmogenic nuclide geochemistry is still in an early stage of development. Presently, only a few cosmogenic isotopes have been applied in geosciences. They include ^{36}Cl ($t_{1/2} = 3.01*10^5$ yrs.), ^{26}Al ($t_{1/2} = 7.05*10^5$ yrs.), ^{10}Be ($t_{1/2} = 1.5*10^6$ yrs.), ^{3}He (stable), and ^{14}C ($t_{1/2} = 5730$ yrs.). The half-lives of these isotopes make them especially valuable dating tools in hydrology, geomorphology, Quaternary stratigraphy and paleogeography, and archaeology.

Before cosmogenic isotope geochronometers can be successfully applied, the production parameters have to be calculated with high precision. The main objective of this research was to calibrate the cosmogenic ^{36}Cl method by using well-dated and geologically well-constrained rock samples and to show its applicability in Quaternary stratigraphy. In this study, we describe how the calibration was performed, point out uncertainties of parameter estimates, and sketch directions for future work. We also give the state-of-the-art description of the cosmogenic ^{36}Cl method as a means of surface exposure dating. Finally, we present two case studies: (1) a chronology of glacial deposits at Bloody Canyon, California, and (2) the impact time of the Meteor Crater meteorite. In both cases obtained dates are in excellent agreement with independent age estimates.

1.1. Major production reactions for ^{36}Cl in minerals at the surface of the earth

Chlorine-36 is produced in rocks exposed at the surface of the earth almost entirely by cosmic-ray induced reactions with ^{35}Cl, ^{39}K, and ^{40}Ca. Cosmic rays are moderated in the atmosphere by interactions with nuclei of atmospheric gases. The major part of the cosmic-ray flux at high (mountain) elevations is neutrons. At sea level, the negative muon flux is comparable to that of neutrons and negative muon capture becomes a significant cosmogenic reaction (Rama and Honda, 1961; Lal and Peters, 1967; Jha and Lal, 1982; Lal, 1987a). Neutrons commonly interact with atoms to produce nuclear disintegrations or emissions. On the other hand, muon energies are low and they rarely produce radionuclides by direct interactions. Instead, they tend to fall into the K shell

of the atom and may be captured by the Coulomb field of positively charged nuclei before they decay (Rama and Honda, 1961). The negative muon stopping rate exceeds neutron activity at depths below 3 mwe (meters of water equivalent) at sea level (Lal, 1987a).

In the top few meters of the lithosphere, thermal neutron activation of ^{35}Cl and spallation of ^{39}K and ^{40}Ca are the dominant production mechanisms for ^{36}Cl (Yokoyama et al., 1977; Bentley et al., 1986; Leavy, 1987; Fabryka-Martin, 1988). Below that depth, the contribution from slow negative muon capture by ^{40}Ca becomes progressively more important (Lal and Peters, 1967; Jha and Lal, 1982; Fabryka-Martin, 1988). Thermal neutron activation of ^{39}K, negative muon capture by ^{39}K, spallation of Ti and Fe by the high energy component of the cosmic-ray flux, and nuclear reactions involving ^{36}Ar and ^{36}S are relatively insignificant reactions in minerals at the surface of the earth; they are responsible for less than 2% of the total *in situ* produced ^{36}Cl (Fabryka-Martin, 1988) and will not be discussed here. The relative contributions of the dominant production reactions in the top 0.5 mwe of the lithosphere (Table 1) depend on the chemical composition of rocks.

Table 1. *Relative importance of major reactions producing ^{36}Cl in the top 0.5 mwe of the lithosphere at sea level in typical crustal rocks (compiled from Fabryka-Martin, 1988).*

Reaction type	Notation	% of total ^{36}Cl
Spallation of K and Ca	$^{39}K(n,2n2p)^{36}Cl$ $^{40}Ca(n,2n3p)^{36}Cl$	16 - 80
Thermal neutron activation of Cl	$^{35}Cl(n,\gamma)^{36}Cl$	11 - 80
Negative muon capture by Ca	$^{40}Ca(\mu,\alpha)^{36}Cl$	0.3 - 10
Thermal neutron activation of K	$^{39}K(n,\alpha)^{36}Cl$	0 - 2
Negative muon capture by K	$^{39}K(\mu,p2n)^{36}Cl$	0 - 0.4

1.2. *Accumulation of* in situ *produced* ^{36}Cl *in geological materials*

The amount of cosmogenic ^{36}Cl accumulated in a given sample after t years of exposure to the cosmic rays and with negligible erosion can be expressed as:

$$R - R_0 = \frac{E_n L_n D_n(\psi_K C_K + \psi_{Ca} C_{Ca} + \Psi_n) + E_\mu L_\mu \Psi_\mu}{\lambda N}\left(1 - e^{-\lambda t}\right)$$

where: R – atomic ratio of ^{36}Cl to stable Cl.

R_0 – background $^{36}Cl/Cl$ ratio supported by U and Th derived neutrons.

ψ_K, ψ_{Ca} – production rates due to spallation of ^{39}K and ^{40}Ca, in atoms per kg of rock per year per unit concentration of K and Ca.

C_K, C_{Ca} – concentration of K or Ca.

Ψ_n – production rate due to thermal neutron activation of ^{35}Cl, in atoms per kg of rock per year.

Ψ_μ – production rate due to negative muon capture by ^{40}Ca, in atoms per kg of rock per year.

E, L, D – correction factors for elevation above sea level (E), geographical latitude and longitude (L), and depth below surface (D), for distribution of neutrons (n) and muons (μ), respectively.

t – time of exposure, in years.

N – concentration of Cl, in atoms per kg of rock.

λ – decay constant for ^{36}Cl ($2.30*10^{-6}$ per year).

The correction factors for elevation above sea level (E_n) and geomagnetic latitude (L_n) have been calculated by Lingenfelter (1963), Lal and Peters

(1967), Rose et al. (1956), Yokoyama et al. (1977, using data from Merker et al., 1973 and Light et al., 1973), and Moraal et al. (1989). The published altitude gradients differ by as much as 100%. Since the correction for geomagnetic latitude varies with solar activity (Lingenfelter, 1963; Merker et al., 1973), for applications over geological periods of time the use of a time-integrated value is necessary. For samples collected at depth d below the surface, the correction factor D can be calculated as $exp(-d/\Lambda_n)$, where Λ_n of 150 g/cm^2 is the mean free path for neutrons (Lal, 1987b). The correction (E_μ) for elevation above sea level is given by $E_\mu = exp\ ((1033-p)/\Lambda_\mu)$, where p is atmospheric pressure (g / cm^2) and Λ_μ is the absorption mean free path for muons (Λ_μ = 247 g / cm^2, for $160 < p < 1033$ g / cm^2 (Conversi, 1950; Rossi, 1952)). The correction factor (L_μ) for geomagnetic latitude is smaller than in the case of neutrons; its value at the equator is about 80% of the value at higher latitudes (Bilokon et al., 1989).

Geomagnetic latitude (λ) can be calculated using the formulation given in Quenby and Webber (1959):

$$\lambda = arcsin(cos\Theta_0 cos\Theta cos(w-w_0) + sin\Theta_0 sin\Theta$$

where Θ is the geographic latitude, w is the geographic longitude, and $\Theta_0 = 78.6°$ and $w_0 = 290.0°$ correspond to the position of the 1945 geomagnetic north pole.

The background ratio, (R_0), of ^{36}Cl due to neutrons from spontaneous fission and (α,n) reactions in the deep subsurface depends largely on the uranium and thorium content of samples (Feige et al., 1968; Kuhn et al., 1984; Bentley et al., 1986; Andrews et al., 1989). Its value is usually small ($5*10^{-15}$ to $5*10^{-14}$ ^{36}Cl/Cl), but may become relatively important for rocks with very short exposure times.

Production rates of ^{36}Cl due to spallation of ^{39}K (ψ_K) and ^{40}Ca (ψ_{Ca}) have been estimated by Yokoyama et al. (1977), who based their calculations on the excitation functions for ^{36}Cl formation. They reported sea-level rates of approximately 15,000 and 5,600 atoms of ^{36}Cl per kg of rock per year per mole of K and Ca, respectively.

Production by thermal neutron activation of ^{35}Cl (Ψ_n) depends on the thermal neutron absorption (stopping) rate, ϕ_n (n/kg/yr), and the chemical composition of exposed material (Davis and Schaeffer, 1955; Phillips et al., 1986):

$$\Psi_n = \phi_n \frac{\sigma_{35} N_{35}}{\sum_i \sigma_i N_i}$$

where σ_{35} is the thermal neutron absorption cross-section for ^{35}Cl ($44*10^{-24}$ cm^2; Stehn et al., 1964; Mughabghab and Garber, 1973), N_{35} the number of atoms of ^{35}Cl per kg of sample, σ_i thermal neutron absorption cross-section for each element i, and N_i the number of atoms of element i per kg of sample. Estimates of the thermal neutron production rates (ϕ_n) due to cosmic ray interactions with air and solids at sea level and high geomagnetic latitudes range from $2*10^5$ to $4*10^5$ n/kg/yr (Montgomery and Montgomery, 1939; Simpson, 1951; Hendrick and Edge, 1966; Yamashita et al., 1966; Andrews et al., 1986).

Chlorine-36 formation due to slow negative muons (Ψ_μ) can be neglected at the surface of the earth for most rock types. However, in carbonates and very calcic igneous rocks (eg. basalts) muons can be responsible for up to 10% of the total cosmogenic ^{36}Cl (Table 1). The production mechanism, although well understood qualitatively, has not been accurately parametrized yet. The production rate can be expressed as (Charalambus et al., 1971):

$$\Psi_\mu = I_\mu(D)\ (f_c)_{Ca}\ f_d\ f_n \quad [\ N_{36}\ kg^{-1}\ yr^{-1}\ ]$$

$I_\mu(D)$ is the stopping rate at depth D below surface. Its surface value ranges

from $1.37*10^5$ to $1.77*10^5$ stopped muons per kg per yr at geomagnetic latitude 40° (Rama and Honda, 1961; Charalambus et al., 1971; Rossi, 1952) and increases slowly with depth to reach a maximum of about 1.15 times the surface value at depth of about 1 m (Charalambus et al., 1971). In this work, we used the value given by Rossi (1952), $1.6*10^5$ muons/kg/yr, at geomagnetic latitude > 50°. The fraction of stopped muons captured by the Coulomb field of the target nucleus, $(f_c)_{Ca}$, can be roughly calculated, with about 25% error, by using the Fermi–Teller Z–law (Charalambus, 1971):

$$(f_c)_{Ca} = r_{Ca}\frac{a_{Ca}Z_{Ca}}{\sum_i a_i Z_i}$$

where r_{Ca} is relative abundance of isotope ^{40}Ca in total Ca (r_{Ca} = 0.96941, CRC, 1980), a is atomic concentration and Z is atomic number. For most rocks the denominator in the above formula is approximately 500 mole–protons/kg. The fraction of muons, f_d, captured by the nucleus of ^{40}Ca is 0.83 , and the default value of probability, f_n, of production of ^{36}Cl from ^{40}Ca by the emission of one α particle was assumed to be 0.15–0.20 (Charalambus, 1971) and later theoretically calculated by Wyttenbach et al. (1978, cited by Fabryka–Martin, 1988) to be 0.005.

2. *Analytical Methods*

The rock samples were analyzed for ^{36}Cl by accelerator mass spectrometry, for total Cl by ion specific electrode, for major elements by XRF spectrometry, and for B and rare earths by inductively coupled plasma emission (ICP/ES) and prompt gamma emission spectrometry.

2.1. Isotopic analysis of ^{36}Cl

2.1.1. Materials

Hot stirring plate.
Constant temperature water bath.
Desktop centrifuge (3,000 rpm).
2.2 μm air filter.
Indicating drierite.
Spatulas.
Polyvinyl gloves.
Teflonware: one 1 L bottle with lid,
1/16 inch ID tubing,
three 50 mL centrifuge tubes,
one 1.5 inch stirring bar.
Glassware: one 600 mL beaker,
three 50 mL centrifuge tubes,
watch glasses,
one 25 mL and one 100 mL graduated cylinders,
Plasticware: one 250 ml graduated cylinder,
one 250 mL separatory funnel,
forceps.

2.1.2. Reagents

Item	Brand	Catalog #	Cl content, ppm
70 % nitric acid	Baker Analyzed	9601-03	< 0.08
48 % hydrofluoric acid	EM Science	HX 0621-2	< 1
30 % ammonium hydroxide	Baker Analyzed Reagent	9721-3	< 0.2
Silver nitrate crystals	Baker Analyzed	3426-04	< 3

Item	Brand	Catalog #	Cl content, ppm
Barium nitrate crystals	Baker Analyzed Reagent	1018–1	< 3
Acetone	Fisher Histological Grade	UN 090	–
18 MΩ deionized water	–	–	0

2.1.3. Sample preparation and analysis

We have developed a wet chemical technique for extraction of Cl from silicate rocks and convertion into a form suitable for AMS measurement (cf. Zreda et al., submitted). The extraction apparatus (Fig. 1) was made of Teflon because of its resistance to hot HF. An air stream was bubbled through the solution to strip the chlorine as HCl. A 2.2 μm air filter and indicating drierite prevented introduction of atmospheric Cl to the sample. The small tubes before and after the chlorine capture tube were included to prevent sample loss in case of sucking back or overspilling of the capture solution.

The rock sample was ground to a fraction equal to or smaller than the mean grain size and leached for 24 hours with 18 MΩ deionized water to remove any meteoric chloride ions from the grain boundaries; basalts were leached for 2 hours in 10% nitric acid to remove any secondary carbonate accumulated in the vesicles. Grinding to much smaller sizes is not advisable because Cl from fluid inclusions can be liberated and removed by leaching. Approximately 100 g of the sample was mixed with 100 ml of concentrated HNO_3 and placed in the 1000–ml reaction bottle on a stirring plate. A separatory funnel with 250 ml of concentrated HF and a 50–ml Teflon capture tube containing Ag^+ ions in an acidic solution were connected to the reaction bottle. Dry air was supplied through a porous teflon loop at a rate sufficient to cause rapid bubbling, and hydrofluoric acid at a rate slow enough to prevent violent reac–

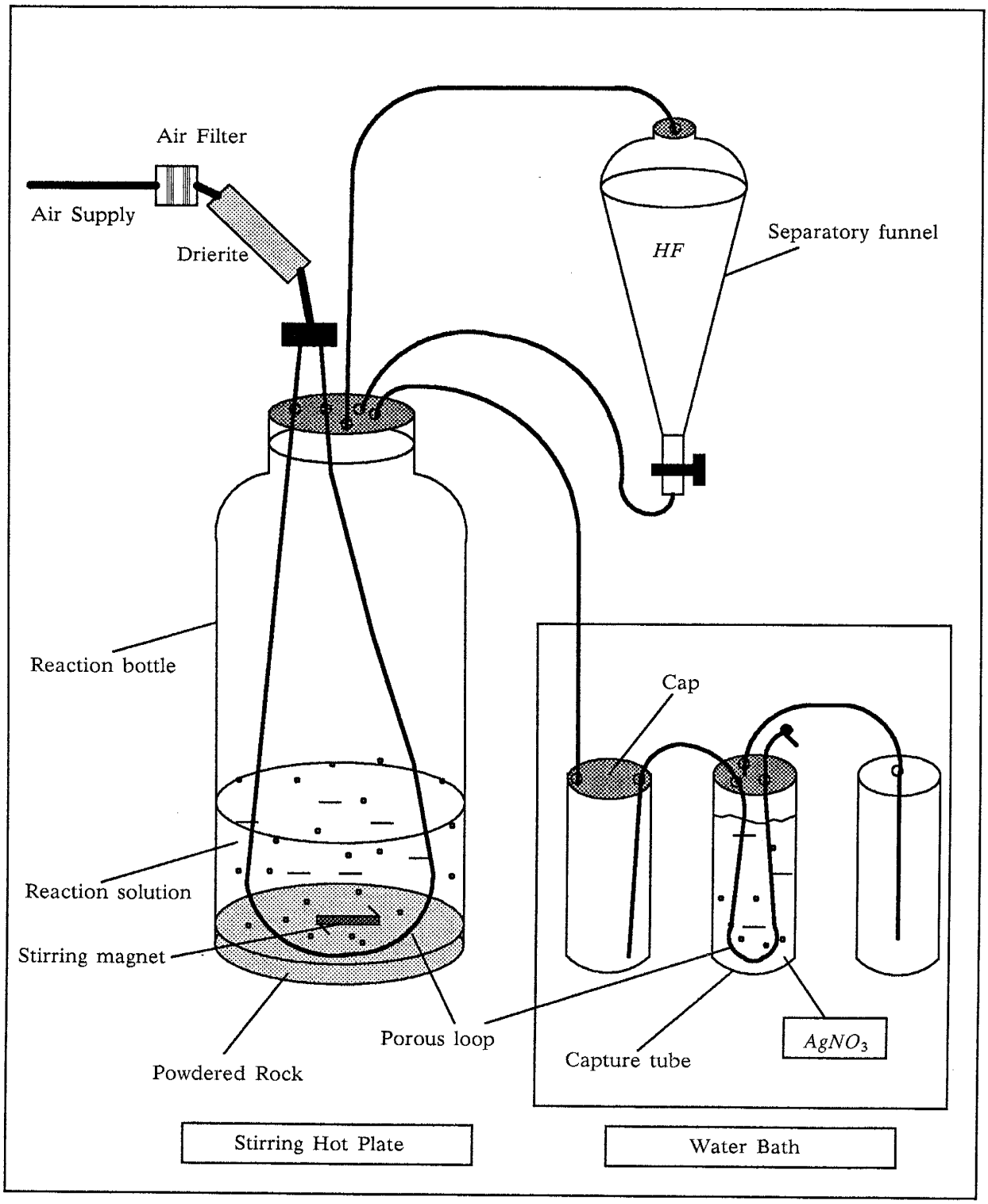

Fig. 1. Chlorine extraction apparatus.

tion. Chloride ions were liberated from the sample, transported with the air stream as HCl or/and Cl_2, and precipitated in the capture tube as AgCl. The time required for complete decomposition of samples varies (depending on mineral composition of the rock) from 6 to 12 hours for acidic and intermediate rocks, respectively. The precipitate was dissolved in NH_4OH and mixed with $BaNO_3$ to remove sulfur; ^{36}S is an interfering isobar and must be removed prior to AMS measurements. After at least 8 hours any $BaSO_4$ precipitated was removed by centrifugation or filtration. Sulfur-free AgCl was recovered by acidifying the remaining base solution. After thorough rinsing, AgCl was placed in an oven at 60°C until it was completely dry (usually at least 1 day). Small samples (less than 2 mg of AgCl) were mixed with a low-sulfur AgBr binder in proportions not exceeding 3 parts of AgBr to one part of AgCl. The samples were loaded into clean, acetone and nitric acid-rinsed, custom-made, low-sulfur tantalum holders.

The samples were analyzed for ^{36}Cl by accelerator mass spectrometry (Elmore et al., 1979) on a tandem Van de Graaff accelerator at the University of Rochester; analytical uncertainty was between 2.2 % and 15.6 % (Fig. 2).

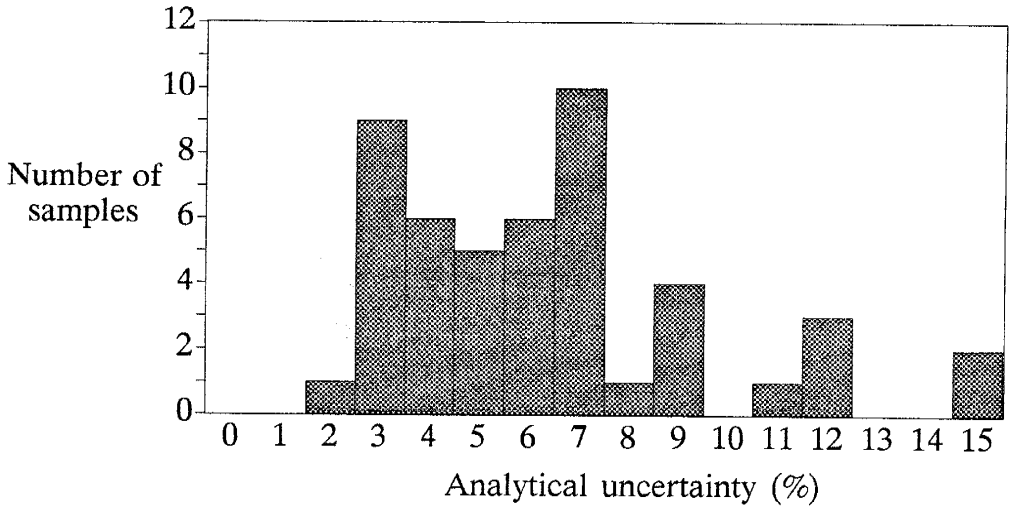

Fig. 2. Analytical uncertainty distribution for ^{36}Cl measurements.

2.2. *Analysis of chlorine content in rock samples*

2.2.1. *Materials*

1. Combination chloride ion-selective electrode (Orion model 9617) and stand.
- pH meter with adapter.
- Custom-made teflon diffusion cells.
- Mechanical shaker (preferably orbital).
- Plastic pipets, beakers, graduate cylinders, and miscellaneous items.

2.2.2. *Reagents*

Item	Brand	Catalog #	Cl content (ppm)
48 % hydrofluoric acid	EM Science	HX 0621-2	< 1
98% sulfuric acid	Fisher A.C.S.	A-300	0.2
Potassium hydroxide	Fluka puriss. p.a.; pellets	60370	< 5
Sodium sulfite anhydrous	Fluka puriss. p.a.	71989	< 50
Potassium permanganate	Fluka puriss. p.a.	60460	< 30
18 MΩ deionized water	-	-	0

The following reagent quantities are sufficient for determination of total Cl in 12 samples:

- Oxidizing solution: 0.4 g $KMnO_4$, 5.6 mL 18 MΩ water, 2.4 mL 50% H_2SO_4, 32 mL HF.
- Reducing solution: 5.6 g KOH, 0.28 g Na_2SO_3, 29 mL 18 MΩ water.

2.2.3. *Cleaning agents for teflon diffusion cells*

- *Chrome–sulfuric acid solution:* 35 mL of saturated $K_2Cr_2O_7$ in 1 L of concentrated H_2SO_4.
- *Peroxide–nitric acid solution:* 1 part of hydrogen peroxide and 4 parts of concentrated HNO_3.

2.2.4. *Sample preparation and analysis*

Chlorine was separated from the rock matrix in teflon diffusion cells and determined by using an ion selective electrode method described by Aruscavage and Campbell (1983) and Elsheimer (1987). A crucial element is a combination chloride selective electrode which can be used directly in the inner chambers of diffusion cells. For this purpose, we machined 12 diffusion cells with lids from teflon rod 2.5 inch OD.

The teflon diffusion cells were carefully cleaned using the standard cleaning solutions: chrome–sulfuric and peroxide–nitric acid. 200 mg of powdered rock sample was weighed into the outer chamber and 2.8 g of the reducing solution into the inner chamber of a diffusion cell. The cells were placed on a gently sloping surface (20° or so) with samples on the upward sides of the cells. Three cm^3 of the oxidizing solution were measured to the outer chamber and the cell was closed immediately. A blank and appropriate standards were prepared similarly using standard chlorine solution. The cells were placed on an orbital shaker; alternatively, a linear shaker can also be used, but will result in poorer reproducibility. After 16–20 hrs. the blank was opened and the electrode conditioned in the blank solution (inner chamber) for 30 min; the potential difference usually drops by about 30 mV during this time. After the electrode had been conditioned, the cells were opened (one at a time) and the potential difference read for a few minutes, until the readings were stable. The calibration

graph (log concentration Cl vs. potential difference) was plotted and the chloride content of the samples determined. Recently, we found that reproducibility can be improved by weighing the reducing solution in the inner cell after the reaction is completed, immediately before measurements. The final weight of the reducing solution ranges from 1.8 to 2.2 g. This variation appears to be normally distributed, and is not associated with any particular cell. It probably results from variation in chemical composition of the rocks analyzed. This variation is accounted for in the calculations; a simple computer program is presented in Appendix 3.

2.3. Major elements analysis

Major elements were determined by standard X–ray fluorescence (XRF) on fused discs (calibration samples) and pressed pellets (remaining samples). Pellets were made from samples ground to a particle size less than 0.075 mm (200 mesh) using a high–speed agate grinder. Eight grams were mixed carefully with 8 drops (0.4 cm^3) of polyvinyl alcohol in an agate mortar. The sample was then pressed to 2 MPa (20 bars) using a hydraulic press and left under this pressure for one minute. The pressure was then slowly released and the sample removed from the press. The analysis was performed on a Rigaku instrument at the New Mexico Bureau of Mines and Mineral Resources. The precision of the measurements was about 2 % for heavy elements (such as K and Ca) and up to 10 % for Si and Al; this precision was adequate for the purpose of my study. The major element analysis on fused discs was performed in an XRF laboratory at the University of New Mexico.

2.4. *Boron and selected rare earth elements analysis*

2.4.1. Inductively coupled argon plasma atomic emission technique (ICAP–AE)

The ICAP–AE technique for rare earth elements (Walsh et al., 1981) and boron (Walsh, 1985) was used in the beginning of the study. One gram sample was mixed with 5 g of sodium carbonate flux in a platinum crucible with a lid. The crucible was placed in a furnace at 950°C for 30 min. The sample was allowed to cool and then dissolved in 50 cm^3 of 6N HCl containing 0.5 g of mannitol. Mannitol prevents evaporation of boron from acid solutions (Feldman, 1961). The solution was transferred to a glass chromatographic column (2 cm OD) filled with 20–cm bed of a cation exchange resin (Dowex Ag 50W–X8, 200–400 mesh; hydrogen form). Major elements were removed by using 400 cm^3 of 1.7N HCl, whereas rare earth elements and boron were quantitatively retained on the resin. They were desorbed later by using 500 cm^3 of 4N HCl. A flow rate of 1 cm^3/min was used in the separation. The final solution was collected in a 500 cm^3 teflon beaker, then slowly evaporated to almost dryness and the residue dissolved in 10 cm^3 of 1.7N HCl. This solution was stored in a polyethylene bottle until the ICP–AE measurements were carried out.

The measurements were performed on a Perkin Elmer spectrometer. The emission lines chosen in this work are listed below (Table 2). All standards were prepared from standard 1000 ppm solutions.

Table 2. *Emission wavelengths of rare earth elements and boron (nm)*

La	Pr	Nd	Sm	Eu
398.85	418.66	401.23	359.26	381.97

Gd	Dy	Yb	Lu	B
342.25	353.17	328.94	261.54	249.77

2.4.2. Prompt gamma emission technique

As the ICP-AE method for REE and boron was expensive and inefficient, it was replaced by a prompt gamma emission technique. The measurements (Gd and B only) were performed by Nuclear Activation Services, Inc., Ann Arbor, Michigan. Gadolinum and boron have exceptionally high thermal neutron absorption cross-sections and had to be considered for the purposes of this study; other REE were neglected as their cross-sections are lower than that of gadolinum by a few orders of magnitude.

3. Cosmogenic ^{36}Cl production rates in terrestrial rocks

Knowledge of the production rates of ^{36}Cl in rocks exposed at the surface of the earth is a prerequisite for using the cosmogenic ^{36}Cl dating method. We have measured the ^{36}Cl content of varnish ^{14}C–dated glacial boulders from the White Mountains in eastern California and in a ^{14}C–dated basalt flow from Utah. We calculated effective, time–integrated parameters for ^{36}Cl production by simultaneous solution of the ^{36}Cl production equation. The production rates due to spallation are 3,560 ± 465 and 2,740±245 atoms ^{36}Cl per yr per mole ^{39}K and ^{40}Ca, respectively, and the thermal neutron stopping rate is $(2.64 \pm 0.42)*10^5$ neutrons per kg of rock per yr. The reported values are normalized to sea level and high (polar) geomagnetic latitudes. Production of ^{36}Cl at different altitudes and latitudes can be obtained by appropriate scaling of the sea level rates. We also performed chlorine–36 dating of late Pleistocene morainal boulders from the Sierra Nevada, California and on carbonate ejecta from Meteor Crater, Arizona. Calculated ^{36}Cl ages are in good agreement with previously reported dates obtained using independent methods.

3.1. Methods

Phillips and coworkers collected several rock samples in the western United States from young glacial moraines and lava flows which had previously been independently dated by means of ^{14}C. We performed mineral separations on some of them and then analyzed the samples and the mineral phases for ^{36}Cl, stable Cl, and for major and trace elements. Based on cosmogenic ^{36}Cl buildup, we calculated effective production rates due to spallation and neutron activation processes. Then we tested the new parameters for internal consis-

tency and tested the validity of previously published corrections for latitude and elevation by dating several rock samples at various locations.

3.1.1. Sample collection and preparation.

In order to provide useful samples for calibrating cosmogenic ^{36}Cl production rates, the materials investigated should be from a well understood geological context, should be precisely dated by independent methods, and should have been in a geomorphically and tectonically stable environment since their exposure to cosmic rays. For these reasons boulders from glacial moraines in the White Mountains of eastern California were selected as the primary reference samples, and lava flow in central Utah as secondary samples.

The glacial samples were collected from a late Quaternary moraine sequence at Chiatovich Creek in the eastern White Mountains. These moraines are in a regionally well–understood context (Elliott–Fisk, 1987) and, because of the relatively arid climate, exhibit enough rock varnish development to allow the application of varnish radiocarbon dating (Dorn et al., 1989). Sample 187 was collected from a small moraine deposited during the Chiatovich Cirque glaciation and has a varnish ^{14}C date of 9.74 ka (Dorn et al., in press). The Chiatovich Cirque glaciation is correlated with the Hilgard glaciation in the Sierra Nevada, which has been assigned an early Holocene (or possibly terminal Pleistocene) age (Fullerton, 1986). Sample 387 was from a late Middle Creek moraine and has a varnish ^{14}C age of 12.51 ka (Dorn et al., in press). The late Middle Creek glaciation in the White Mountains is correlated with the late Tioga phase in the Sierra Nevada (Elliott–Fisk, 1987), which has a ^{14}C date for its termination of 11 ka (Fullerton, 1986). Rock varnish on a late Tioga moraine at Pine Creek, in the Sierra Nevada west of the White Mountains, yielded a varnish ^{14}C date of 13.9 ± 0.4 ka (Dorn et al., 1987). Finally, sample

787 was collected from an early Middle Creek moraine with a varnish ^{14}C age of 17.78 ka (Dorn et al., in press). The early Middle Creek is correlated with the early Tioga glaciation in the Sierra Nevada. The Tioga glaciation was initiated between 21 ka (Lebetkin, 1980) and 25 ka (Atwater et al., 1986). An early Tioga moraine at Pine Creek gave a varnish ^{14}C date of 18.9 ± 0.8 ka (Dorn et al., 1987). In summary, the varnish ^{14}C dates from the Chiatovich Creek moraines are in good agreement with both conventional ^{14}C dating of the regional glacial sequence and with varnish ^{14}C dates on correlative moraines from a nearby part of the Sierra Nevada. The varnish ^{14}C dates are therefore considered to be reliable enough to use for calibrating the cosmogenic production rate of ^{36}Cl.

Presumably, some finite length of time is required to initiate varnish generation (and thus accumulation of organic carbon) on boulder surfaces. This should result in some time lag between the emplacement of the boulder and the ^{14}C date that would be measured on the basal 10 percent of the varnish. Unfortunately, this time lag is unknown for the White Mountains environment. For sites in the western United States where varnish ^{14}C dates were tested against precise independent chronologies the lag was found to be generally less than 5 percent (Dorn et al., 1989). Due to its relatively small but uncertain length, we have chosen to calibrate to the measured, varnish–^{14}C ages of the moraines. When the varnish lag can be accurately quantified, the ^{36}Cl production rates can be appropriately corrected. At present, the magnitude of the correction would appear to be well within the uncertainty of the calculated production rates.

In order to assure that the sample geometries have remained unchanged since the time of deposition, only large boulders with glacially altered surfaces

from young moraines were sampled. Another rationale behind choosing relatively young glacial deposits was to minimize the influence of any elevation changes due to tectonic uplift of the White Mountain block. The average Quaternary vertical uplift rate of the White Mountains with respect to sea level has been estimated to be 0.5 mm/yr (Bachman, 1978), which is similar to the late Quaternary displacement rate of 0.25 mm/yr of the Sierra Nevada block along the Owens Valley fault zone (Martel et al., 1987). This uplift rate is equivalent to an offset of 5–9 m since the deposition time of the two Middle Creek and the Chiatovich Cirque moraines. Displacement of this magnitude does not require any corrections.

We performed mineral separation in a heavy liquid (sodium metatungstate) on the three granitic samples from the White Mountains (187, 387, and 787) and obtained three impure phases: microcline/albite, quartz, and anorthite/biotite (Table 3). Potassium–rich microcline yielded information on the production rate due to spallation on ^{39}K, whereas relatively pure quartz, in which

Table 3. *Composition of mineral separates. Bold, underlined letters indicate mineral separates that have been used for calibration. Key to abbreviations: A – albite–rich plagioclase, An – anorthite–rich plagioclase, B – biotite, M – microcline, Q – quartz, P – undifferentiated plagioclase. Plagioclases form pertites and therefore could not be completely separated from other minerals.*

	C–187–3	C–387–1	C–787–1
Density, g/cm^3	Minerals present – mass, g		
>2.80	B, An – 16	**B – 36**	B – 9
2.63–2.80	An, Q, **B –14**	An, B – 9	P, **B**, Q – **9**
2.62–2.63	**Q**, M – **104**	M, Q – 19	**Q – 71**
2.60–2.62	**Q**, M – **44**	**Q – 98**	Q,P – 23
2.58–2.60	A, Q, **M – 19**	A, M, Q – 50	A, M – 9
2.56–2.58	**M**, A – **108**	**M**, A – **172**	M, P – 12
<2.56	–	–	**M**, A – **122**
Total mass, g	305	374	255

most of ^{36}Cl should be from thermal neutron activation of ^{35}Cl, was used to estimate the effective thermal neutron stopping rate. Small impurities in microcline and quartz are not critical because chemical composition is accounted for in the production equation. The third mineral phase consisted of plagioclase and heavy minerals which did not completely decompose during sample preparation. Chlorine could not be reliably quantified and therefore these mineral separates were not used in the calibration.

Two additional calibration samples were obtained from the Tabernacle Hill basalt flow in Utah (samples 9353 and 9354). The eruption age is bracketed by a ^{14}C–dated organic matter incorporated into volcanic ash below the flow and tufa above (Oviatt and Nash, 1989; Cerling, 1990); the eruption occurred between 14.3 and 14.5 ka. The dates are consistent with the intensively–studied Lake Bonneville chronology. These two calcium–rich samples were chosen to provide information on the production rates due to spallation of Ca and neutron activation of ^{35}Cl.

We analyzed four basalts from late Pleistocene moraines on Mauna Kea, Hawaii (samples MK–MAKY–16, MK–MAKT–29, MK–MAKO–12, and MK–W–5) to test the proposed geomagnetic latitude correction factors (Lal and Peters, 1967; Yokoyama et al., 1977; Rose et al., 1956; Lingenfelter, 1963). In addition, we dated five siliceous dolomites from Meteor Crater, Arizona, and morainal boulders from the Sierra Nevada, California, to test the internal consistency of the calculated ^{36}Cl production rates (see Chapter 4 and 5).

3.1.2. Calculations

We obtained production rates due to the different mechanisms discussed below by solving equation (1) for the parameters: ϕ_n, ψ_K, and ψ_{Ca}. We developed a computer algorithm for iterative solution of equations for all samples

Table 4. Geochemistry of samples used for calibration.

Sample ID	SiO_2 %	TiO_2 %	Al_2O_3 %	Fe_2O_3 %	MgO %	CaO %	MnO %	Na_2O %	K_2O %	P_2O_5 %	Cl ppm	B ppm	Gd ppm	$^{36}Cl/Cl$ 10^{-15}
187–Bulk	76.00	0.21	13.80	1.22	0.14	0.21	0.03	4.26	5.44	0.02	130	2.6	4.9	473 ± 74
187–Quartz	84.90	0.04	10.20	0.35	0.18	0.14	0	4.60	3.61	0	125	2.6	2.7	493 ± 48
187–Microcline	70.30	0.02	17.00	0.32	0	0.16	0	5.34	7.80	0	130	0.9	0.9	616 ± 61
387–Quartz	94.80	0.02	3.99	0.27	0.10	0.26	0.01	2.27	0.37	0	101	0	1.26	342 ± 32
387–Microcline	69.70	0.01	18.10	0.28	0	0.22	0.01	5.57	8.78	0	142	0	0.96	856 ± 101
787–Bulk	76.50	0.21	14.00	13.50	0.12	0.49	0.02	4.83	5.43	0.05	160	6.3	4.7	595 ± 74
787–Quartz	92.50	0.05	4.67	0.35	0.16	0.25	0	2.60	0.54	0	135	1.8	0.8	344 ± 26
9353	47.91	1.31	14.03	10.22	6.81	10.93	0.16	2.06	0.86	0.46	94	10	5.4	244 ± 16
9354	46.13	1.42	14.84	11.65	6.75	10.69	0.17	2.37	0.78	0.42	111	10	5.7	226 ± 15

Major elements were measured by XRF spectrometry on pressed pellets (analytical error 2% except for Si and Al), B and Gd by ICP–AE and prompt gamma emission spectrometry. Total Cl was measured by ion–selective electrode (analytical error less than 5%). Chlorine–36 was measured by AMS.

Table 5. Location and calculated production parameters for calibration samples[a]

Sample ID	Altitude [km]	Latitude (°N)	Longitude (°E)	ELD_n	ELD_μ	$\frac{\sigma_{35}N_{35}}{\sum_i \sigma_i N_i}$	^{14}C age [ka]	Production from activation of Cl [atoms/kg rock/yr]	Production from spallation of K [atoms/kg rock/yr]	Production from spallation of Ca[c] [atoms/kg rock/yr]
187–Bulk	3.75	37.5	242	14.54	3.80	0.01416	9.74[b]	3,259	3,444	–
187–Quartz	3.75	37.5	242	14.54	3.80	0.01361	9.74[b]	4,636	–	–
187–Microcline	3.75	37.5	242	14.54	3.80	–	9.74[b]	–	5,720	–
387–Quartz	3.70	37.5	242	14.16	3.74	0.01061	12.51[b]	2,862	–	–
387–Microcline	3.70	37.5	242	14.16	3.74	–	12.51[b]	–	7,620	–
787–Bulk	3.27	37.5	242	11.06	3.27	0.01677	17.78[b]	4,064	3,550	–
787–Quartz	3.27	37.5	242	11.06	3.27	0.01415	17.78[b]	3,456	–	–
9353	1.445	38.94	247.48	3.35	1.76	0.00822	14.4 ± 0.1	1,834	–	5,021 (4,349)
9354	1.445	38.94	247.48	3.35	1.76	0.00923	14.4 ± 0.1	2,772	–	5,578 (4,943)

[a] Production values are for sea level and polar latitudes. Only values used in calculations are shown (see text for details).
[b] Estimated uncertainty is less than 10%.
[c] For calcium, the first values refers to $f_n = 0.005$ and values in parentheses refer to $f_n = 0.15$ (see text for details).

(Appendix 7.2.). First, the equations were solved for the thermal neutron stopping rate and the individual values were averaged. The mean value was then used in solving the appropriate equations for the production rate due to direct spallation of K. Again, they were averaged, and the mean value was used for solving for the remaining parameter – the production rate due to direct spallation of Ca. The procedure was repeated until no change in calculated mean values was observed, which was achieved after 6–8 iterations. We ran the program with several different sets of initial values for ψ_K, ψ_{Ca}, and ϕ_n to check the uniqueness of the solution; the final figures were always identical. We plotted (Fig. 3, 4, 5) the calculated values of total production due to each mechanism (Table 5) versus respective concentrations (Table 4) and fitted straight lines of the form $y=ax$ to the data points using a least squares algorithm; the slopes are equal to the thermal neutron stopping rate (for Cl) and to production rates per percent of oxide (for K and Ca). The reported values are normalized to sea level and high geomagnetic latitudes (90°).

3.2. Results and discussion

The results of chemical and isotopic analyses are summarized in Table 4. Sample locations, correction factors, and calculated parameters are presented in Table 5; geographical longitude is to the east of Greenwich.

3.2.1. Production rates

The calculated thermal neutron absorption rate of $(2.64 \pm 0.42)\times10^5$ neutrons per kg of rock per yr (Fig. 3) is in fairly good agreement with measured values at different locations. The reported values of the thermal neutron flux range from 10^{-3} to $2*10^{-3}$ n/cm^2/s (Montgomery and Montgomery, 1939;

Simpson, 1951; Hendrick and Edge, 1966; Yamashita et al., 1966; Andrews et al., 1986) which is equivalent to a flux density of $2*10^5$ to $4*10^5$ n per kg per year. The variability between the flux estimates can be partly explained by analytical uncertainty in the thermal neutron measurements, which can be as high as 50 % (Yamashita et al., 1966). This error arises mainly from uncertainty concerning the energy distribution of the thermal and epithermal neutrons and the anisotropic nature of the neutron flux at the air/rock interface. The anisotropy

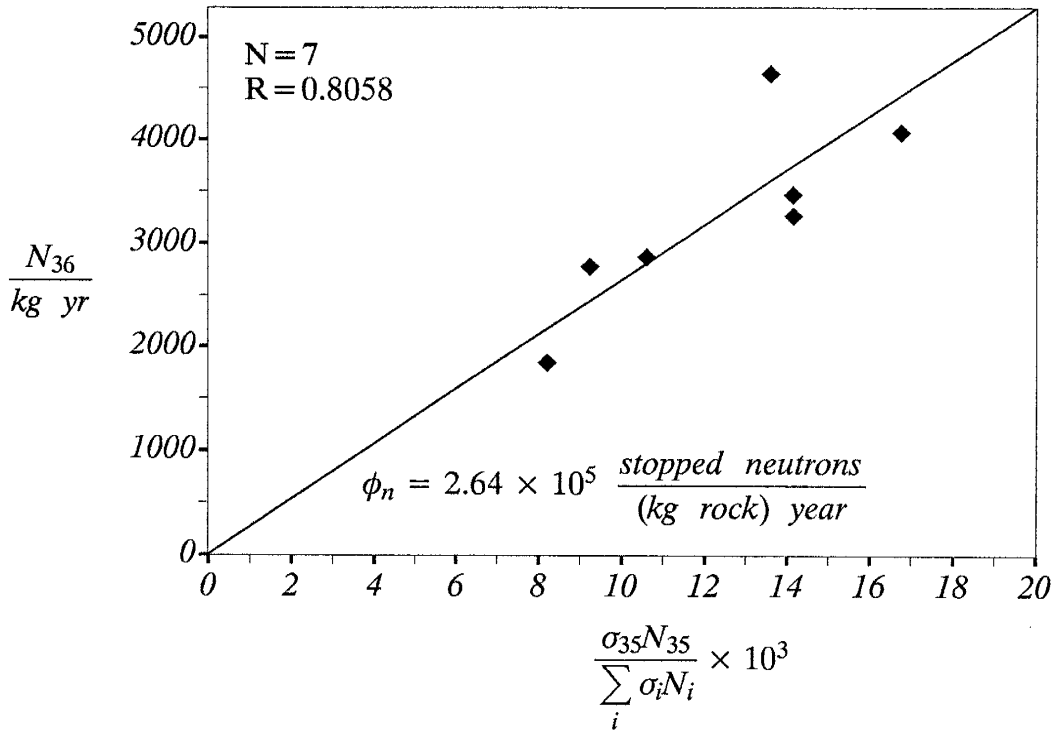

Fig. 3. Thermal neutron stopping rate in rocks at the surface of the earth. Horizontal axis shows ^{36}Cl produced per one thermal neutron; vertical axis represents total ^{36}Cl produced by neutron activation of ^{35}Cl; slope of the fitted line is equal to the thermal neutron absorption rate.

of the neutron flux may be a source of an additional error introduced during conversion from the flux units (n/cm^2/yr) to the stopping rate units (n/kg/yr). This may underestimate converted values by about 15 % (Yamashita et al.,

channel $^{40}Ca(\mu,\alpha)^{36}Cl$: 0.15 (Charalambus, 1971) and 0.005 (Wyttenbach et al., 1978, cited by Fabryka–Martin, 1988). Both values of f_n are theoretically calculated and need to be verified experimentally. If the real value of f_n were close to 0.005, the muon term could be safely omitted in the production equation (Eq. 1), because its contribution to ^{36}Cl production would be only about 1 % of that of direct spallation of ^{40}Ca. If, on the other hand, its value were 0.15, the production rate due to negative muon capture by ^{40}Ca would be as high as 14 % of that of direct spallation of ^{40}Ca and this reaction would have to be treated quantitatively. These figures are valid at sea level; at high elevations, the muon contribution decreases because of the larger attenuation length for muons than for neutrons. The production rate due to negative muons was subtracted from the total ^{36}Cl formed from Ca which yielded production rate due to spallation. The calculated production rates due to spallation of ^{40}Ca for the two values of f_n are presented in Table 6. They differ by 14% and, since spallation of ^{40}Ca usually accounts for no more than 50% of the total ^{36}Cl production, the introduced total uncertainty should be smaller than 7%.

Table 6. *Production rates of ^{36}Cl due to direct spallation of ^{40}Ca for different values of the muon component* f_n.

f_n	Production rate due to direct spallation of ^{40}Ca	
	$\frac{\text{atoms } ^{36}Cl}{\text{(mole Ca) yr}}$	$\frac{\text{atoms } ^{36}Cl}{\text{(kg rock) \%CaO yr}}$
0.005	2,740 ± 245	490 ± 45
0.15	2,400 ± 245	430 ± 45

Both production rates are considerably lower than the previously published values (Yokoyama et al., 1977). The same factors that affect potassium spallation may account for this discrepancy. The calculated values may have to be adjusted in the future when more accurate estimates for f_n are available. Until then, since reactions involving muons are not of critical importance for

sumes that ^{36}Cl is produced over the entire cosmic-ray energy spectrum which is not valid for earth surface conditions because energetically different components of the cosmic radiation are moderated at different rates. Similar discrepancies between theoretically calculated and experimentally derived production rates for ^{3}He (Kurz, 1986; Cerling, 1990) and ^{10}Be (Nishiizumi et al., 1989) have been explained by the lack of availability of excitation functions for the formation of those nuclides from their target elements. The value calculated in this study is the first reported, experimentally derived effective terrestrial production rate reported for ^{36}Cl due to spallation of ^{39}K.

Calcium is a target element for ^{36}Cl formation due to two different cosmogenic reactions: spallation (Fig. 5) and negative muon capture. We calculated a production rate due to negative slow muon capture using the formulation of Charalambus (1971) and two different values for probability, f_n, of reaction

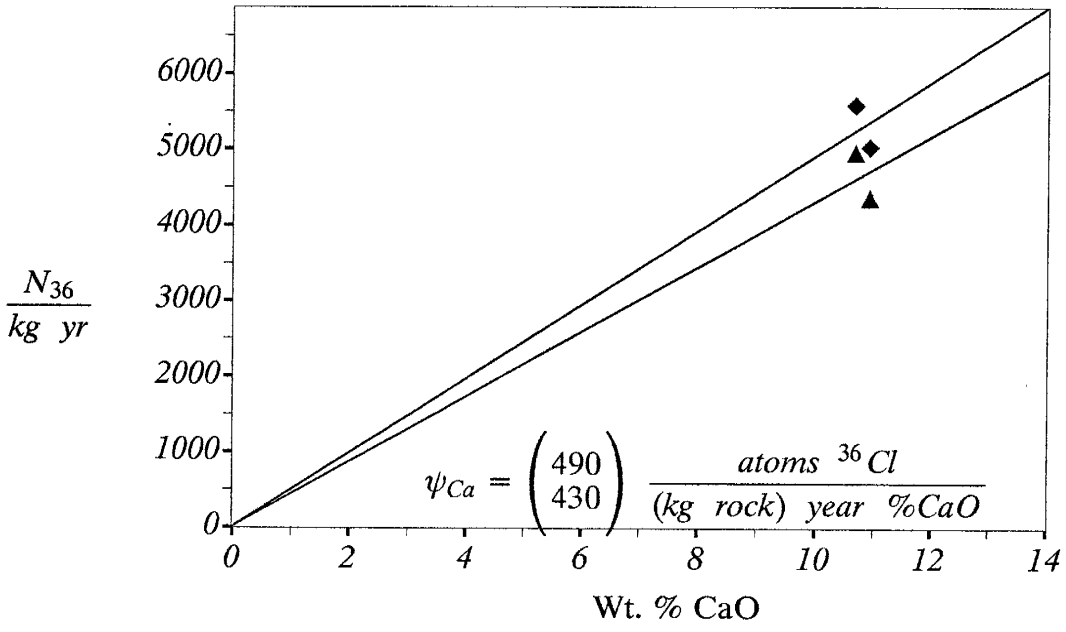

Fig. 5. Production of ^{36}Cl due to direct spallation of ^{40}Ca for different values of contribution of muons, f_n: solid line and squares are for $f_n = 0.005$, dashed line and crosses are for $f_n = 0.15$. The slopes of the lines represent the production rates ψ_{Ca} of ^{36}Cl from ^{40}Ca.

1966). It should be stressed that the measured, present-time fluxes may not be representative for the past conditions because of possible major changes in the earth's magnetic field strength (O'Brien, 1979) and the galactic cosmic ray flux. The value calculated in this study represents the effective, sea-level, high-latitude thermal neutron stopping rate time-integrated over the last 10-18 ka.

The production rate due to spallation of potassium (Fig. 4) is 3,560 ± 465 atoms ^{36}Cl per mole K per yr (760 ± 100 atoms per kg of rock per yr per % K_2O). This value is smaller than that obtained by Yokoyama et al. (1977) by a factor of four. The production rates of Yokoyama et al. (1977) were theoretically calculated using the excitation functions for ^{36}Cl production given by

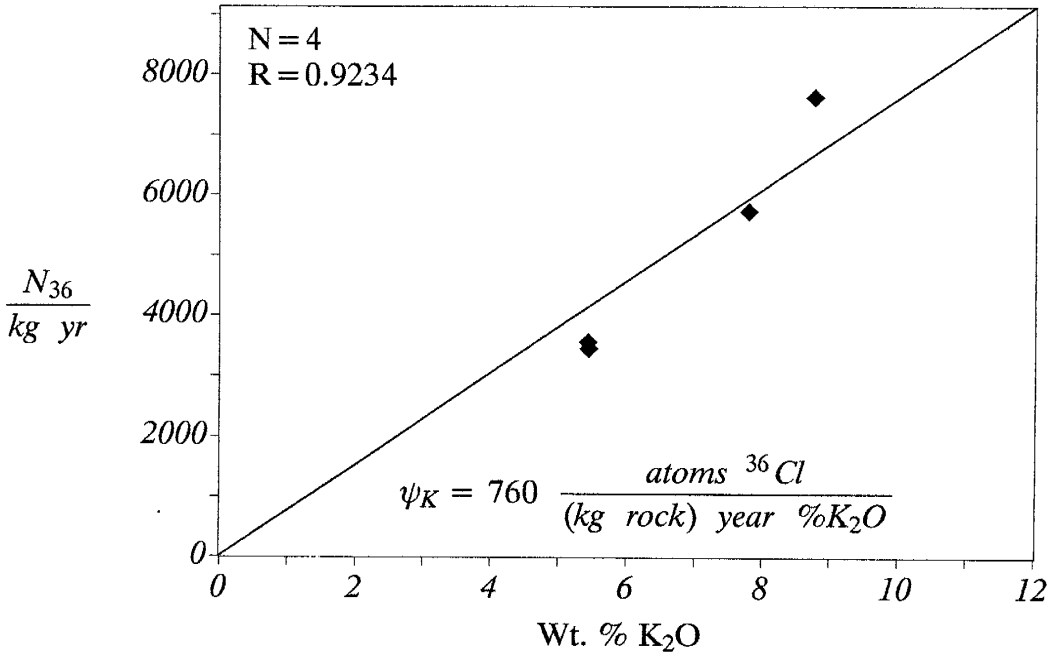

Fig. 4. Production of ^{36}Cl due to direct spallation of ^{39}K. The slope of the line is equal to the production rate ψ_K of ^{36}Cl from ^{39}K.

Reedy and Arnold (1972) for lunar conditions. These conditions, however, may not be applicable on the surface of the earth because of atmospheric moderation and magnetic field effects. The model of Reedy and Arnold (1972) as-

most surface samples, the slow negative muon component can be omitted in the production equation and the higher of the two reported values for spallation of calcium used.

3.2.2. Test of the production parameters

Four basaltic boulders from late Pleistocene moraines on Mauna Kea (Porter, 1979) were collected at elevations similar to those for samples in the White Mountains but at different geomagnetic latitude. The results of chemical and isotopic analyses and other data are presented in Tables 7 and 8. Chlorine-36 buildup ages calculated using the geomagnetic correction factors of Yokoyama et al. (1977) and Lingenfelter (1963) exceeded the corresponding ^{14}C ages by as much as 50 %. The geomagnetic latitude dependence of Lal (1990) yielded calculated ages (Table 8) almost identical with those obtained by the varnish ^{14}C method (Dorn et al., in preparation). This excellent agreement supports the latitude dependence formulation of Lal (1990) and indicates that cosmogenic ^{36}Cl buildup dates can be corrected for geomagnetic latitudes differing from the calibration latitude.

The formulation of Lal used in this study is in the form of cubic polynomials: $EL = a_0 + a_1x + a_2x^2 + a_3x^3$ where EL is the correction factor for elevation and geomagnetic latitude, x is the elevation (km) above sea level and a's are the polynomial coefficients for different geomagnetic latitudes (Table 9). In this study, we normalized the correction factor EL to polar geomagnetic latitudes by dividing calculated EL by coefficient a_0 for 60° geomagnetic latitude (i.e. 1.8109). For latitudes differing from those in Table 9, we obtained the polynomial coefficients using straight line interpolation between the given values.

Snow cover can potentially attenuate the cosmic-ray flux reaching rock surfaces. Nishiizumi et al. (1989) have calculated that in the Sierra Nevada as

Table 7. Geochemistry of samples from late Pleistocene moraines, Mauna Kea, Hawaii

Sample ID	SiO_2 %	TiO_2 %	Al_2O_3 %	Fe_2O_3 %	MgO %	CaO %	MnO %	Na_2O %	K_2O %	P_2O_5 %	Cl ppm	B ppm	Gd ppm	$^{36}Cl/Cl$ 10^{-15}
MK-MAKO-12	54.93	2.37	17.98	9.85	2.04	6.82	0.19	5.44	1.99	1.04	49	10	3.0	1121 ± 82
MK-MAKY-16	51.90	2.37	18.80	10.00	1.90	6.72	0.20	5.61	2.04	0.96	84	9	5.2	708 ± 30
MK-MAKT-29	52.90	2.22	18.00	9.47	1.51	6.22	0.20	5.97	2.12	0.95	45	10	4.9	1110 ± 36
MK-W-5	46.88	4.65	17.64	14.96	4.72	9.39	0.18	3.91	0.99	0.76	40	10	5.0	2991 ± 111

Major elements were measured by XRF spectrometry on pressed pellets (analytical error 2% except for Si and Al), B and Gd by ICP-AE and prompt gamma emission spectrometry. Total Cl was measured by ion selective electrode (analytical error less than 5%). Chlorine-36 was measured by AMS.

Table 8. Carbon-14 (Dorn et al., 1989) and ^{36}Cl ages of late Pleistocene moraines, Mauna Kea, Hawaii.

Sample ID	Altitude [km]	Latitude	Longitude (to the East)	ELD_n	^{14}C age [ka]	^{36}Cl age [ka]
MK-MAKO-12	3.500	19.8	204.5	7.09	21.5	22.9
MK-MAKY-16	3.584	19.8	204.5	7.66	20.2	20.8
MK-MAKT-29	4.054	19.8	204.5	9.72	15.9	16.0
MK-W-5	3.109	19.8	204.5	5.74	66.0 (cation ratio age)	68.0

ELD_n was calculated according to the latitude dependence of Lal (1990).
Chlorine-36 ages were calculated using the production equation, solved for t.

Table 9. *The polynomial coefficients for altitudinal/latitudinal dependence formulation of Lal (1990).*

Geomagnetic latitude	a_0	a_1	a_2	a_3
0	1.0486	0.8116	0.3121	0.0650
10	1.0715	0.7995	0.3521	0.0657
20	1.2116	0.8628	0.4201	0.0787
30	1.4881	1.2513	0.3100	0.1497
40	1.6667	1.6025	0.4503	0.1867
50	1.7864	1.8649	0.5419	0.2414
60	1.8109	1.9718	0.5622	0.2502

much as 10 % decrease in radionuclide production could have occurred on horizontal surfaces. In order to minimize this effect, the field party (F. Phillips et al.) sampled the tops of high boulders that should be rapidly swept free of snow by the wind. The White Mountains are in the rain shadow of the Sierra Nevada and receive much less precipitation than the Sierra Nevada does. The eastern slopes of the White Mountains are virtually snowless for most of the year (The California Water Atlas). A the time of sampling there were only a few small, isolated snow patches away from our sample locations. Therefore, the effect of attenuation of the cosmic rays due to snow cover should be negligible for the calibration samples collected in the White Mountains. The excellent agreement between varnish ^{14}C and ^{36}Cl ages of the Hawaiian samples indicate that this was also the case on Mauna Kea. Three of the Hawaiian samples (MK–MAKO–12, MK–MAKY–16 and MK–MAKT–29) were collected at locations where snow cover was unlikely to develop and persist for long periods of time. They yielded ^{36}Cl ages identical to the varnish ^{14}C ages (Table 8). The ^{36}Cl age of the fourth sample (MK–W–5) is only slightly older than the cation–ratio age. Although attenuation of the cosmic ray flux by snow was not a problem in my

study areas, it should not be overlooked; in all locations where snow cover is significantly thick and persists for long periods of time, appropriate corrections for additional attenuation of the cosmic rays should be made using correction factor, D, for depth below surface.

Five dolomite samples from Meteor Crater, Arizona were analyzed and the time of the meteorite impact calculated (Phillips et al., in preparation). They were collected at geomagnetic latitudes similar to the calibration latitude, but at differing elevations. The mean age of 50.8 ± 6.5 ka (Chapter 5) is in excellent agreement with the age of 49.0 ± 3.0 ka obtained from thermoluminescence studies of shock-metamorphosed minerals (Sutton, 1985). The ^{36}Cl data are very consistent. Four out of five samples yielded almost identical ages, with standard deviation smaller than analytical uncertainty of the individual AMS measurements. This suite of samples indicates that given favorable geological conditions, such as low erosion rates in arid environments, the cosmogenic ^{36}Cl buildup method gives reliable and accurate exposure ages. It also shows that by appropriate scaling of the sea level production rates, the ^{36}Cl buildup method can be applied at different elevations.

We established a chronology of late Pleistocene glaciations in Bloody Canyon, eastern Sierra Nevada (Phillips et al., 1990). Obtained dates (Chapter 4) are in excellent agreement with both 'cold' stages of marine ^{18}O record and solar intensity curve. They also agree well with varnish radiocarbon ages of late Wisconsin moraines from Pine Creek, 60 km S of Bloody Canyon (Dorn et al., 1987). These encouraging results show that ^{36}Cl can indeed be used for dating geomorphic surfaces.

3.2.3. *Suggestions for future work*

Uncertainty concerning published corrections for elevation above sea level and for geomagnetic latitude are probably the greatest source of error in the calculated ages. The formulation proposed by Lal (1990) for correcting for altitude and geomagnetic latitude worked well in this study because almost all samples were collected at approximately similar altitudes (except for the Meteor Crater samples). However, if application of the ^{36}Cl method to other areas is intended, further testing of the latitude/altitude dependence would be necessary. The correction factor for elevation can be verified by processing samples of approximately the same age from different elevations. Suitable samples have already been collected from Hawaii and are being processed.

The production rate of ^{36}Cl due to spallation of ^{40}Ca is poorly constrained by this study because its derivation was based on only two samples. Uncertainty of this parameter does not allow precise dating of high–Ca rocks. It is therefore imperative that suitable calibration samples be obtained and the production rate due to spallation of ^{40}Ca verified.

An experimental estimate of the probability, f_n, of ^{36}Cl production due to negative muon capture by ^{40}Ca is necessary to quantify this process. The knowledge of the correct value of this parameter will allow for more precise estimate of the production rate due to direct spallation of ^{40}Ca. This mechanism is particularly important for high–Ca samples from low elevations, such as those from Death and Panamint Valleys, California.

3.3. *Summary*

We investigated cosmogenic ^{36}Cl buildup in rocks exposed at the surface of the earth and parametrized different production mechanisms. Effective pro-

duction rates due to direct spallation of ^{39}K and ^{40}Ca are 3,560 ± 465 and 2,740±245 atoms ^{36}Cl per yr per mole ^{39}K and ^{40}Ca, respectively. We have shown that these values, although considerably lower than those reported elsewhere, should be valid for late Pleistocene conditions. An effective thermal neutron stopping rate of (2.64 ± 0.42)x10^5 neutrons per kg of rock per yr compares well with the present–day, measured values.

We also investigated production of ^{36}Cl due to negative muon capture using two previously reported values of probability of the reaction leading to ^{36}Cl formation. The maximum sea–level production rate due to this process is less than 15% of that of spallation of calcium. This proportion becomes negligibly small at high (mountain) altitudes.

The latitudinal/altitudinal distribution of cosmic–ray intensity of Lal (1990) is supported by agreement obtained between the ^{36}Cl buildup and ^{14}C dates. We applied the new production rates to dating rocks of various ages and at various geomagnetic latitudes and elevations. The results are in excellent agreement with ages obtained by independent methods. They show that the cosmogenic ^{36}Cl dating method can be successfully applied for samples at differing locations by appropriate scaling of the reported sea–level rates.

The cosmogenic ^{36}Cl dates compare well with the ages obtained using different dating methods. Similar cosmogenic production rates of ^{36}Cl were obtained using samples collected at different locations (the White Mountains and Tabernacle Hill) and independently dated by both varnish ^{14}C and classical ^{14}C techniques. The ^{36}Cl ages of the glacial moraines in the Sierra Nevada compare well with ^{14}C–dated organic material below and above the glacial sequence. Finally, the cosmogenic ^{36}Cl dating of the impact time of the Meteor Crater meteorite yielded ages almost identical to the age obtained from inde-

pendent thermoluminescence studies. These results strengthen our confidence in the calculated production parameters and indicate that the cosmogenic ^{36}Cl geochronology can be successfully applied in the earth sciences.

4. Cosmogenic ^{36}Cl chronology for glacial deposits at Bloody Canyon, eastern Sierra Nevada, California

4.1. Introduction

The Sierra Nevada is a westward–tilted fault block composed of deformed Paleosoic and Mesosoic metamorphic rocks intruded by a granitic batholith. The block is uplifted to elevations of 2,500 to 4,400 m above sea level. Its eastern side is a wall rising 750 to 3,100 m at a slope of 15%. Volcanic rocks of Miocene to Holocene age are present locally and provide limited radiometric control for associated glacial deposits.

The range forms a natural barrier to the eastward flow of maritime air masses off the Pacific Ocean. Precipitation is highest on the western slopes (up to 1,600 mm/yr) and drops to 400–500 mm/yr to the east of the crest. Snowfall may amount to 11.5 m per season at altitudes 2,300 to 2,600 m and remains for significant periods at elevations above 1,300 m.

In the Pleistocene, snowline was about 750 m lower than it is now. A region 55 km wide along the crest was intensively glaciated. Ice was most abundant in the southern and central Sierra, between latitudes 37 and 38°N. To the north, the lower elevation of the range resulted in smaller volume of ice; to the south, the higher temperatures kept the volume small. The largest glaciers were 100 km long on the western slope and only 16 km on the eastern one (Wahrhaftig and Birman, 1965). This difference reflects spatial distribution of precipitation in the range. Main glaciers descended to altitudes of 1,300 to 2,200 m on the eastern slope of the Sierra Nevada (Blackwelder, 1931).

4.2. Stratigraphy of glacial sequences

The lateral and terminal glacial moraines in canyons along the eastern front of the Sierra Nevada are relatively well studied because they are well preserved and not hidden from view by forest vegetation. They have been a focus of modern geological investigations since the early 1930's. Blackwelder (1931) first used semiquantitative criteria, such as granite weathering ratios and boulder frequency counts, for differentiation of glacial advances. He recognized deposits of four glaciations: the Tioga (youngest), Tahoe, Sherwin, and Mc Gee, and a possible advance between the Sherwin and Tahoe. Blackwelder correlated these glaciations with glacial events in the Basin Ranges and Rocky Mountains and with the standard mid–continent stratigraphy. He assigned the Tioga and Tahoe to the Wisconsin, the Sherwin to the Kansan, and the Mc Gee to the Nebraskan of the standard mid–continent section. In addition, he closely estimated the time of the Tioga maximum at 25 ka by correlating it with the Würm stage dated by using varve–clay lake deposits in Sweden (De Geer and Antevs, 1925, cited by Blackwelder, 1931). Blackwelder was also aware of the fact that the lengths of the established glacial periods were different; he believed that the Tahoe was deposited between 90 and 150 ka, and the Sherwin about 1.4 ma ago.

Investigations in the 1950's and 1960's provided evidence for two additional advances in the Sierra Nevada (Sharp and Birman, 1963). The Tenaya was found between Tioga and Tahoe and was correlated with the Wisconsin. Tenaya moraines were found to be "distinctly fresher, sharper, and topographically more ragged than Tahoe" (Sharp and Birman, 1963) and more weathered than the Tioga moraines. The Mono Basin, tentatively assigned to the Illinoian, preceded the Tahoe and was also less extensive. It is usually obscured by the Tahoe

and can be found only in areas where the Tahoe glaciers did not follow the Mono Basin path. The Tenaya and Mono Basin were described in Bloody Canyon where "one of the most clean–cut and spectacular sets of lateral moraines of the east Sierra Nevada" can be found (Sharp and Birman, 1963).

Burke and Birkeland (1979), however, suggested that the Tenaya is not a distinct glaciation but rather an early phase of the Tioga. The authors used multiparameter relative dating techniques in four valleys along the eastern Sierra Nevada and normalized the data to similar vegetation conditions. They concluded that there were only two major post–Sherwin glaciations – the Tahoe and Tioga. They grouped the Mono Basin till with the Tahoe, and the Tenaya with Tioga in some drainages but with the Tahoe in others.

The problem with the Tenaya indicates that the relative dating techniques may be useful in differentiating first–order glaciations, but are not sensitive enough to correlate second–order fluctuations, which may not be synchronous.

In order to detect second–order events one needs more precise, quantitative chronological tools. The establishment of an absolute chronology was initiated in 1950's with developments in isotope geochemistry. Stable isotopes provided means for inferring paleotemperatures whereas radioisotopes were used for measuring time.

The Sherwin till was bracketed by underlying basalt dated at 3.26 ma, and overlying Bishop Tuff dated at 738 ka (Dalrymple, 1964). Both dates were obtained by means of K–Ar method. On the basis of development of the paleosol, Sharp (1968) and Birkeland et al. (1980) estimated that the till is at least 50 ka older than the tuff. The till is also correlated with reversed–polarity continental till that was deposited 800–890 ka ago (Hallberg, cited in Fullerton, 1986).

Numerical ages bracketing younger glacial deposits were obtained in Sawmill Canyon (near Independence, California) by Darlymple (1964). An olivine basalt flow between two tills was dated at 93 ± 116 and 58 ± 73 ka. The till below the flow was considered to be pre–Tahoe and was correlated with the Mono Basin by Dalrymple (1964) and with the Tahoe by Burke and Birkeland (1979) and Dalrymple et al. (1982). The same volcanic rocks were redated by means of more precise ^{39}Ar–^{40}Ar technique at 119 ± 7 ka (Gillespie et al., 1984), and the underlying flow at 463 ± 40 ka (Gillespie, 1982). The author concluded that the lower till was deposited before 119 ka ago and thus is pre–Tahoe or pre–Wisconsin; the upper till is younger than 119 ka and is thus correlative with the Tahoe (early Wisconsin). No radiometric dates are available from the Bloody Canyon – Sawmill Canyon (Mono Lake region) area.

The Tioga glaciation, commonly represented by multiple end moraines, has been bracketed by ^{14}C dates on associated lacustrine sediments at Tulare Lake at 26 ka (Atwater et al., 1986), and peat overlying the Tioga till and basal lake sediments at 10–11 ka (Fullerton, 1986; Mezger and Burbank, 1986). The end moraines at Pine Creek, 60 km south of Bloody Canyon, were directly dated at 19 ka by rock varnish ^{14}C (Dorn et al., 1987).

4.3. Methods

4.3.1. Introduction

Most of the radiometric dates discussed above do not represent actual ages of glacial deposits. They are limiting maximum and minimum ages and do not allow a definitive chronology to be established. One solution to this problem would be to apply methods that directly date glacial landforms. However, as Phillips (Phillips et al., 1990) points out, such dating methods are intrinsically

difficult to develop because virtually all glacial landforms are constructed out of geologically preexisting rocks and most classical radiometric techniques measure the age of the rock or mineral formation rather than the age of geomorphic redistribution. One approach that has been applied with apparent success is rock varnish ^{14}C and cation ratio methods (Dorn et al., 1987). However, its use is limited to arid climate where rock varnish can be preserved; at most Sierra Nevada sites this preservation is questionable (Phillips et al., 1990).

An alternative surface exposure method, devised by Schaeffer and Davis (1955), utilizes cosmogenic ^{36}Cl accumulation in rocks exposed at the surface of the earth. Glacial moraines meet the fundamental assumption of the chlorine method of complete shielding followed by rapid exposure (due to glacial excavation).

In this study, we report the use of the ^{36}Cl method to date glacial moraines at Bloody–Sawmill Canyon, eastern Sierra Nevada. This area was selected for cosmogenic ^{36}Cl studies because of the large number of previous investigations, the relatively large number of morphologically distinct moraines that are preserved, and the clear–cut relative age sequence that can be inferred from the geometries of the moraines (Phillips et al., 1990). Bloody Canyon contains the type locality of the Mono Basin and one of the first Tenaya tills described east of the Sierra Nevada crest (Sharp and Birman, 1963).

4.3.2. Sample collection

Most samples were collected by F. Phillips and S. Smith (cf. Smith, 1988; Phillips et al., 1990) in 1986/87. They sampled the largest boulders that could be located along the crest of each of the moraines (Fig. 6). The crest itself is an almost horizontal surface on which boulders are not likely to roll or shift

after deposition. Only large (0.6 to 5.4 m tall) boulders were selected because they were most likely to have been exposed at the surface prior to any degradation of the moraine crest, and because they are more likely to be snow–free due to projecting above the average snow depth. All samples were collected from the top 5 cm of rock, as close to the center of the boulder as possible, using a hammer and a chisel. This procedure should minimize any shielding effect by rock material present above the sampling point (rocks attenuate cosmic rays) and any edge effect (due to anisotropy of the cosmic ray flux at the boundary between rock and air).

The samples were labelled as follows. BC and SC mean Bloody Canyon and Sawmill Canyon, respectively, 86 or 87 indicate date of the sample collection, the next number is a sequential number of the sample, and the last two letters designate moraine/glaciation: Tioga (TI), Tenaya (TE), Tahoe (TA), and Mono Basin (MB) according to Sharp and Birman (1963).

A few additional samples were collected by F. Phillips and myself in 1988 (BC88 and SC88). We followed the same sampling criteria as stated above.

Edited field notes are enclosed in Appendix 4.4.

The samples were analyzed for ^{36}Cl, major and selected minor elements, rare earths, and Cl as described in Chapter 3.

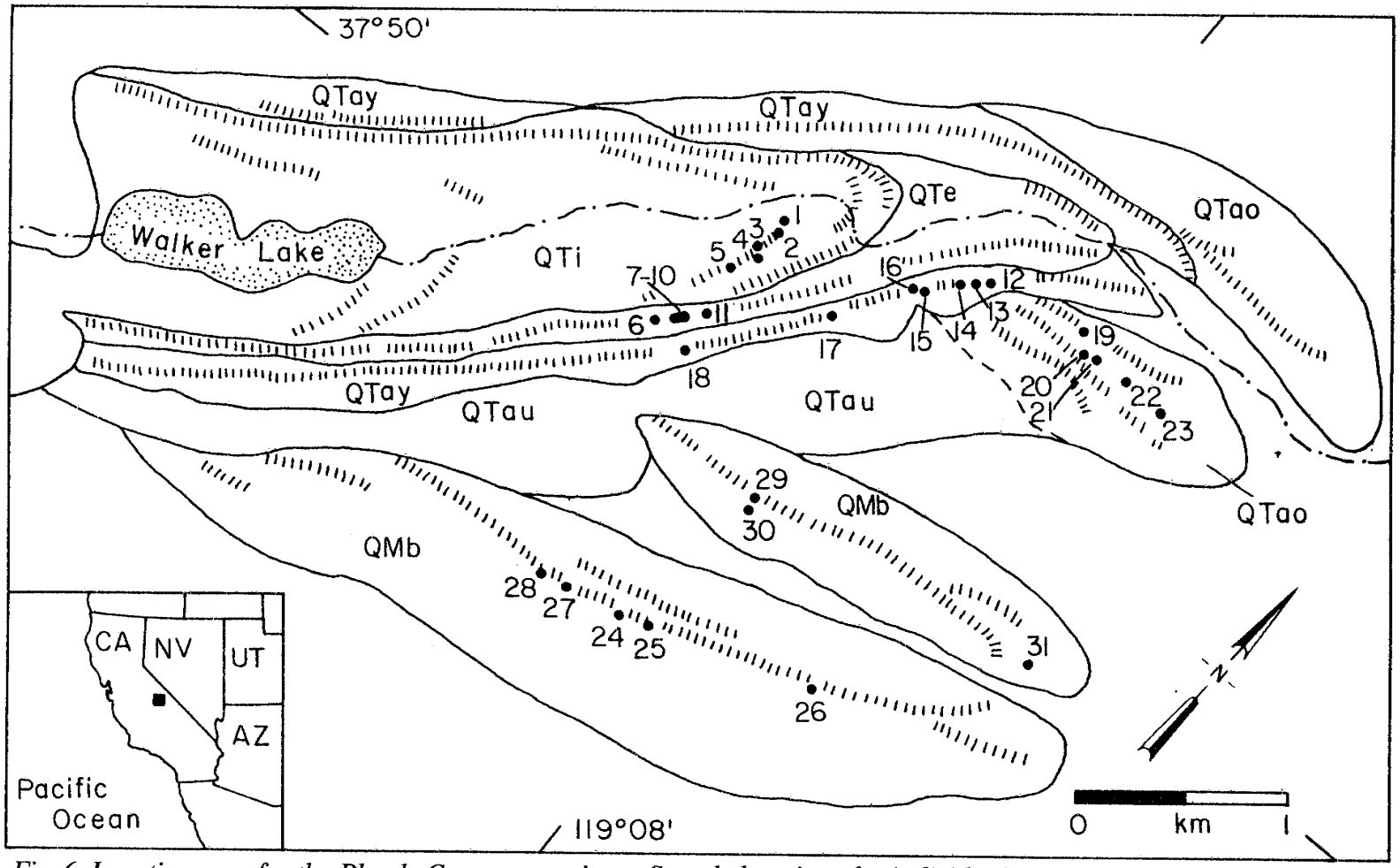

Fig. 6. Location map for the Bloody Canyon moraines. Sample locations for individual boulders are indicated by dots and numbers (keyed to Tables 10 and 11). Late Quaternary (Q) moraines are indicated by the subscripts: Ti–Tioga, Te–Tenaya, Tay–younger Tahoe, Tao–older Tahoe, Tau–undifferentiated Tahoe, and Mb–Mono Basin. Hatchures indicate moraine crests. (Mapping modified from Gillespie, 1982).

4.3.3. Exposure time calculations

The time of exposure was calculated using the production equation solved for time:

$$t = \frac{-1}{\lambda} \ln \left[1 - \frac{(R - R_0)\lambda N}{E_n L_n D_n \left(\psi_K C_K + \psi_{Ca} C_{Ca} + \phi_n \frac{\sigma_{35} N_{35}}{\Sigma \sigma_i N_i} \right)} \right]$$

The meaning of all symbols is explained in Chapter 3. The production due to slow negative muons was neglected because the rocks sampled are low in calcium and because at high elevations muons are relatively less important in production of ^{36}Cl. Calculations were performed using a PASCAL program 'cl.lal' (Appendix 4.1.). The value R_0 for radiogenic ^{36}Cl was assumed to be $30*10^{-15}$ which is typical for granitic rocks (Bentley et al., 1986). The production parameters and corrections are calculated and discussed in Chapter 3.

4.4. Results and discussion

The results of chemical and isotopic analyses are reported in Table 10. Sample locations, correction factors, and calculated time of exposure are presented in Table 11. The calculated ^{36}Cl exposure times are graphed for each moraine in Figure 7; the moraine names correspond to those on Fig. 5. and to those of Sharp and Birman (1963).

The mean of the boulder ages from the Tioga moraine, 21 ka, is in good agreement with limiting ^{14}C ages of 26 ka of the corresponding lake sediments (Atwater et al., 1986; Mezger and Burbank, 1986). A limiting minimum varnish ^{14}C age of 19 ka was obtained for a Tioga moraine in the corresponding position at Pine Creek, 60 km south along the Sierra crest (Dorn et al.,1987).

Table 10. Chemical and isotopic data for glacial moraine samples at Bloody Canyon, California.

Map number	Sample ID	SiO_2 %	TiO_2 %	Al_2O_3 %	Fe_2O_3 %	MgO %	CaO %	MnO %	Na_2O %	K_2O %	P_2O_5 %	Cl ppm	B ppm	Gd ppm	$^{36}Cl/Cl$ 10^{-15}
1	BC-86-1-TI	78.18	0.05	12.41	0.80	0.01	0.84	0.03	3.21	5.09	0.08	24	5[a]	6.0	1770 ± 136
2	BC-86-2-TI	65.66	0.18	12.74	1.82	0.78	2.27	0.03	3.54	2.96	0.38	71	5[a]	3.0	402 ± 17
3	BC-86-3-TI	74.77	0.31	15.42	2.66	1.24	2.12	0.08	3.92	4.38	0.25	103	8.6	1.8	536 ± 39
4	BC-86-4-TI	79.34	0.05	12.06	0.69	0	0.79	0.03	3.67	4.64	0.05	44	5[a]	1.2	±
5	BC-86-5-TI	72.32	0.56	15.54	4.23	1.99	2.89	0.11	3.34	3.44	0.34	141	3.1	3.6	455 ± 22
6	BC-86-6-TE	76.88	0.17	14.18	1.82	0.41	2.14	0.10	3.37	3.75	0.09	34	5[a]	3.9	1350 ± 96
7	BC-86-7-TE	64.04	0.19	12.91	0.97	0.70	3.69	0.04	3.11	1.68	0.12	40	5[a]	3.0	244 ± 37
8	BC-86-8-TE	77.24	0.25	15.93	2.58	1.46	1.47	0.11	3.86	3.30	0.20	67	5[a]	3.6	697 ± 38
9	BC-86-9-TE	65.61	0.22	14.59	1.74	0.68	1.94	0.05	3.57	4.32	0.28	74	5[a]	4.2	839 ± 54
10	BC-86-10-TE	73.19	0.18	12.73	1.97	0.41	1.52	0.09	3.54	3.96	0.12	64	5[a]	2.2	469 ± 28
11	BC-86-11-TE	75.21	0.08	14.84	1.02	0.49	0.98	0.07	5.16	5.34	0.02	26	5[a]	4.5	1951 ± 160
12	BC87-1TA	76.44	0.20	14.61	1.98	1.29	2.02	0.11	3.98	4.05	0.58	74	5[a]	3.6	1638 ± 211
13	BC87-2TA	73.80	0.09	14.40	0.78	0.25	0.79	0.04	4.85	5.57	0.28	31	5[a]	3.0	3763 ± 133
14	BC87-3TA	74.87	0.16	13.73	1.64	0.46	2.04	0.06	3.51	3.88	0.22	64	5[a]	3.0	1309 ± 87
15	BC87-4TA	75.62	0.18	13.24	1.97	0.54	2.18	0.08	3.10	2.48	0.36	74	5[a]	4.8	1461 ± 180
16	BC87-5TA	69.60	0.23	14.90	2.25	0.87	1.83	0.11	3.47	4.31	0.29	100	5[a]	3.3	1699 ± 94
17	BC88-1	75.64	0.12	13.64	0.63	0.27	1.61	0.04	3.01	4.70	0.06	38	0.9	1.1	315 ± 18
18	BC88-5	68.80	0.54	15.09	3.03	1.05	2.72	0.07	3.09	4.41	0.44	90	5.6	5.1	1701 ± 162

[a] indicates samples which have not been analyzed for B and for which a typical value of 5 ppm was assumed.

Table 10. Chemical and isotopic data for glacial moraine samples at Bloody Canyon, California.

Map number	Sample ID	SiO_2 %	TiO_2 %	Al_2O_3 %	Fe_2O_3 %	MgO %	CaO %	MnO %	Na_2O %	K_2O %	P_2O_5 %	Cl ppm	B ppm	Gd ppm	$^{36}Cl/Cl$ 10^{-15}
19	BC-86-12-TA	63.40	1.29	9.41	8.56	3.95	7.37	0.25	3.41	1.06	0.48	73	5[a]	6[b]	3155 ± 238
20	BC-86-13-TA	67.80	0.40	14.48	2.82	1.25	2.20	0.07	3.77	4.37	0.51	75	5[a]	8.4	4313 ± 248
21	BC-86-14-TA	77.12	0.20	14.80	1.88	1.44	1.19	0.10	4.12	3.74	0.33	49	5[a]	4.0	5736 ± 256
22	BC-86-15-TA	75.30	0.51	9.40	3.41	3.13	1.46	0.06	3.07	3.85	0.95	76	5[a]	6[b]	4211 ± 240
23	BC-86-16-TA	72.16	0.58	16.18	4.18	2.82	3.82	0.09	4.38	3.92	0.64	115	5[a]	5.7	2790 ± 197
24	SC86-17MB	75.20	0.15	11.40	1.36	0.95	0.56	0.07	3.24	3.93	0.94	57	5[a]	4[b]	3123 ± 223
25	SC86-18MB	74.68	0.25	15.27	2.15	2.08	1.22	0.13	2.83	3.90	0.52	122	5[a]	2.2	2001 ± 153
26	SC86-19MB	75.22	0.20	14.64	2.09	0.67	2.40	0.13	3.51	3.22	0.32	113	5[a]	6.0	1959 ± 122
27	SC86-20MB	74.68	0.10	14.65	1.06	0.48	1.18	0.05	3.43	5.16	0.17	28	5[a]	3.4	5289 ± 178
28	SC86-21MB	72.3	0.05	13.30	0.47	0.00	0.66	0.03	3.85	5.52	0.18	26	5[a]	4.4	7031 ± 250
29	SC88-1	70.75	0.43	14.64	2.73	0.89	2.36	0.07	3.14	4.73	0.30	76	1.0	3.2	2848 ± 62
30	SC88-2	69.48	0.50	14.67	3.13	1.06	2.64	0.07	3.27	4.38	0.34	111	6.7	4.0	1916 ± 67
31	SC88-3	67.24	0.60	15.76	3.17	1.24	3.41	0.08	3.74	4.19	0.30	157	4.8	3.6	2266 ± 167

[a] indicates samples which have not been analyzed for B and for which a typical value of 5 ppm was assumed.
[b] indicates samples which have not been analyzed for Gd and for which a typical value for a given moraine was assumed.

Table 11. Locations, ELD factors, macroscopic cross sections, and ^{36}Cl ages for samples from Bloody Canyon, California.

Map number	Sample ID	Elevation km	Latitude	Longitude	ELD_n	$\Sigma\sigma_i N_i$ cm^2/kg	$^{36}Cl/Cl$ 10^{-15}	Boulder age ka	Moraine age ka
1	BC-86-1-TI	2.38	37.9	240.8	6.34	4.97	1770 ± 136	23.1	
2	BC-86-2-TI	2.38	37.9	240.8	6.34	4.06	402 ± 17	12.2[a]	Tioga
3	BC-86-3-TI	2.38	37.9	240.8	6.34	4.88	536 ± 39	20.4	21.4 ± 1.4
4	BC-86-4-TI	2.38	37.9	240.8	6.34	–	–	–	
5	BC-86-5-TI	2.38	37.9	240.8	6.34	5.24	455 ± 22	20.8	
6	BC-86-6-TE	2.45	37.5	240.8	6.61	4.71	1350 ± 96	24.0	
7	BC-86-7-TE	2.33	37.9	240.8	6.14	3.71	244 ± 37	5.1[a]	
8	BC-86-8-TE	2.40	37.6	240.8	6.39	4.83	697 ± 38	23.3	Tenaya
9	BC-86-9-TE	2.44	37.5	240.8	6.56	4.65	839 ± 54	24.4	24.3 ± 0.9
10	BC-86-10-TE	2.33	37.9	240.8	6.14	4.38	469 ± 28	13.5[a]	
11	BC-86-11-TE	2.43	37.5	240.8	6.51	5.13	1951 ± 160	25.5	
12	BC87-1TA	2.34	37.5	240.8	6.15	4.88	1638 ± 211	55.9	
13	BC87-2TA	2.34	37.5	240.8	6.15	4.75	3763 ± 133	60.6	
14	BC87-3TA	2.37	37.5	240.8	6.25	4.46	1309 ± 87	38.6[a]	Younger
15	BC87-4TA	2.39	37.5	240.8	6.35	4.55	1461 ± 180	57.0	Tahoe
16	BC87-5TA	2.41	37.5	240.8	6.46	4.79	1699 ± 94	65.8	59.8 ± 4.5
17	BC88-1	2.34	37.5	240.8	6.15	3.87	315 ± 18	5.2	
18	BC88-5	2.34	37.5	240.8	6.15	5.47	1701 ± 162	63.2	

[a] indicates boulder ages that have not been used for calculations of mean moraine ages because of their position off the main clusters

Table 11. Locations, ELD factors, macroscopic cross sections, and ^{36}Cl ages for samples from Bloody Canyon, California.

Map number	Sample ID	Elevation km	Latitude	Longitude	ELD_n	$\Sigma\sigma_i N_i$ cm^2/kg	$^{36}Cl/Cl$ 10^{-15}	Boulder age ka	Moraine age ka
19	BC–86–12–TA	2.20	37.5	240.9	5.57	6.38	3155 ± 238	133[b]	Older
20	BC–86–13–TA	2.24	37.5	240.8	5.75	6.10	4313 ± 248	189[c]	Tahoe
21	BC–86–14–TA	2.24	37.5	240.8	5.75	4.84	5736 ± 256	214[c]	141 ± 11[b]
22	BC–86–15–TA	2.20	37.5	240.9	5.57	5.45	4211 ± 240	218[c]	207 ± 16[c]
23	BC–86–16–TA	2.21	37.5	240.8	5.63	6.04	2790 ± 197	149[b]	
24	SC86–17MB	2.29	37.9	240.8	5.96	4.73	3123 ± 223	114	
25	SC86–18MB	2.29	37.9	240.8	5.96	4.51	2001 ± 153	103	
26	SC86–19MB	2.41	37.9	240.8	6.49	5.07	1959 ± 122	92	Mono
27	SC86–20MB	2.41	37.9	240.1	6.48	4.70	5289 ± 178	79[a]	Basin
28	SC86–21MB	2.41	37.8	240.0	6.45	4.30	7031 ± 250	97	103 ± 11
29	SC88–1	2.38	37.9	240.8	6.34	5.23	2848 ± 62	93	
30	SC88–2	2.38	37.9	240.8	6.34	5.28	1916 ± 67	80[a]	
31	SC88–3	2.38	37.9	240.8	6.34	5.41	2266 ± 167	119	

[a] indicates boulder ages that have not been used for calculations of mean moraine ages because of their position off the main clusters
[b c] Older Tahoe may be interpreted as a composite moraine for which two distinct exposure ages were calculated

The ^{36}Cl ages are slightly older than the varnish ^{14}C ones probably because my samples were taken from the down-valley end of the moraine and therefore should indicate maximum of the Tioga glaciation. In addition, varnish ^{14}C ages are usually underestimated by about 5 % (Dorn, personal communication) because the basal varnish sample integrates carbon accumulated during the first 500–2000 years of exposure of the rock at the surface.

The Tenaya moraine, although morphologically distinct from the Tioga, is only 3,000 years older. The mean age of 24 ka place it together with the Tioga in the late Wisconsin. This is in line with conclusions of Burke and Birkeland (1979), who did not detect any major differences between the two, and combined them in a single unit, the Tioga. The slightly older age of the Tenaya crest can indicate an early advance of the Tioga glaciation, followed by recession,

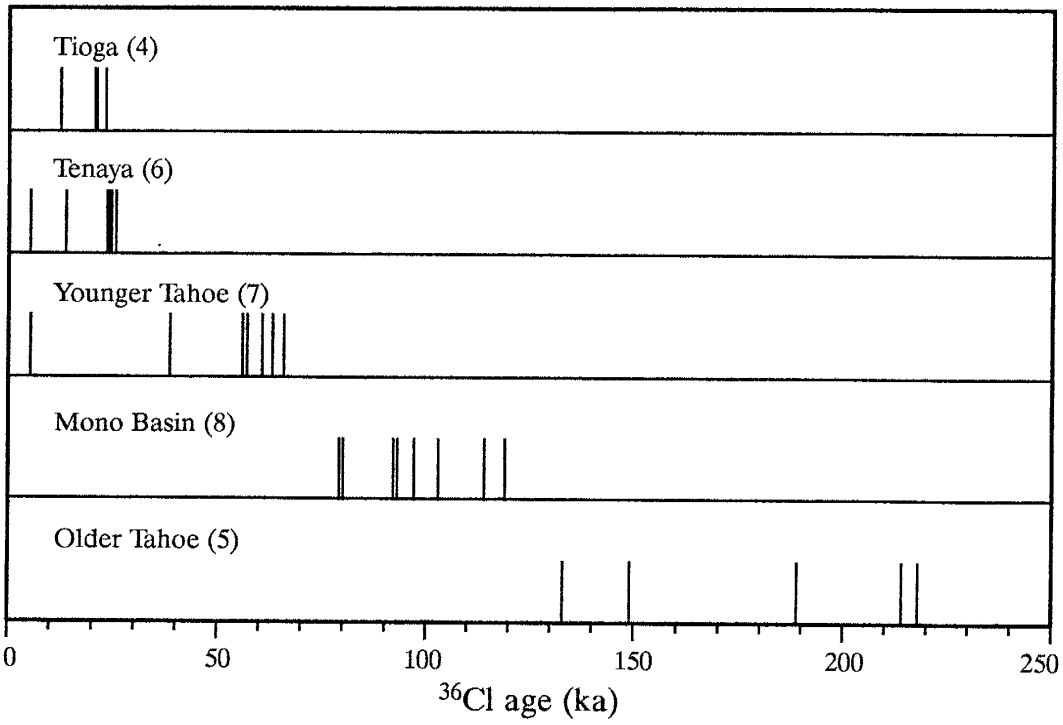

Fig. 7. Distribution of cosmogenic ^{36}Cl boulder ages among the moraines at Bloody Canyon. The ages were calculated using the production equation solved for the exposure time (p. 40). The numbers in parentheses indicate number of samples from each moraine.

and another advance 3,000 years later. There is a concern, however, that the Tenaya age may be affected by fire shattering because the Tenaya crest lies between the highly forested Tioga and Tahoe moraines, and might have experienced more forest fires than other moraines (Burke and Birkeland, 1979). Intense fire shattering could result in a bias toward anomalously young ages of analyzed rocks. In such a case one would expect data points scattered over the entire time interval since deposition of the moraine. However, four out of six Tenaya samples are clustered around 24 ka, with two younger outliers. This distribution, unless caused by coincidence, leads to a conclusion that the four 24 ka samples accurately represent the glacial event.

Based on the ^{36}Cl ages, the Tioga and Tenaya moraines of Sharp and Birman (1963) are grouped together and correlated with late Wisconsin. Late Wisconsin glacial deposits have been identified in all the glaciated mountain ranges in the western United States. The maximum occurred between 23 and 25 ka in Alaska, about 23 ka ago in Colorado, and 24 ka ago in Wyoming (Richmond and Fullerton, 1986) which correspond well with the ^{36}Cl dates presented in this study.

On the basis of the ^{36}Cl dates, the Tahoe moraine of Sharp and Birman (1963) was divided into an older and younger Tahoe (Phillips et al., 1990). The boulder dates for the younger Tahoe are clustered at 55–65 ka, whereas the older Tahoe dates group between 130 and 220 ka. In both cases two anomalously young rocks were sampled. Their young ages can be explained by the same factors that affected the young outliers at the Tenaya crest. The younger and older Tahoe dates are very distinct and there is no overlap between the maximum of the younger Tahoe (66 ka) and the minimum of the older Tahoe (133 ka). The Tahoe crest, although uniform morphologically, can thus be interpreted as a composite moraine. Sample BC–86–12–TA was obtained from

the main body of the older Tahoe and BC–86–16–TA from the terminal portion of the moraine. They both yielded ages close to 140 ka. On the other hand, boulders BC–86–13 through 15–TA were located close together on the outside part of the moraine. They all yielded ages older than the two former samples and are therefore interpreted as having recorded the inception of the older Tahoe glacial advance at about 200 ka. The two younger samples then indicate the culmination of the older Tahoe episode at about 140 ka. This subdivision closely resembles that proposed by Gillespie (1982) based on relative dating parameters. The younger Tahoe is correlative with the middle Wisconsin, whereas the older Tahoe corresponds to the Illinoian of the standard mid–continent stratigraphy. The older Tahoe till can be correlated with an early advance of the late Illinoian glaciation in Yellowstone Park, which is younger than 225 ka, and older than 174–183 ka (Richmond and Fullerton, 1986). The culmination of the older Tahoe can be correlated with "main" Tahoe of Dorn et al. (1987 and personal communication, 1989) at Pine Creek which was dated at 150 ka by varnish cation–ratio. The young Tahoe correlates well with revised varnish cation–ratio ages of 65 ka obtained at Pine Creek (Dorn, personal communication, 1989). It also correlates well with ice–dammed lake sediments in Yellowstone Park, which were deposited between 54 and 70 ka ago. Ages from 47 to 65 ka were reported for middle Wisconsin sediments from the Olympic Mountain and Puget lobe area, Washington, northeastern United States, and New England (Richmond and Fullerton, 1986 and references therein).

The Mono Basin boulder ages cluster in the range between 80 and 119 ka. The boulders on the Mono Basin moraine crests exhibit indications of advanced weathering and spalling (Phillips et al., 1990), which would result in removal of the original surface and thus in minimum ^{36}Cl ages. The most likely age for the Mono Basin moraine should then lie in the range 110–120 ka. The

scatter in calculated ages may also indicate that the Mono Basin moraine is a product of multiple glaciations which occurred between 80 and 120 ka (cf. Gillespie, 1982; Gillespie et al., 1984). There is some evidence from moraine morphology to support this interpretation (Phillips et al., 1990). The Mono Basin moraine was deposited between the younger and older Tahoe and is correlative with the early Wisconsin. This age corresponds well with the maximum limiting age of 119 ka (Gillespie et al., 1984) obtained for a basalt flow between two tills at Sawmill Canyon (near Independence, California). That lower till, however, was described by this author as the pre–Tahoe rather than the Mono Basin. There is a well documented early Wisconsin glaciation in Yellowstone Park bracketed by ages of 131 and 106 ka, with the glacial maximum at 117 ka (Richmond and Fullerton, 1986). A later glacial advance is bracketed by ages 102 and 80 ka with the maximum at 90 ka. The ^{36}Cl ages fit well in either of the two ranges; therefore, it is possible that the two younger samples can actually represent a later advance of the early Wisconsin glaciation.

On the global correlation scale the time intervals represented by glacial deposits correlate with the 'cold' marine isotope stages (Emiliani 1964; Martinson et al., 1987) and with periods of low insolation (Brouwer and van Woerkem, 1953; Berger 1978, 1984). The marine ^{18}O record exhibits important positive anomalies at 20, 60–70, 100–120, and 220–230 ka, and minimum insolation values are at 26, 70, 120, and 230 ka. Both are in excellent agreement with the ^{36}Cl ages of the Tioga/Tenaya, younger Tahoe, Mono Basin, and older Tahoe dates obtained in this study.

The calculated exposure ages exhibit interesting characteristics. The samples from the young moraines are fairly tightly clustered with little scatter, whereas the older samples are progressively more scattered (Fig. 7). This pattern can be explained by examining the factors that may alter the measured val-

ues from that given by hypothetical accurate analysis on a rock that perfectly conforms to the exposure–age model:

2. *Analytical errors* would cause an approximately random distribution of sample ages from a single moraine. This error is probably responsible for scatter of data points for the younger moraines, and becomes progressively less significant with age.

3. *Chlorine–36 inherited from a previous exposure history* will show up as anomalously old samples and can be easily detected for young rocks if a suite of 5 or more samples is analyzed. This kind of error can pass undetected for older rocks with large scatter due to other factors.

4. *Preferential leaching of ^{36}Cl compared to stable Cl* would produce bias towards younger ages. The process of leaching is difficult to evaluate quantitatively. It seems likely to become progressively more important with increasing age of the landform, especially in humid climates and for porous rocks and sediments. Most rocks described in this study are granites with porosity about 0.5%, sampled in a semiarid climate. We find no correlation between moraine age and chlorine concentration. Therefore, the leaching of chlorine is probably negligible, and should not affect the calculated ages. Preliminary studies we have conducted on effects of weathering on retention of ^{36}Cl support the assumption that leaching should be negligible in arid climate and thus should not introduce a large uncertainty in the final age determination.

5. *Spalling, shattering, or erosion of the rock surface* will change rock geometry by removing the top layer and exposing new surfaces to the cosmic rays. The calculated ages would underestimate true exposure times. These are continuous processes and they can be expected to have stronger effect on older sam-

ples and to be negligible for the younger ones. The correct sampling technique is absolutely essential for minimizing this error.

6. *Gradual exposure of the rock due to moraine crest denudation* will give ages that underestimate the true age of the moraine. In this study, a few young outliers in each moraine could be attributed to this factor. The gradual exposure can be inferred independently from weathering characteristics of the rock surface.

7. *Snow cover* can attenuate cosmic rays and lower production rates of cosmogenic isotopes. This process produces bias towards younger ages unless appropriate corrections are applied. In this study snow cover is probably not a significant influence because the samples were collected from relatively snow–free surfaces on tops of large boulders.

In summary, for young moraines (such as the Tioga and Tenaya) the boulder ages show an approximately normal distribution due to analytical errors, but as the moraines grow older this distribution becomes skewed towards ages younger than the age of the landform. Similarly, ages of the younger moraines are more compactly clustered, whereas the older ones are more scattered. For these older moraines a value close to the maximum age rather than the average may give the best estimate of the true age of the landform. However, the older surfaces are more likely to had been exposed to the cosmic radiation prior to glacial deposition and thus yield ages that are older than the true age of the moraine. At this point it is practically impossible to quantify the two sources of variation: previous exposure and erosion processes. One has to use a second nuclide, with significantly different half–life than that of ^{36}Cl. Likely candidates include radioactive ^{10}Be and ^{26}Al (Nishiizumi et al., 1989) and stable ^{3}He (Kurz, 1986).

4.5. Preliminary remarks on paleoclimatic implications of the new ^{36}Cl chronology

Establishment of correlation between glaciations and the global climate changes has been attempted for the past three decades. One commonly accepted model, first proposed by Milankovitch (1941), is based on the cyclic changes in the intensity and the distribution of solar radiation over the Earth. These changes are driven by astronomical factors: tilt of the earth's axis (period 41 ka), the shape of the earth's orbit (period 100 ka), and precession of the earth's spin axis (period 23 ka). Similar periodicities were found in the globally synchronous ^{18}O record of deep sea sediments (Emiliani, 1950; Imbrie et al., 1984; Shackleton, 1987). The classical Milankovich theory fails to provide explanation for the global extent of glacial events. It also cannot explain synchroneity of the glacial events on both hemispheres and rapid transitions from full glacial to full interglacial conditions (Broecker and Denton, 1989). It is likely that no single physical process can be responsible for severe climate changes during the Pleistocene. Instead, a number of external (orbital) and internal (atmospheric) processes have to act in accord in order to cause major reorganizations of the earth's atmosphere and hydrosphere (Broecker and Denton, 1989; Schneider and Thompson, 1979). Fingerprints of these interactions can be found in marine and terrestrial glacial deposits. It is essential that precise chronologies for these sediments be established in order to estimate extent, timing, and duration of the Pleistocene glacial events.

The basic glacial chronology is derived from the marine ^{18}O record (Imbrie et al., 1984). The same record is commonly used as an indicator of the global ice volume. However, this is based on the oversimplified assumptions that the mean ^{18}O composition of glacier ice is independent on ice sheet size and loca-

tion. Actually, the isotopic composition of foraminifera is a non-linear function of ice volume and it may thus misrepresent the true amplitude of the ice-volume signal and lag the true ice volume by a few thousands of years (Mix and Ruddiman, 1984). This lag may be further increased by buffering properties of the global ocean system due to its large size. In addition, the marine isotopic record integrates global ice-volume changes and therefore cannot serve as an indicator of climate variations in a given region (Porter, 1989).

Terrestrial glacial sediments are more robust indicators of timing, duration, and extent of the glaciations and the critical information lies in their chronologies. These sediments are, in general, not amenable to the standard relative and absolute dating techniques. Only recently has this chronological control become possible by direct dating of glacial moraines using the cosmogenic nuclide buildup and the varnish/cation ratio methods. The new ^{36}Cl chronology of glacial moraines at Bloody Canyon strongly supports synchroneity of glacial events in the Sierra Nevada with both the global glacial indications of the marine ^{18}O record (Emiliani, 1950; Emiliani 1964; Imbrie et al., 1984; Martinson et al., 1987; Shackleton, 1987) and with minima in summer insolation (Brouwer and van Woerkem, 1953; Berger 1978, 1984). However, we found an inverse relationship between the glacial magnitudes indicated by the marine ^{18}O and glacial ^{36}Cl records (Phillips et al., 1990). The marine record shows a progressive buildup of continental ice sheets from the previous interglacial through the last glacial maximum, whereas at Bloody Canyon the earlier mountain glaciers were the most extensive (Fig. 8.). In addition, the ^{36}Cl dates show a rapid transition from full interglacial to full glacial conditions which is in conflict with much slower changes in the marine ^{18}O record. This discrepancy may indicate that small mountain glaciers, in contrast to continental ice

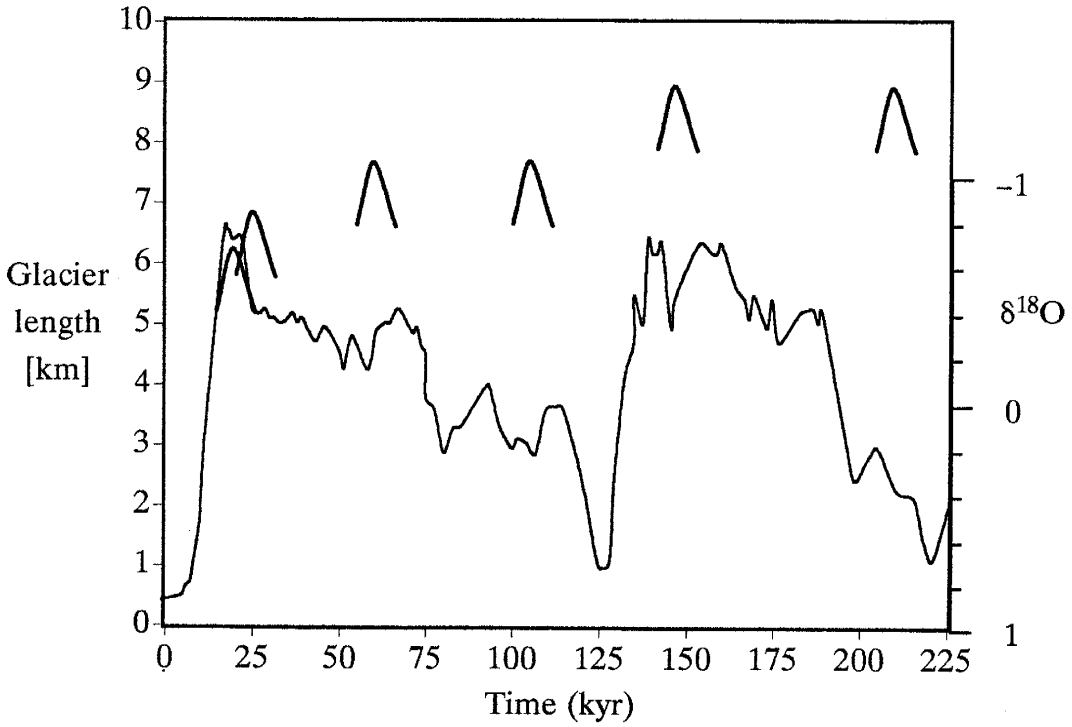

Fig. 8. A comparison of Bloody Canyon glacier lengths with the marine $\delta^{18}O$ record (after Martinson et al., 1987). The glacier lengths were measured from the cirque to the terminal moraine. The Bloody Canyon glacial maxima are indicated by the heavy, discontinuous lines and the marine $\delta^{18}O$ by the light line. The scale on the normalized $\delta^{18}O$ has been reversed from Martinson et al. (1987) so that glacial maxima correspond to the top of the graph for both records.

sheets, responded rapidly (without time lag) and linearly to abrupt changes of mode in the global ocean and atmosphere circulation. Further studies should therefore be concentrated on mountain glacial deposits which have potential to provide additional information on changes of the global climate in the past and aid predictions for the future.

4.6. Summary and conclusions

A chronology has been established for glacial moraines at Bloody Canyon, California, by direct dating of morainal boulders using the cosmogenic ^{36}Cl method. The ^{36}Cl accumulation indicates glaciations at about 21 ka, 24 ka, 55–65 ka, 95–115 ka, 130–150 ka and 190–220 ka. In the proposed glacial

chronology the Tenaya is grouped with Tioga and correlated with the late Wisconsin. The Tahoe is subdivided into the older and younger glaciations, with the Mono Basin placed between them. Thus, the term 'Tahoe Glaciation' is confusing and should be either abandoned or limited to the early Wisconsin glacial stage (the younger Tahoe).

The timing of the glaciations correlates well with peaks of the marine ^{18}O record and minima in the summer insolation curve. The relative magnitudes of the glacial intensity in the marine ^{18}O and terrestrial ^{36}Cl records, however, are different. This discrepancy may indicate that mountain glaciers responded more rapidly and linearly than continental ice sheets to global climatic changes.

More work needs to be done in other drainages of the eastern Sierra Nevada in order to resolve the problem of correlation of glacial events. There were very possibly more than 4 major advances during the last 200 ka. Until now, they could not be easily distinguished from each other because of lack of chronologic control. The limiting ages of associated volcanic rocks often left more than ample room for interpretations. Direct dating of glacial landforms by using the cosmogenic ^{36}Cl method should provide more accurate dates and should lead to better understanding of glacial geology and stratigraphy and of the past climatic conditions.

5. *Cosmogenic ^{36}Cl age of Meteor Crater, Arizona*

5.1. Introduction

Impact craters are uncommon at the earth's surface because its dynamic nature relatively quickly erases the evidence of most older impacts; only about 120 such structures are recognized. The impact structures are characterized by a circular form, structural disturbance at the surface, and presence of shock–metamorphosed minerals. They provide information on the characteristics of impact bodies, on metamorphic changes produced by the passage of the shock wave, and on cratering rate (Grieve, 1987). Some of the largest impacts have played an important role in the earth's evolution. It is believed that large–scale impacts have the potential to be responsible for major reorganizations in the earth's climatological and biological conditions. However, the evidence to date is inconclusive and the problem of the great mass extinctions still remains open.

Meteor Crater is a simple, bowl–shaped crater located in north–central Arizona near the southern edge of the Colorado Plateau (Fig. 9). The impact resulted in an uplifted rim area covered by fallout ejecta. Before the impact, the area was virtually flat with a regional slope of 0.5° to the northeast (Roddy, 1978) which reflects the underlying structure. The upper part of the stratigraphic sequence consists of 8.5 m of Triassic Moenkopi formation overlying 80 m of Permian Kaibab formation. The Moenkopi formation is formed of thin to massive bedded sandstone and siltstone with calcareous cements. The Kaibab unit consists of thin to medium bedded quartz dolomite and dolomitic sandstone. Beneath the two top formations there is a 1000–m thick sequence of Mesozoic and Paleozoic sedimentary rocks which overlies a Precambrian

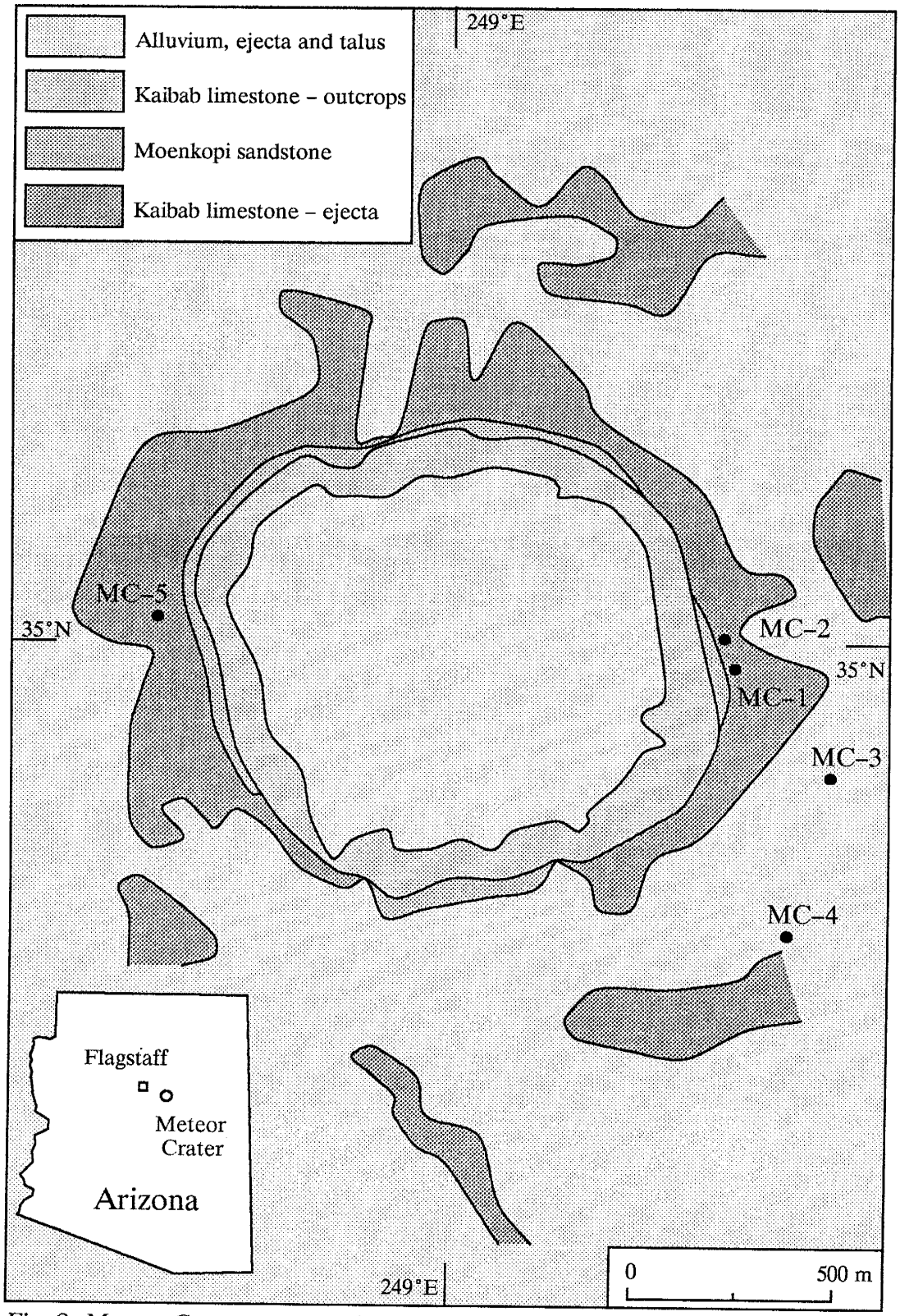

Fig. 9. Meteor Crater area (modified from Schoemaker, 1987). Locations for individual boulders are indicated by dots and sample names. The Kaibab formation was originally covered by 8.5 m layer of the Moenkopi sandstone.

crystalline basement (Roddy, 1978). The impact formed a 170–m deep crater and exposed dolomites of the Kaibab formation at the surface of the earth. Therefore, these rocks should be a model case study for the cosmogenic ^{36}Cl method as they perfectly meet the requirement of complete shielding followed by sudden exposure to cosmic radiation.

Meteor Crater is one of the youngest and best preserved impact craters at the surface of the earth. The age of the impact is uncertain. Schoemaker estimated that the impact took place between 20 and 30 ka ago. This age is based on soil development on the ejecta blanket (Schoemaker, 1960), geological correlations with ^{14}C dated exposures in the Hopi Buttes region 80 km northeast (Roddy, 1978), and stratigraphy of sediments within the crater and their correlation with radiometrically dated $\delta^{18}O$ maxima (Schoemaker, 1983). However, thermoluminescence studies on ejected dolomites and sandstones (Sutton, 1985) indicated an age of 49 ka. This date is also supported by "dead varnish radiocarbon" obtained by Dorn (Phillips et al., in preparation). The correct estimate of the time of impact is important for determining cratering rate (or rate of meteorite bombardment).

5.2. The ^{36}Cl dating

F. Phillips and S. Smith collected five samples (MC 1 through 5) from the tops of the tallest (1.3 to 12 m tall) dolomitic boulders ejected from the crater and deposited at the surrounding rim. The original ejecta blanket was about 2 m thick (Roddy, 1987, personal communication cited by Smith, 1988) which was less than the heights of the tallest boulders. The shorter boulders might have been covered by fine–grained material for a short period of time and then swept free of this material by wind (cf. Smith, 1988).

The samples were analyzed for ^{36}Cl, major elements, Cl, rare earth elements, and boron (Table 12). Total chlorine was determined by XRF fluorescence on pressed pellets. This technique was adequate in this case because of sufficiently high chlorine content of the samples (130–270 ppm). The other measurements were performed as described in Chapter 2.

We calculated the exposure time (Table 13) of the ejected boulders using the production equation solved for time (Chapter 4.3.3.). The mean age of 50.8 ± 6.5 ka is in excellent agreement with the thermoluminescence age of 49 ± 3 ka (Sutton, 1985) obtained from shock–metamorphosed quartz and dolomite (Fig. 10). Varnish–^{14}C study performed on the same material yielded "dead radiocarbon" (Phillips et al., in preparation) which also supports our results; low activity of ^{14}C results from decay rather than from contamination by ancient carbonate carbon. An interesting feature of the calculated ages is that four out of five samples are clustered around 54 ka, whereas one sample (MC–2) is significantly younger. The standard deviations of the mean of the four samples is smaller than analytical uncertainty of the individual AMS measurements. The younger sample can thus be interpreted as being partially shielded by loose material for time longer than the other samples or as having rolled over. Although there is no independent field evidence confirming either of the two hypotheses, the separation of the age of MC–2 from the mean of the other four by approximately 10 standard deviations argues strongly that the low value for MC–2 is not an analytical artifact. For practical purposes of calculating meteorite impact rates the two means are not significantly different.

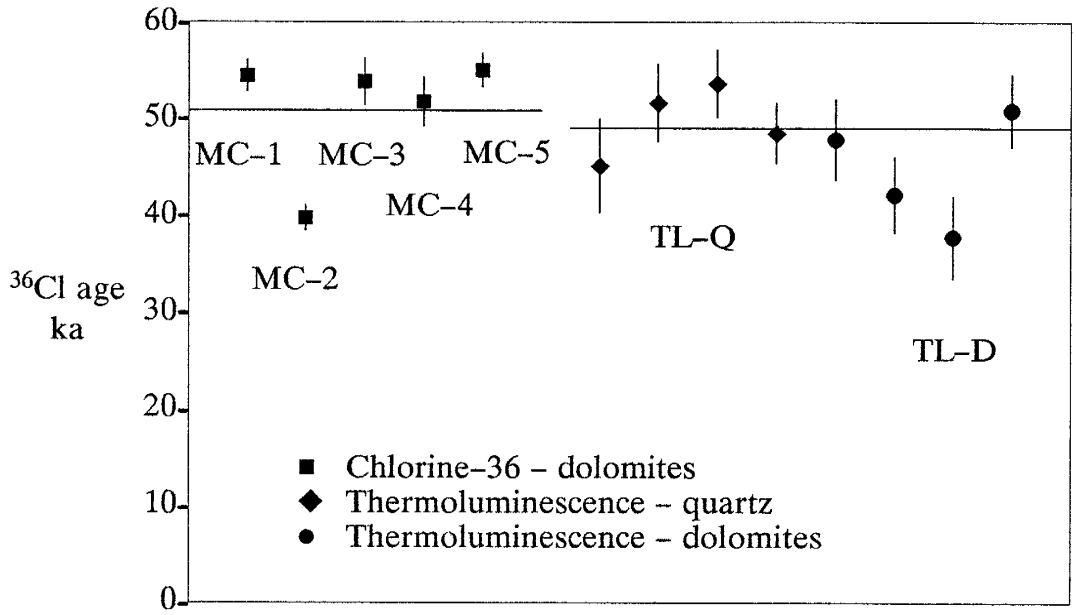

Fig. 10. Age distribution for Meteor Crater samples. Average ^{36}Cl age of all 5 samples is 50.8 ± 6.5 ka, whereas mean age of the 4 oldest samples is 53.7 ± 1.4 ka. Mean thermoluminescence age is 49 ± 3 ka, and varnish ^{14}C age > 50 ka (dead ^{14}C).

The consistency of the ^{36}Cl data shows that the cosmogenic ^{36}Cl dating method is particularly well suited for, although not limited to, dating sudden events like meteorite impacts, volcanic eruptions etc.

Table 12 *Chemical and isotopic data for ejected boulders at Meteor Crater, Arizona.*

Sample ID	SiO_2 [%]	TiO_2 [%]	Al_2O_3 [%]	Fe_2O_3 [%]	MgO [%]	CaO [%]	MnO [%]	Na_2O [%]	K_2O [%]	P_2O_5 [%]	LOI [%]	Cl [ppm]	B [ppm]	Gd [ppm]	$^{36}Cl/Cl$ [10^{-15}]
MC-1	28.78	0.13	2.52	0.33	17.16	21.13	0.05	0.16	0.47	0.23	26.18	143	3.5	0.2	1462 ± 44
MC-2	23.96	0.13	2.24	0.36	17.56	23.38	0.02	0.05	0.47	0.28	27.10	131	5.3	0.4	1194 ± 39
MC-3	10.74	0.15	2.38	0.73	19.36	29.21	0.07	0.11	0.43	0.39	25.84	217	5.8	0.3	1280 ± 57
MC-4	27.00	0.24	4.97	0.60	16.19	23.78	0.03	0.17	0.78	0.19	23.46	132	7.6	0.0	1469 ± 71
MC-5	12.95	0.14	2.20	0.61	18.84	28.16	0.10	0.13	0.44	0.48	27.80	259	1.7	0.3	1207 ± 38

Major elements and Cl were analyzed by XRF spectrometry, B and Gd by ICP-AE spectrometry, and ^{36}Cl by accelerator mass spectrometry (AMS).

Table 13 *Locations, ELD factors, macroscopic cross sections, and ^{36}Cl ages for samples from Meteor Crater, Arizona.*

Sample ID	Elevation [km]	Latitude	Longitude	ELD_n	$\Sigma\sigma_i N_i$ cm^2/kg	Boulder age [ka]
MC-1	1.55	35.0	249.0	3.44	2.28	54.4
MC-2	1.55	35.0	249.0	3.44	2.37	39.7
MC-3	1.55	35.0	249.0	3.44	2.65	53.8
MC-4	1.55	35.0	249.0	3.44	2.73	51.7
MC-5	1.55	35.0	249.0	3.44	2.50	55.0
Mean age	-	-	-	-	-	50.8 ± 6.5 53.7 ± 1.4[a]

ELD_n was calculated using formulation of Lal (1990). See Chapter 3 for details.
[a] Sample MC-2 was not used for calculation of this mean age.

6. Conclusions

Looking at surface exposure dating from the perspective of the early 1990's, it is clear that the major advances in this field occurred during the last decade. One of the milestones in surface exposure dating was the development of accelerator mass spectrometry. This development lagged many years after the first ideas of using *in situ* cosmogenic nuclides had emerged and cosmogenic isotope studies were possible only due to joint efforts of physicists and geoscientists who made analyses at extremely low concentrations feasible.

Once measuring nuclide concentrations was no longer the major limitation for the *in situ* cosmogenic nuclide studies, scientists' attention was focused on estimating nuclide production rates. Two approaches have been attempted: (1) measurements of cosmogenic nuclide concentrations in terrestrial materials of known ages and (2) theoretical calculations based on the cosmic ray fluxes and reaction cross sections. In this study, the empirical approach was chosen and yielded time–integrated production rates.

The production rates of cosmogenic ^{36}Cl (as well as some constraining parameters) have been well established by this study. The chlorine research efforts should now be focused on applications rather than on the method development. However, there are still unsolved problems that should be addressed in the future. In the next few years, we need new geophysical data about time and space variations in the cosmic–ray flux and about space variations of nuclide productions in the earth's rocks.

Before the 1980's Quaternary geologists could not quantitatively and directly date terrestrial glacial sequences. Existing surface exposure methods yielded relative ages and did not permit quantitative interpretations. New

techniques of absolute surface exposure dating have demonstrated the potential to channel the interests of Quaternary geologists towards more quantitative analysis of glacial chronologies and conditions leading to their formation. To date, two complementary surface exposure dating techniques have been used to obtain valuable information about the past glacial conditions: (1) rock varnish methods (varnish ^{14}C and cation–ratio) and (2) cosmogenic ^{36}Cl. The varnish method is limited to relatively arid climates, whereas the chlorine method can be applied also under more humid conditions. Precise dating of terrestrial glacial moraines by using the cosmogenic ^{36}Cl method should allow establishment of numerical chronologies and paleoclimatic interpretations that are more reliable than similar interpretations based on correlation with global glacial indicators. This new approach to the old and controversial problem of local and global correlation of glaciations should stimulate further research in this field.

The newly developed cosmogenic ^{36}Cl dating technique has helped reach new horizons in understanding the latest geological history of the earth. The numerical output of the ^{36}Cl dating can itself be a goal or can be a tool for achieving other, higher goals by constituting input data in modelling of processes and conditions related to terrestrial glaciations. This higher goals, which should dominate in the future, include paleoclimatic interpretations and quantitative description of conditions that lead to glaciations. We believe that these goals can be achieved by using the surface exposure dating techniques together with other modelling efforts.

7. References

D.P. Adam, 1967, Late–Pleistocene and recent palynology in the Sierra Nevada, California, in: *Quaternary Palynology*, E.J. Cushing, H.E. Wright Jr., eds., 275–301, Yale University Press, New Haven, Connecticut.

J.N. Andrews, J.–Ch. Fontes, J.–L. Michelot and D. Elmore, 1986, In–situ neutron flux, ^{36}Cl production and groundwater evolution in crystalline rocks at Stripa, Sweden, *Earth and Planet. Sci. Lett.* 77, 49–58.

J.N. Andrews, S.N. Davis, J. Fabryka–Martin, J–Ch. Fontes, B.E. Lehmann, H.H. Loosli, J.–L. Michelot, H. Moser, B. Smith and M. Wolf, 1989, The *in situ* production of radioisotopes in rock matrices with particular reference to the Stripa granite, *Geochim. Cosmochim. Acta* 53, 1803–1815.

B.F. Atwater, D.P. Adam, J.P. Bradbury, R.M. Forester, R.K. Mark, W.R. Lettis, G.R. Fisher, K.W. Gobalet and S.W. Robinson, 1986, A fan dam for Tulare Lake, California, and implications for the Wisconsin glacial history of the Sierra Nevada, *Geol. Soc. Amer. Bull.* 97, 97–109.

P.J. Aruscavage and E.Y. Campbell, 1983, An ion–selective electrode method for determination of chlorine in geological materials, *Talanta* 30, 745–749.

S.B. Bachman, 1978, Pliocene–Pleistocene break–up of the Sierra Nevada–White–Inyo Mountains block and formation of Owens Valley, *Geology* 6, 461–463.

H.W. Bentley, F.M. Phillips and S.N. Davis, 1986, Chlorine–36 in the terrestrial environment, in: *Handbook of Environmental Isotope Geochemistry, Vol. 2, The Terrestrial Environment, B*, P. Fritz and J.–Ch. Fontes, eds., 427–480, Elsevier, New York.

A. L. Berger, 1978, Long–term variations of caloric insolation resulting from the earth's orbital elements, *Quaternary Res.* 9, 139–167.

A. Berger and P. Pestiaux, 1984, Accuracy and stability of the Quaternary terrestrial insolation, in *Milankovitch and Climate, Part 1*, A. Berger et al., eds., 83–111, D. Reidel.

H. Bilokon, G. Cini Castagnoli, A. Castellina, B. D'Ettore Piazzoli, G. Mannocchi, E. Meroni, P. Picchi and S. Vernetto, 1989, Flux of the vertical

negative muons stopping at depths 0.35–1000 hg/cm^2, *J. Geophys. Res.* 94, 12, 145–152.

P. W. Birkeland, R. M. Birke and A. L. Walker, 1980, Soils and subsurface rock–weathering features of Sherwin and pre–Sherwin glacial deposits, eastern Sierra Nevada, California, *Geol. Soc. Amer. Bull.* 91, 238–244.

E. Blackwelder, 1931, Pleistocene glaciation in the Sierra Nevada and Basin Ranges, *Geol. Soc. Amer. Bull.* 42, 865–922.

W.S. Broecker and G.H. Denton, 1989, The role of ocean–atmosphere reorganizations in glacial cycles, *Geochim. Cosmochim. Acta* 53, 2465–2501.

J. Brouwer and A. J. J. van Woerkem, 1953, in *Climatic change*, Shapley, Harlow, ed., 318 p., Harvard Univ. Press, Cambridge, Massachusetts.

R.M. Burke and P.W. Birkeland, Reevaluation of multiparameter relative dating techniques and their application to the glacial sequences along the eastern escarpment of the Sierra Nevada, California, *Quaternary Res.* 11, 21–51; 1979.

The California Water Atlas, 1979, W.L. Kahrl, ed., 113 p., California Governor's Office.

T.E. Cerling, 1990, Dating geomorphic surfaces using cosmogenic ^{3}He, *Quaternary Res. 33, 148–156.*

S. Charalambus, 1971, Nuclear transmutations by negative stopped muons and the activity induced by the cosmic–ray muons, *Nucl. Phys.* A166, 145–161.

N.J. Conard, D. Elmore, P.W. Kubik, H.E. Gove, L.E. Tubbs, B.A. Chrunyk and M. Wahlen, 1986, The chemical preparation of AgCl for measuring ^{36}Cl in polar ice with accelerator mass spectrometry, *Radiocarbon* 28, 556–560.

M. Conversi, 1950, Experiments on cosmic–ray mesons and protons at several altitudes and latitudes, *Phys. Rev.* 79, 749–767.

G. B. Dalrymple, 1964, Potassium–argon dates of three Pleistocene interglacial basalt flows from the Sierra Nevada, California, *Geol. Soc. Amer. Bull.* 75, 753–758.

G. B. Dalrymple, R. M. Burke and P. W. Birkeland, 1982, Concerning K–Ar dating of a basalt flow from the Tahoe–Tioga interglaciation, Sawmill

Canyon, southeastern Sierra Nevada, California, *Quaternary Res.* 17, 120–122.

R. Davis, Jr. and O.A. Schaeffer, 1955, Chlorine–36 in nature, *Ann. N. Y. Acad. Sci.* 62, 105–122.

R.I. Dorn, B.D. Turrin, A.J.T. Jull, T.W. Linick and D.J. Donahue, 1987, Radiocarbon and cation–ratio ages for rock varnish on Tioga and Tahoe morainal boulders of Pine Creek, eastern Sierra Nevada, California, and their paleoclimatic implications, *Quaternary Research* 28, 38–49.

R.I. Dorn, A.J.T. Jull, D.J. Donahue, T.W. Linick and L.J. Toolin, Latest Pleistocene lake shorelines and glacial chronology in the western Basin and Range province, USA: Insights from AMS radiocarbon dating of rock varnish and paleoclimatic implications, *Palaeogeogr., Palaeoclimat., Palaeoecol.*, In press.

R.I. Dorn, A.J.T. Jull, D.J. Donahue, T.W. Linick and L.J. Toolin, 1989, Accelerator mass spectrometry radiocarbon dating of rock varnish, *Geol. Soc. Amer. Bull.* 101, 1363–1372.

D.L. Elliott–Fisk, 1987, Glacial geomorphology of the White Mountains, California and Nevada: establishment of glacial chronology, *Phys. Geogr.* 8, 299–323.

D. Elmore, B.R. Fulton, M.R. Clover, J.R. Marsden, H.E. Gove, H. Naylor, K.H. Purser, L.R. Kilius, R.P. Beukins and A.E. Litherland, 1979, Analysis of ^{36}Cl in environmental water samples using an electrostatic accelerator, *Nature* 277, 22–25.

D. Elmore and F.M. Phillips, 1987, Accelerator mass spectrometry for measurements of long–lived radioisotopes, *Science* 236, 543–550.

H.N. Elsheimer, 1987, Application of an ion–selective electrode method to the determination of chloride in 41 international geochemical reference materials, *Geostandards Newsletter* 11, 115–122.

C. Emiliani, 1955, Pleistocene temperatures, *J. Geol.* 63, 538–578.

C. Emiliani, 1964, Paleotemperature analysis of the Caribbean cores A254–BR–C and CP–28, *Geol. Soc. Amer. Bull.* 75, 129–144.

J.T. Fabryka–Martin, 1988, Production of radionuclides in the earth and their hydrogeologic significance, with emphasis on chlorine–36 and iodine–129, 400 p., Ph.D. dissertation, University of Arizona.

Y. Feige, B.G. Oltman and J. Kastner, 1968, Production rates of neutrons in soils due to natural radioactivity, *J. Geophys. Res.* 73, 3135–3142.

C. Feldman, 1961, Evaporation of boron from acid solutions and residues, *Anal. Chem.* 33, 1916–1920.

D.S. Fullerton, 1986, Chronology and correlation of glacial deposits in the Sierra Nevada, California, in: *Quaternary Glaciations in the Northern Hemisphere–Report of the International Geological Correlation Programme Project 24*, V. Sibrava, D.Q. Bowen and G.M.Richmond, eds., 161–169, Pergamon Press.

A.R. Gillespie, 1982, Quaternary glaciation and tectonism in the southern Sierra Nevada, Inyo County, California, 695 p., Ph.D. dissertation, California Institute of Technology.

A.R. Gillespie, J.C. Huneke and G.J. Wasserburg, 1984, Eruption age of a ~ 100,000–year–old basalt from ^{40}Ar–^{39}Ar analysis of partially degassed xenoliths, *J. Geoph. Res.* 89, 1033–1048.

R.A.F. Grieve, 1987, Terrestrial impact structures, *Ann. Rev. Earth Planet. Sci.*, 15, 245–270.

G. R. Hallberg, 1986, Pre–Wisconsin glacial stratigraphy of the Central Plains region in Iowa, Nebraska, Kansas, and Missouri, in *Quaternary Glaciations in the Northern Hemisphere–Report of the International Geological Correlation Programme Project 24*, V. Sibrava, D.Q. Bowen and G.M.Richmond, eds., 11–15, Pergamon Press.

Handbook of Chemistry and Physics (CRC), 1980, R.C. Weast, ed., B249–342.

L.D. Hendrick and R.D. Edge, 1966, Cosmic–ray neutrons near the earth, *Phys. Rev.* 145, 1023–1025.

J. Imbrie, J. D. Hays, D. Martinson, A. McIntyre, A. Mix, J. Morley, N. Pisias, W. Prell and N. J. Shackleton, 1984, The orbital theory of Pleistocene climate: support from a revised chronology of the marine $\delta^{18}O$ record, in *Milankovitch and Climate, Part 1*, A. L. Berger et al., eds., 269–305, D. Reidel.

R. Jha and D. Lal, 1982, On cosmic ray produced isotopes in surface rocks, in: *Natural Radiation Environment*, K.G. Vohra et al., eds., Proc. Second Special Symp. on Natural Radiation Environment, 629–635, Halsted Press, .

M.W. Kuhn, S.N. Davis, H.W. Bentley and R. Zito, 1984, Measurements of thermal neutrons in the subsurface, *Geophys. Res. Lett.* 11, 607–610.

M.D. Kurz, 1986, Cosmogenic helium in a terrestrial igneous rock, *Nature* 320, 435–439.

D. Lal, 1987a, Cosmogenic nuclides produced *in situ* in terrestrial solids, *Nucl. Inst. Meth. Phys. Res.* B29, 238–245.

D. Lal, 1987b, Production of ^{3}He in terrestrial rocks, *Chem. Geol. (Isotope Geosc. Section)* 66, 89–98.

D. Lal and B. Peters, 1967, Cosmic ray produced radioactivity on earth, in: Encyclopedia of Physics, S. Fluegge, ed., Vol. 46/2, Cosmic Rays II, K. Sitte, ed., 551–612, Springer–Verlag, Berlin.

B.D. Leavy, 1987, Surface–exposure dating of young volcanic rocks using the *in situ* buildup of cosmogenic isotopes, 197 p., Ph.D. dissertation, Department of Geosciences, New Mexico Institute of Mining and Technology, Socorro, New Mexico.

L.K. Lebetkin, 1980, Late Quaternary activity along the Lone Pine fault, Owens Valley fault zone, California, 85 p., thesis, Stanford University.

E.S. Light, M. Merker, H.J. Verschell, R.B. Mendell and S.A. Korff, Time dependent world–wide distribution of atmospheric neutrons and of their products, 2. Calculation, *J. Geophys. Res.* 78, 2741–2762, 1973.

R.E. Lingenfelter, 1963, Production of carbon–14 by cosmic–ray neutrons, *Rev. Geophys.* 1, 35–55.

S.J. Martel, T.M. Harrison and A.R. Gillespie, 1987, Late Quaternary vertical displacement rate across the Fish Springs Fault, Owens Valley Fault Zone,California, *Quaternary Research* 27, 113–129.

D. G. Martinson, N. G. Pisias, J. D. Hays, J. Imbrie, T. C. Moore, Jr. and N.J. Shackleton, 1987, Age dating and the orbital theory of the ice ages: Development of a high–resolution 0 to 300,000–yr chronostratigraphy, *Quaternary Res.* 27, 1–29.

M. Merker, E.S. Light, H.J. Verschell, R.B. Mendell and S.A. Korff, 1973, Time dependent world–wide distribution of atmospheric neutrons and of their products, 1. Fast neutron observations, *J. Geophys. Res.* 78, 2727–2740.

L. Mezger and D. Burbank, The glacial history of the Cottonwood Lakes area, southeastern Sierra Nevada, *Geol. Soc. Amer. Abstract with Programs* 18, 157, 1986.

N. M. Milankovitch, 1941, Canon of insolation and the ice–age problem, *Koniglich Serbische Akademie, Beograd* (English translation by the Israel Program for Scientific Translation), U.S. Dept. of Commerce and Nat. Sci. Fdn., Washington, D.C.

A.C. Mix and W.F. Ruddiman, 1984, Oxygen–isotope analyses and Pleistocene ice volumes, *Quaternary Research* 21, 1–20.

C.G. Montgomery and D.D. Montgomery, 1939, The intensity of neutrons of thermal energy in the atmosphere at sea level, *Phys. Rev.* 56, 10–12.

H. Moraal, M.S. Potgieter, P.H. Stoker and A.J. van der Walt, 1989, Neutron monitor latitude survey of cosmic ray intensity during the 1986/1987 solar minimum, *J. Geophys. Res.* 94, 1459–1464.

S.F. Mughaghab and D.I. Garber, 1973, Neutron Cross Sections, Vol. 1, Resonance Parameters, Brookhaven National Laboratory.

L.L. Newkirk, 1963, Calculation of low–energy neutron flux in the atmosphere by the S_n method, *J. Geophys. Res.* 68, 1825–1833.

K. Nishiizumi, E.L. Winterer, C.P. Kohl, J. Klein, R. Middleton, D. Lal and J.R. Arnold, 1989, Cosmic ray production rates of ^{10}Be and ^{26}Al in quartz from glacially polished rocks, *J. Geoph. Res.* 94, 17,907–17,915.

K. O'Brien, H.A. Sandmeier, G.E. Hansen and J.E. Campbell, 1978, Cosmic ray induced neutron background sources and fluxes for geometries of air over water, ground, iron, and aluminum, *J. Geophys. Res.* 83, 114–120.

K. O'Brien, 1979, Secular variations in the production of cosmogenic isotopes in the earth's atmosphere, *J. Geophys. Res.* 84, 423–431.

C.G. Oviatt and W.P. Nash, 1989, Late Pleistocene basaltic ash and volcanic eruptions in the Bonneville basin, Utah, *Geol. Soc. Amer. Bull.* 101, 292–303.

F.M. Phillips, B.D. Leavy, N.D. Jannik, D. Elmore and P.W. Kubik, 1986, The accumulation of cosmogenic chlorine–36 in rocks: A method for surface exposure dating, *Science* 231, 41–43.

F.M. Phillips, M.G. Zreda, S.S. Smith, D. Elmore, P.W. Kubik, and P. Sharma, 1990, A cosmogenic chlorine–36 chronology for glacial deposits at

Bloody Canyon, Eastern Sierra Nevada, California, *Science* 248, 1529–1532.

S.C. Porter, 1979, Hawaiian glacial ages, *Quaternary Research* 12, 161–187.

S.C. Porter, 1989, Some geological implications of average Quaternary glacial conditions, *Quaternary Research* 32, 245–261.

J.J. Quenby and W.R. Weber, 1959, Cosmic ray cut–off rigidities and the earth's magnetic field, *Philos. Mag.* Eight Series, v. 4, 90–113.

Rama and M. Honda, 1961, Cosmic–ray–induced radioactivity in terrestrial materials, *J. Geophys. Res.* 66 (10), 3533–3539.

R.C. Reedy and J.R. Arnold, 1972, Interaction of solar and galactic cosmic–ray particles with the moon, *J. Geophys. Res.* 77, 537–555.

G.M. Richmond and D.S. Fullerton, 1986, Introduction to Quaternary glaciations in the United States of America, in: Quaternary Glaciations in the Northern Hemisphere–*Report of the International Geological Correlation Programme Project 24*, V. Sibrava, D.Q. Bowen and G.M.Richmond, eds., 3–10, Pergamon Press.

D.J. Roddy, 1978, Pre–impact geologic conditions, physical properties, energy calculations, meteorite and initial crater dimensions and orientations of joints, faults and walls at Meteor Crater, Arizona, *Proc. Lunar Planet. Sci. Conf.* 9^{th}, 3891–3930.

D.C. Rose, K.B. Fenton, J. Katzman and J.A. Simpson, 1956, Latitude effect of the cosmic ray nucleon and meson components at sea level from the Arctic to the Antarctic, *Canadian J. Phys.* 34, 968–984.

B. Rossi, 1952, High Energy Particles, 569 p., Prentice Hall, New Jersey.

S.H. Schneider and S.L. Thompson, 1979, Ice ages and orbital variations: some simple theory and modelling, *Quaternary Research* 12, 188–203.

E.M. Schoemaker, 1960, Penetration mechanics of high velocity meteorites illustrated by Meteor Crater, Arizona, In: *Structure of the Earth's Crust and Deformation of Rocks*, Rept. 18, 418–434, Internat. Geol. Congr., XXI Session, Copenhagen.

E.M. Schoemaker, 1983, Asteroid and comet bombardment of the earth, *Annu. Rev. Earth Planet. Sci.*, 461–494.

E.M. Schoemaker, 1987, Meteor Crater, Arizona, *Geol. Soc. Amer. Centennial Field Guide – Rocky Mountain Section, 399–404.*

N. J. Shackleton, 1987, Oxygen isotopes, ice volume and sea level, *Quaternary Sci. Rev.* 6, 183–190.

R. P. Sharp, 1968, Sherwin Till – Bishop Tuff geological relationships, Sierra Nevada, California, *Geol. Soc. Amer. Bull.* 83, 2233–2260.

R.P. Sharp and J.H. Birman, 1963, Additions to classical sequence of Pleistocene glaciations, Sierra Nevada, California, *Geol. Soc. Amer. Bull.* 74, 1079–1086.

J.A. Simpson, 1951, Neutrons produced in the atmosphere by the cosmic radiations, *Phys. Rev.* 83, 1175–1188.

S. S. Smith, 1988, Cosmogenic ^{36}Cl research: chlorine extraction procedures and application of dating techniques at Meteor Crater, Arizona and Bloody Canyon, California, 154 p., New Mexico Institute of Mining and Technology.

J.R. Stehn, M.D. Goldberg, B.A. Magurno and R. Wiener–Chasman, 1964, Neutron Cross Sections, vol. 1, Z = 1 to 20, Brookhaven National Laboratory.

S.R. Sutton, 1985, Thermoluminescence measurements on shock–metamorphosed sandstone and dolomite from Meteor Crater, Arizona: 2. Thermoluminescence age of Meteor Crater, *J. Geophys. Res.* 90, 3690–3700.

C. Wahrhaftig and J. H. Birman, 1965, The Quaternary of the Pacific Mountain system in California, in *The Quaternary of the United States*, H. E. Wright, Jr. and D. G. Frey (eds.), 299–340, Princeton Univ. Press.

J.N. Walsh, 1985, Determination of boron at trace levels in rocks by inductively coupled plasma spectrometry, *Analyst* 110, 959–962.

J.N. Walsh, F. Buckley and J. Baker, 1981, The simultaneous determination of the rare–earth elements in rocks using inductively coupled plasma source spectrometry, *Chem. Geology* 33, 141–153.

A. Wyttenbach, P. Baertschi, S. Bajo, J. Hadermann, K. Junker, S. Katcoff, E.A. Hermes and H.S. Pruys, 1978, Probabilities of muon induced nuclear reactions involving charged particle emission, *Nucl. Phys.* A294, 278–292.

M. Yamashita, L.D. Stephens and H.W. Patterson, 1966, Cosmic–ray–produced neutrons at ground level: neutron production rate and flux distribution, *J. Geophys. Res.* 71, 3817–3834.

Y. Yokoyama, J.–L. Reyss and F. Guichard, 1977, Production of radionuclides by cosmic rays at mountain altitudes, *Earth Planet. Sci. Lett.* 36, 44–50.

M.G. Zreda, F.M. Phillips, D. Elmore, P.W. Kubik and P. Sharma, 1990, Cosmogenic chlorine–36 production rates in terrestrial rocks, Submitted to *Earth Planet. Sci. Lett.*

8. Appendices

8.1. PASCAL program for exposure age calculation

```
{cl1.pas with modified EL correction factor after Lal (personal communication,1989)}
{the program is interactive, i.e. the user is always prompted for input of parameters/variables}
{the program will run on MS-DOS computers; neither graphics card nor math coprocessor are}
{necessary, however, if present, they may improve performance or/and screen output effects}

type DateStr = string[10];

functionDate: DateStr;   { reads date from the operating system }
type regpack = record
                 ax,bx,cx,dx,bp,si,di,ds,es,flags: integer;
               end;

var  recpack:regpack;                {record for MsDos call}
     month,day: string[2];
     year:string[4];
     dx,cx: integer;

begin
  with recpack do
  begin
    ax := $2a shl 8;
  end;
  MsDos(recpack);                    { call function }
  with recpack do
  begin
   str(cx,year);                   {convert to string}
   str(dx mod 256,day);                { " }
   str(dx shr 8,month);                { " }
  end;
  date := month + '/' + day + '/' + year;
end;

type TimeString = string[8];

function time: TimeString;           { reads time from the operating system }
type regpack = record
                 ax,bx,cx,dx,bp,si,di,ds,es,flags: integer;
               end;

var  recpack:      regpack;          {assign record}
     ah,al,ch,cl,dh:  byte;
     hour,min,sec:    string[2];

begin
  ah := $2c;                         {initialize correct registers}
  with recpack do
  begin
    ax := ah shl 8 + al;
  end;
  intr($21,recpack);                  {call interrupt}
  with recpack do
  begin
    str(cx shr 8,hour);               {convert to string}
    str(cx mod 256,min);                  { " }
    str(dx shr 8,sec);                  { " }
  end;
  if length(hour) = 1 then hour: = '0' + hour;
  if length(min) = 1 then min: = '0' + min;
```

```
  if length(sec)=1 then sec:='0'+sec;
  time := hour+':'+min+':'+sec;
end;

type s20 = string[70];
  {x1,y1,x2,y2 - widow coordinates
  c1 - head text color
  c2 - head background
  head - window head}

procedure Frame(x1, y1, x2, y2: Integer);          { draws input/output windows }
var  I : Integer;

begin {Frame}
  GotoXY(x1, y1);
  Write(chr(218));                                 { draws lines }
  for I := (x1 + 1) to (x2 - 1) do
  begin
    Write(chr(196));
  end;
    Write(chr(191));
  for I := (y1 + 1) to (y2 - 1) do
  begin
    GotoXY(x1 , I);  Write(chr(179));
    GotoXY(x2, I);  Write(chr(179));
  end;
  GotoXY(x1, y2);
    Write(chr(192));
  for I := (x1 + 1) to (x2 - 1) do
  begin
    Write(chr(196));
  end;
    Write(chr(217));
end; {Frame}

procedure makewindow(x1,y1,x2,y2,c1,c2:integer;head:s20); { makes windows }
var   v,k,l,i:integer;
      a1,a2,b1,b2:integer;
begin

  textcolor(c1);textbackground(c2);
  v:=length(head);
  k:=x2-x1;
  l:=round((k-v)/2 );
  if head <>'' then
  begin
    gotoxy(x1,y1);
    write(' ':l,head,' ':l);
  end;
  textcolor(c2);textbackground(c1);
  a1:=x1;a2:=y1+1;
  b1:=x2;b2:=y2+1;
  frame(a1,a2,b1,b2);
  window(x1+1,y1+2,x2-1,y2);
  clrscr;
end;

const  psiK:real=759.0;                { production rate due to spallation on K }
       psiCa:real=490.0;               { production rate due to spallation on Ca }
       fiN:real=2.64E5;                { thermal neutrons stopping rate }
       Rnot:real=10.9e-15;             { radiogenic chlorine-36 }
type brn1_type=record
                 v:real;               {input value (% of oxide)}
                 vb:real;              {barns from v %}
               end;
```

```
const major = 10;
type str80 = string[80];
type brnm_type = record
                   m:integer;          {mass of 1 mole of an element (g)}
                   e:string[2];        {element's symbol}
                   x:string[5];        {oxide formula}
                   b:real;             {thermal neutron absorption (barns)}
                   c:real;             {% of an element in an oxide}
                   at:byte;
                 end;

const brn1:array[1..major] of brn1_type =
    ((v:0.0;vb:0.0),
    (v:0.0;vb:0.0),
    (v:0.0;vb:0.0),
    (v:0.0;vb:0.0),
    (v:0.0;vb:0.0),
    (v:0.0;vb:0.0),
    (v:0.0;vb:0.0),
    (v:0.0;vb:0.0),
    (v:0.0;vb:0.0),
    (v:0.0;vb:0.0));

const brnm:array[1..major] of brnm_type =
    ((m:28;e:'Si';x:'SiO2 ';b:0.16;c:0.4667;at:1),
    (m:48;e:'Ti';x:'TiO2 ';b:6.1;c:0.6;at:1),
    (m:27;e:'Al';x:'Al2O3';b:0.23;c:0.5294;at:1),
    (m:56;e:'Fe';x:'Fe2O3';b:2.55;c:0.70;at:1),
    (m:24;e:'Mg';x:'MgO  ';b:0.063;c:0.6;at:1),
    (m:40;e:'Ca';x:'CaO  ';b:0.43;c:0.7143;at:1),
    (m:55;e:'Mn';x:'MnO  ';b:13.3;c:0.7746;at:1),
    (m:23;e:'Na';x:'Na2O ';b:0.53;c:0.7419;at:1),
    (m:39;e:'K';x:'K2O  ';b:2.1;c:0.8298;at:1),
    (m:31;e:'P';x:'P2O5 ';b:0.19;c:0.4366;at:1));

type brn2_type = record
                   e2:string[2];       {element's symbol}
                   b2:real;            {thermal neutron absorption x-section}
                 end;

const brn2:array[1..2] of brn2_type = ((e2:'O';b2:0.0002),
                                       (e2:'C';b2:0.0034));

const trace = 12;

type brn3_type = record
                   v3:real;            {input concentration (ppm)}
                   vb3:real            {barns from v3 ppm}
                 end;

type brnt_type = record
                   e3:string[2];       {element's symbol}
                   b3:real;            {thermal neutron abs. x-section (barns)}
                   m3:real;            {atomic mass of an element (mg)}
                 end;

const brn3:array[1..trace] of brn3_type =
    ((v3:0.0;vb3:0.0),
    (v3:0.0;vb3:0.0),
    (v3:0.0;vb3:0.0),
    (v3:0.0;vb3:0.0),
    (v3:0.0;vb3:0.0),
    (v3:0.0;vb3:0.0),
    (v3:0.0;vb3:0.0),
    (v3:0.0;vb3:0.0),
    (v3:0.0;vb3:0.0),
```

```
      (v3:0.0;vb3:0.0),
      (v3:0.0;vb3:0.0),
      (v3:0.0;vb3:0.0));

const brnt:array[1..trace] of brnt_type =
      ((e3:'Cl';b3:43;m3:35500.0),
      (e3:'B ';b3:759;m3:11000.0),
      (e3:'Ce';b3:0.63;m3:140000.0),
      (e3:'Pr';b3:0.00;m3:141000.0),
      (e3:'Nd';b3:50.5;m3:144000.0),
       (e3:'Sm';b3:5800.0;m3:150000.0),
      (e3:'Eu';b3:4600.0;m3:152000.0),
      (e3:'Gd';b3:49000.0;m3:157000.0),
      (e3:'Tb';b3:25.5;m3:159000.0),
      (e3:'Dy';b3:930;m3:162000.0),
      (e3:'Yb';b3:36.6;m3:173000.0),
      (e3:'Lu';b3:77;m3:175000.0));

type data = record
              name:string[12];
              brn1:array[1..major] of brn1_type;
              brn3:array[1..trace] of brn3_type;
              sigmaN:real;          { macroscopic absorption cross section }
              psiN:real;            { production of 36-Cl from 35-Cl }
              el,la,lo,de:real;     { elevation, latitude, longitude, depth }
              ELD1:real;            { ELD factor }
              Cl36:real;            { 36-Cl/Cl ratio in 10^-15 units }
              Cl36er:real;          { error on 36-Cl ratio }
              PR:real;              { total production of 36-Cl }
              nf:real;              { normalized 36-Cl }
              nfer:real;            { error on normalized 36-Cl }
            end;

const  AV = 6.022045E23;            { Avogadro number }
       max = 20;                    { maximum number of samples in one series }
var   o:text;                       { output device selector }
      avg:real;                     { dummy average }
      filnam:string[14];            { filename }
      rname:string[14];             { filename }
      fs:integer;                   { filesize }
      found:boolean;                { boolean selector }
      dta:array[0..max] of data;    { array of data records }
      filvar:file of data;          { file containing the data records }
      sd,mean,sum:real;             { statistical dummies }
      R:real;                       { ratio of 36Cl to Cl }
      PR,psi_n,sigmaN:real;         { production of 36Cl due to all reactions }
      CK,CCa,NCl,NClppm:real;       { CK, CCa - % oxide of K, Ca }
                                    { NCl - # of atoms of Cl }
                                    { NClppm - ppm of Cl }
      t,ter:real;                   { exposure time and standard error }
      tasdmin,tasdmax,tssdmin,tssdmax:real;
                                    { range of calculated exposure time for }
                                    { analytical (asd) and statistical (ssd) }
                                    { standard deviation }
      i,ii,j,k:integer;             { dummy loop counting variables }
      choice,c,ch:char;             { switch variables }
      sname:string[15];             { sample name }
      samname:array[1..max] of string[15];  { array of sample names }
      ele,lat,lon:real;             { elevation, latitude, longitude }
      spchar:char;                  { dummy switching variable }
      time1,time2,deltat:real;      { }
      error:integer;                { }

function p(base:real;exponent:integer):real;    {power function}
begin
  if exponent = 0 then p:= 1.0
```

```
  else if exponent = 1 then p: = base
  else p: = base*p(base,exponent-1);
end;

function glat(lat,long:real):real;                    { L correction factor }
const lat_0:real = 78.6; long_0:real = 290.0;         { lat_0 - magnetic pole latitude }
var sing,cosg:real;                                   { sine and cosine of geomagnetic latitude }
begin
  sing: = cos(lat_0*pi/180)*cos(lat*pi/180)*cos((long-long_0)*pi/180)
      + sin(lat_0*pi/180)*sin(lat*pi/180);
  cosg: = sqrt(1-sqr(sing));
  glat: = arctan(sing/cosg)*180/pi;                   { glat - geomagnetic latitude }
end; {glat}

function ELD(ele,lat,lon:real):real;                  { ELD factor }
const a:array[0..6,0..3] of real =                    { polynomial fit parameters }
        ((1.0486,0.81161,0.31213,6.5e-2),
        (1.0715,0.79948,0.3521,6.575e-2),
        (1.2116,0.86277,0.4201,7.872e-2),
        (1.4881,1.2513,0.3100,0.14968),
        (1.6667,1.6025,0.4503,0.18667),
        (1.7864,1.8649,0.54185,0.241386),
        (1.8109,1.97177,0.56215,0.25022));

var  x,y,y1:real;
     i,j:integer;
     g:real;
     gmod,gmod1:integer;
begin
  g: = glat(lat,lon);
    if g > = 60 then gmod: = 6 else gmod: = round(g) div 10;
    if g > = 60 then gmod1: = gmod else gmod1: = gmod + 1;
    if ele > 10 then ele: = ele/1000;
      y: =  a[gmod,0] + a[gmod,1]*ele + a[gmod,2]*ele*ele +
            a[gmod,3]*ele*ele*ele;
      y1: = a[gmod1,0] + a[gmod1,1]*ele + a[gmod1,2]*ele*ele +
            a[gmod1,3]*ele*ele*ele;
    y: = y/1.8109;
    y1: = y1/1.8109;
    ELD: = y + (y1-y)*(g-10*gmod)/10;
end; {ELD}

procedure coltextin(c:integer);                       { select text color }
begin
  textcolor(black);textbackground(c);
end;

procedure coltextoff;                                 { undo text color }
begin
  textcolor(yellow);textbackground(black);
end;

procedure windowoff;                                  { go back to full-screen window }
begin
  window(1,1,80,25);
end;

procedure tofile;                                     { write record to file on a disk }
begin
  windowoff;
  makewindow(5,19,35,22,black,yellow,' SAVING');
  buflen: = 12;write('Filename : ');readln(filnam);   { input mask }
  if filnam = '' then filnam: = 'PROD.DTA';
  assign(filvar,filnam);                              { assign file name }
    rewrite(filvar);                                  { write file }
  for i: = 1 to j do                                  { j = file size }
```

```
    write(filvar,dta[i]);
  if filesize(filvar)=0 then erase(filvar);
  close(filvar);                                    { close file variable }
  coltextoff;
  windowoff;
end; {tofile}

procedure readdata;                                 { reads record from a disk }
begin
  clrscr;                                           { clears screen }
  makewindow(1,1,30,20,black,yellow,'READING');     {set up window }
  write('Filename : ');
  {$I-}                                             { turn off I/O checking }
  repeat                                            { input file name }
    gotoxy(12,1);
    clreol;
    read(filnam);
    if filnam='' then filnam:='PROD.DTA';
    assign(filvar,filnam);
    reset(filvar);
  until ioresult=0;                                 { until input iscorrect }
  {$I+}                                             { turn on I/O checking }
  writeln;
  fs:=filesize(filvar);                             { # of samples in the file }
  j:=fs;
  for i:=1 to j do read(filvar,dta[i]);             { read content of the file }
  close(filvar);
  writeln;
  writeln(fs,' samples have been read :');
  writeln;
  for i:=1 to fs do writeln(dta[i].name);
  windowoff;
end;

procedure input(k:byte);                            { input data }
label 10;
begin
  makewindow(30,2,78,20,yellow,black,'INPUT OF DATA');
  j:=k;
  repeat
    j:=j+1;
    with dta[j] do                                  { dta[j] is the record containing all data }
    begin
      write('Name : ');readln(name);if name='' then goto 10; { sample name }
      for k:=1 to length(name) do name[k]:=upcase(name[k]); { in upper case letters}

      write('Elevation [m]          : ');readln(el);ele:=el;
      write('Latitude  [deg]        : ');readln(la);lat:=la;
      write('Longitude [deg to East] : ');readln(lo);lon:=lo;
      ELD1:=ELD(ele,lat,lon);
      writeln('Calculated ELD1=',ELD1);             { ELD1 equals ELD }

    write('36Cl [in 1E-15] =');read(Cl36);
      write(' ',chr(241),' ');readln(Cl36er);       { chr(241) is '±' sign in ASCII code }
      if Cl36>1 then Cl36:=Cl36*1E-15;
      if Cl36er>1 then Cl36er:=Cl36er*1E-15;

      sigmaN:=0.0;                                  { rock absorption cross section zeroed }
      writeln;writeln('Input major elements (% of sample) :');
      for i:=1 to major do
      with brn1[i] do
      begin
        write(brnm[i].x,':');
        readln(v);
          vb:=v*10*brnm[i].c/brnm[i].m*brnm[i].at*AV*brnm[i].b*1e-24;
                                                    { vb is absorption cross section for a given element }
```

```
        sigmaN:=sigmaN+vb;
      end;
      writeln;writeln('Input REE, B and Cl (ppm) :');
      for i:=1 to trace do
      with brn3[i] do
      begin
        write(brnt[i].e3,':');
        readln(v3);
          vb3:=v3/brnt[i].m3*AV*brnt[i].b3*1e-24;
        sigmaN:=sigmaN+vb3;
      end;
      writeln('sigmaN=',sigmaN);                { total absorption cross section of the sample }
      writeln(brnt[1].e3,'  ',brn3[1].v3);
      psiN:=fiN*43e-24*0.75*brn3[1].v3/35500.0*AV/sigmaN;
                                                { psiN = production from 35Cl at sea level }
      writeln('psiN=',psiN);
        PR:=ELD1*(psiK*brn1[9].v+psica*brn1[6].v+psiN)/brn3[1].v3/35500.0*AV;
                                                { total production at a given elevation }
      writeln('PR=',PR);
    end;
    10:
  until dta[j].name='';                         { do input until sample name is <RETURN> }
  j:=j-1;
  windowoff;
  tofile;                                       { write the record to a file on a disk }
end;

procedure printdta(j:integer);                  { show an entire record for a single sample }
begin
  makewindow(1,1,80,22,black,white,dta[j].name);
  with dta[j] do
  begin
    for i:=1 to major do
    begin
      gotoxy(1,i);
      write(brnm[i].x,'  ',brn1[i].v);
    end;
    for i:=1 to trace do
    begin
      gotoxy(41,i);
      write(brnt[i].e3,'  ',brn3[i].v3);
    end;
    gotoxy(1,14);
    writeln('sigmaN   ',sigmaN,'          psiN   ',psiN);
    writeln('PR       ',PR);
    writeln('Cl36     ',Cl36,' ',chr(241),' ',Cl36er);
    writeln('Elevation ',el);
    writeln('Latitude  ',la);
    writeln('Longitude ',lo);
    write('ELD1     ',ELD1);
  end;
  windowoff;
end;

procedure add;                                  { add sample to existing file }
begin
  clrscr;
  makewindow(1,15,27,20,black,white,'ADD ANOTHER FIELD');
  writeln('Filesize=',j);
  windowoff;
  input(fs);
end;

procedure del;                                  { delete sample from file }
var  nam:string[12];
     found1:boolean;
```

```
      c:char;
      i,l:integer;
begin
  clrscr;
  makewindow(1,1,30,12,black,yellow,'DELETE');
  write('Name to delete : ');
  found1:=false;
  repeat
    gotoxy(18,1);                                   { position of cursor }
    clreol;
    read(nam);                                      { read sample name to be deleted }
    for k:=1 to length(nam) do nam[k]:=upcase(nam[k]);
                                                    { convert name to upper case }
    i:=0;
    repeat
      i:=succ(i);
      found1:=(nam=dta[i].name);
    until found1 or (i=j);
  until found1 or (nam='');
  windowoff;
  if nam<>'' then  printdta(i)
  else
  begin
    exit
  end;
  lowvideo;                                         { lower screen intensity }
  gotoxy(50,20);
  write('Delete ',dta[i].name,' (y/n) ?');
  normvideo;                                        { normal screen intensity }
  repeat                                            { keep making choice }
    read(kbd,c);
    c:=upcase(c);
  until c in ['Y','N'];                             { until choice is made }
  writeln;
  case c of
    'Y':begin                                       { if choice was 'yes' then delete }
          j:=j-1;
          for l:=1 to (i-1) do
          begin
            k:=l;
            dta[l]:=dta[k];
          end;
          for l:=i to j do
          begin
            k:=l+1;
            dta[l]:=dta[k];
          end;
          tofile;
        end;
    'N':;                                           { else do not delete }
  end; {case}
end; {del}

procedure change;                                   { change any field in record }
var   t:integer;
      c:char;
      sname:string[14];
begin
  repeat
    makewindow(1,1,40,16,black,white,'CHANGING');
    found:=false;
    writeln('Press ENTER to exit');
    write('Name of sample to be changed : ');readln(sname);
    for i:=1 to length(sname) do sname[i]:=upcase(sname[i]);
    for i:=1 to j do  if dta[i].name = sname then                    { sample found }
    begin
```

```
  writeln('Found # ',i);
  found:=true;
  k:=i;
end;
if found then                                   { if sample was found then make changes }
begin
  with dta[k] do
  begin
    t:=1;
    while not (t=0) do
    begin
      windowoff;
      makewindow(39,3,79,21,black,yellow,'OPTIONS');
      writeln(' 1-name          2-elevation');
      writeln(' 3-latitude      4-longitude');
      writeln(' 5-Cl36  [in 1E-15 units ]  ');
      writeln(' 6-SiO2                16-Cl');
      writeln(' 7-TiO2                17-B ');
      writeln(' 8-Al2O3                18-Ce');
      writeln(' 9-Fe2O3                19-Pr');
      writeln(' 10-MgO                 20-Nd');
      writeln(' 11-CaO                 21-Sm');
      writeln(' 12-MnO                 22-Eu');
      writeln(' 13-Na2O                23-Gd');
      writeln(' 14-K20                 24-Tb');
      writeln(' 15-P205                25-Dy');
      writeln('                     26-Yb');
      writeln('                     27-Lu');
      writeln(' Which field do you want to change ?');   { specify field to be changed }
      write('  /1-27 /  press ENTER to exit ');          { or press <ENTER> to skip }
      t:=0; lowvideo;read(t);normvideo;
      windowoff;
      makewindow(1,1,40,16,black,white,'CHANGING');
      gotoxy(1,6);clreol;
      gotoxy(1,5);clreol;
      if t in [1..27] then
      write('Field ',t,' ');
      case t of
        1:  begin
              writeln(name);
              write('name of sample ');readln (name);
              for i:=1 to length(name) do name[i]:=upcase(name[i]);end;
        2:  begin writeln(el);write('elevation ');  readln(el); ele:=el;end;
        3:  begin writeln(la);write('latitude ');  readln(la); lat:=la;end;
        4:  begin writeln(lo);write ('longitude '); readln(lo); lon:=lo;end;
        5:  begin
              writeln(cl36,' ',chr(241),' ',cl36er);
              write('Cl36 ');read(Cl36);Cl36:=Cl36*1E-15;
              write(' ',chr(241),' ');readln(Cl36er);
              Cl36er:=Cl36er*1E-15;
            end;
        6..15:begin
                writeln(brnm[t-5].x,' : ',brn1[t-5].v);
                write(brnm[t-5].x,':');readln(brn1[t-5].v);
              end;
        16..27:begin
                 writeln(brnt[t-15].e3,' : ',brn3[t-15].v3);
                 write(brnt[t-15].e3,':');readln(brn3[t-15].v3);
               end;
      end;
    end; {while}
    sigmaN:=0.0;
    ELD1:=ELD(el,la,lo);
    for i:=1 to major do
    with brn1[i] do
```

```
        begin
          vb:=v*10*brnm[i].c/brnm[i].m*brnm[i].at*AV*brnm[i].b*1e-24;
          sigmaN:=sigmaN+vb;
        end;
        for i:=1 to trace do
        with brn3[i] do
        begin
          vb3:=v3/brnt[i].m3*AV*brnt[i].b3*1e-24;
          sigmaN:=sigmaN+vb3;
        end;
        psiN:=fiN*43e-24*0.75*brn3[1].v3/35500.0*AV/sigmaN;
        PR:=ELD1*(psik*brn1[9].v+psica*brn1[6].v+psiN)/brn3[1].v3/35500.0*AV;
    end;

    end
    else
    begin
      if sname<>'' then begin
                          coltextin(yellow);write(^g,' Not found ! ');
                          coltextoff;
                        end;
      windowoff;tofile;exit;
    end;
    writeln;
    writeln;
    windowoff;
  until c='N';
  windowoff;
  tofile;
end;

procedure analyse;                          { perform exposure time calculations }
var   ssd,asd:real;
      mean1:real;
      tp,Clsec:real;
      strg:string[80];
      ch:char;
const s:string[5]=' E-15';
begin
  clrscr;
  {$I-}
   rewrite(o);
  {$I+}
  clrscr;
  write('Name of reference sample  :');      { reference sample }
  readln(rname);
  found:=false;
  for k:=1 to length(rname) do rname[k]:=upcase(rname[k]);
  for k:=1 to j do
  begin
    if dta[k].name=rname then
    begin
      dta[0]:=dta[k];
      found:=true;
    end;
  end;
  if not found then
  begin
    coltextin(yellow);write(^g,' Not found ! ');coltextoff;
  end
  else
  begin
    clrscr;
    writeln(o,date,'  ',time);
    writeln(o,'PARAMETERS : psiK=',psiK:3:0,' psiCa=',psica:3:0,' fiN=',fiN:6:0);
                                            { production rates and neutron stopping rate }
```

```
writeln(o);
strg:=' Filename :'+filnam+'  Reference sample : '+rname;
makewindow(1,4,80,23,black,white,strg);

{ make a table of all samples with calculated ages, secular equilibrium ratio,}
{ and production from K, Ca, and Cl }

write(o,'Sample        36Cl  36Cl norm.    Age');

  writeln(o,'    Sec. Cl  psiK  psiCa  psiN');
write
  (o,'            *1E15    *1E15      yrs');
writeln(o,'    *1E15       atoms/yr/kg');
writeln
  (o,'===================================
=========================================
');
for i:=1 to j do
begin

  { normalized ratio (normalized to reference sample chemical composition) }

  dta[i].nf:=(dta[i].Cl36-Rnot)
            *(dta[i].brn3[1].v3/dta[0].brn3[1].v3)
            *(dta[0].brn1[9].v*psiK+dta[0].brn1[6].v*psiCa
             +dta[0].psiN)/
            (dta[i].brn1[9].v*psiK+dta[i].brn1[6].v*psiCa
             +dta[i].psiN)*
            dta[0].ELD1/dta[i].ELD1;
  dta[i].nfer:=dta[i].Cl36er*(dta[i].nf/dta[i].Cl36); { error of normalized ratio }
  with dta[i] do
  begin

    { calculate exposure time (tp) for single samples }

    tp:=-ln(1-((Cl36-Rnot)*2.3e-6*brn3[1].v3/35500.0*AV)/
        (ELD1*(brn1[9].v*psiK+brn1[6].v*psiCa+psiN)))/2.3e-6;

    { calculate secular equilibrium ratio for single samples }

       Clsec:=ELD1*(psiK*brn1[9].v+psiCa*brn1[6].v+psiN)/
              (2.3E-6*(brn3[1].v3/35500.0*AV))+Rnot;
    write(o,name,' ':(12-length(name)));
    write(o,Cl36*1E15:6:0,chr(241),Cl36er*1E15:3:0);
    write(o,nf*1E15:6:0,chr(241),nfer*1E15:3:0,'    ',tp:6:0,'     ');
  writeln(o,Clsec*1E15:6:0,ELD1*brn1[9].v*psiK:8:0,ELD1
            *brn1[6].v*psiCa:8:0,ELD1*psiN:8:0);
  end;
end;
writeln(o);
mean:=0;
for i:=1 to j do mean:=mean+dta[i].nf;
mean:=mean/i;                                { mean age from all samples in file }
write(o,'              Mean : ',mean*1E15:6:0);
with dta[0] do
  t:=-ln(1-(mean*2.3e-6*brn3[1].v3/35500.0*AV)/
    (ELD1*(brn1[9].v*psiK+brn1[6].v*psiCa+psiN)))/2.3e-6;
asd:=0;                                      { analytical standard deviation }
for i:=1 to j do asd:=asd+dta[i].nfer;
asd:=asd/i;
ssd:=0.0;                                    { statistical standard deviation }
for i:=1 to j do ssd:=ssd+sqr(mean-dta[i].nf);
if i>1 then ssd:=sqrt(ssd/(i-1)) else ssd:=0;
writeln(o,' ',chr(241),' ',asd*1E15:2:0);
writeln;
writeln(o,'              Statistical SD  =',ssd*1E15:6:0,s);
```

```
    writeln(o,'            Analytical SD = ',asd*1E15:6:0,s);

    { tasdmin and tasdmax are ranges of exposure ages according to }
    { analytical standard deviations for calculated ages }

    tasdmin:=-ln(1-((mean-asd)*2.3e-6*dta[0].brn3[1].v3/35500.0*AV)/
              (dta[0].ELD1*(dta[0].brn1[9].v*psiK+dta[0].brn1[6].v*psiCa+
              dta[0].psiN)))/2.3e-6-t;
    tasdmax:=-ln(1-((mean+asd)*2.3e-6*dta[0].brn3[1].v3/35500.0*AV)/
              (dta[0].ELD1*(dta[0].brn1[9].v*psiK+dta[0].brn1[6].v*psiCa+
              dta[0].psiN)))/2.3e-6-t;
    writeln(o);
    write(o,'          ');
    writeln
      (o,'Calculated age : ',t:5:0,' +',tasdmax:5:0,'/',tasdmin:5:0,' (ASD)');

    { tssdmin and tssdmax are ranges of exposure ages according to }
    { statistical standard deviations for calculated ages }

    tssdmin:=-ln(1-((mean-ssd)*2.3e-6*dta[0].brn3[1].v3/35500.0*AV)/
          (dta[0].ELD1*(dta[0].brn1[9].v*psiK+dta[0].brn1[6].v*psiCa+
             dta[0].psiN)))/2.3e-6-t;
    tssdmax:=-ln(1-((mean+ssd)*2.3e-6*dta[0].brn3[1].v3/35500.0*AV)/
          (dta[0].ELD1*(dta[0].brn1[9].v*psiK+dta[0].brn1[6].v*psiCa+
            dta[0].psiN)))/2.3e-6-t;
    writeln(o,'                              +', tssdmax:5:0,'/', tssdmin:5:0,' (SSD)');
    end;
    writeln(o);
    writeln(o);
    windowoff;
    {$I-} close(o); {$I+}                              { close file }
end;

procedure combine;                                     { merge two files together }
var  i,j,k:integer;
     filnam1,filnam2,filnam3:string[14];
     filvar1,filvar2,filvar:file of data;

begin
  makewindow(40,4,78,11,white,black,'MERGE');
  {$I-}
  write('Source file #1 : ');
  repeat                                               { first file }
    gotoxy(1,2);clreol;gotoxy(18,1);clreol;
    read(filnam1);
    assign(filvar1,filnam1);
    reset(filvar1);
  until (IOresult=0) or (filnam1='');
  if filnam1='' then begin windowoff; exit; end;
  writeln;
  write('Source file #2 : ');
  repeat                                               { second file }
    gotoxy(1,3);clreol;gotoxy(18,2);clreol;
    read(filnam2);
    assign(filvar2,filnam2);
    reset(filvar2);
  until (IOresult=0) or (filnam2='');
  if filnam2='' then begin windowoff; exit; end;
  {$I+}
  writeln;
  write('Destination file : ');
  readln(filnam3);                                     { output file }

  if filnam3='' then begin windowoff; exit; end;
```

```
  assign(filvar,filnam3);
  rewrite(filvar);

  j:=0;
  for i:=1 to filesize(filvar1) do
  begin
    read(filvar1,dta[i]);
    j:=j+1;
    dta[j]:=dta[i];
    write(filvar,dta[j]);
  end;

  for i:=1 to filesize(filvar2) do
  begin
    read(filvar2,dta[i]);
    j:=j+1;
    dta[j]:=dta[i];
    write(filvar,dta[j]);
  end;
  writeln; write('Merged ');
  close(filvar1);close(filvar2);close(filvar);
  windowoff;
end;

procedure help;                                    { calls help window }
var  t:text;
     c:string[80];
     i:integer;
begin
  clrscr;
  i:=0;
  makewindow(1,1,80,20,black,white,'H E L P');
  assign(t,'HELP.TXT');
  reset(t);
  while not eof(t) do
  begin
    readln(t,c);
    writeln(c);
    i:=i+1;
    if (i mod 16 )=0   then
    begin
      textcolor(yellow);
      gotoxy(1,18);
      write('              < Press any key to continue >');
      textcolor(white);
      repeat until keypressed;
      gotoxy(1,18);clreol;
    end;
  end;
  close(t);
  windowoff;
end;

procedure refsample;                               { writes reference sample to file }
var  refname:string[12];                           { the file will have extension '.ref' }
     k:integer;
     found:boolean;
begin
  makewindow(40,13,78,20,white,black,'WRITE SAMPLE TO FILE');

  write('Name of sample: ');readln(refname);
  for  k:=1 to length(refname) do refname[k]:=upcase(refname[k]);

  found:=false;
  for i:=1 to j do
  begin
```

```
    if refname=dta[i].name then
    begin
      filnam:=refname + '.REF';
      k:=i;
      found:=true;
    end;
  end;
  if not found then writeln('Not found !')
  else
    begin
      assign(filvar,filnam);
      rewrite(filvar);
      write(filvar,dta[k]);
      close(filvar);
      writeln;
      writeln;write('Reference sample ',filnam,' saved');
    end;
    windowoff;
end;

procedure ff;                                   { calls sub menu from main menu }
begin
  gotoxy(1,25);
  coltextin(15);
  write
    (' File processsing: <R>ead <A>dd <D>elete <C>hange <W>rite <M>erge
<Q>uit ');
  coltextoff;
  repeat
    read(kbd,ch);
    until upcase(ch) in ['R','W','M','C', 'A','D','Q'];
  ch:=upcase(ch);
  case ch of
    'A':add;
    'D':del;
    'Q':begin clrscr; exit; end;
    'C':change;
    'M':combine;
    'W':refsample;
    'R':readdata;
  end;
end;

procedure hidemenu;                             { hides menu line }
begin
  gotoxy(1,25);
  clreol;
  repeat until keypressed;
end;

procedure report;                               { gives all adta for all samples in file }
var  y,i,k,m,n:integer;
      els:string[20];
      s:array[1..36] of string[80];
      name1:string[80];
type s20=string[20];

    function conv(co:real):s20;                 { floating numbers to strings }
    var cs:string[20];
    begin
      str(co,cs);
      delete(cs,8,7);
      conv:=cs;
    end;

begin
```

```
  {$I-}
  rewrite(o);
  {$I+}
  s[1]:='Sample   ';
  s[2]:='Elev.  ';
  s[3]:='Lat.   ';
  s[4]:='Long.  ';
  s[5]:='ELD    ';
  s[6]:='Cl36   ';
  s[7]:='Cl36 SD';
  s[8]:='Sigma  ';
  s[9]:='psiN   ';
  for k:= 10 to 19 do s[k]:=brnm[k-9].x+'  ';
  for k:= 20 to 31 do s[k]:=brnt[k-19].e3+'    ';

  for i:=1 to j do
  with dta[i] do
  begin
    name1:=name;
    for n:=1 to (12-length(name1)) do name1:=name1+' ';
      s[1]:=s[1]+name1;
      s[2]:=s[2]+conv(el)+' ';
      s[3]:=s[3]+conv(la)+' ';
      s[4]:=s[4]+conv(lo)+' ';
      s[5]:=s[5]+conv(eld1)+' ';
      s[6]:=s[6]+conv(Cl36)+' ';
      s[7]:=s[7]+conv(Cl36er)+' ';
      s[8]:=s[8]+conv(sigmaN)+' ';
      s[9]:=s[9]+conv(psiN)+' ';
    for m:=10 to 19 do
      s[m]:=s[m]+conv(brn1[m-9].v)+' ';
    for m:=20 to 31 do
      s[m]:=s[m]+conv(brn3[m-19].v3)+' ';
  end;
  writeln(o,s[1]);
  for n:=1 to (length(s[1])-2) do write(o,'=');writeln(o);
  for i:=2 to 9 do writeln(o,s[i]);writeln(o);
  for i:=10 to 19 do writeln(o,s[i]);
  writeln(o);
  y:=whereY;
   if choice='M' then
  begin
    write('<Press any key>');
    repeat until keypressed;
    gotoxy(1,y);clreol;
  end;
  for i:=20 to 31 do writeln(o,s[i]);
  {$I-} close(o); {$I+}
end;

procedure config;                          { changes production parameters }
var  e:integer;
     c:char;
type par_type=record
                nm:string[8];
                vl:real;
              end;
const  par:array[1..4] of par_type =
         ((nm:'fin  ';vl:2.64e5),(nm:'psik ';vl:759.0),
         (nm:'psica';vl:490.0),(nm:'rnot ';vl:10.9e-15));
begin
  clrscr;
  write('<M>onitor or <P>rinter');
  repeat
    read(kbd,choice);
    choice:=upcase(choice);
```

```
  until choice in ['M','P'];
  clrscr;
  if choice='M' then assign(o,'TRM:') else assign(o,'LST:');
  writeln('Setting the following parameters:');
  writeln;
  for i:=1 to 4 do writeln('<',i,'> ',par[i].nm,'  ',par[i].vl);
  writeln;
  repeat
    writeln('Choose one of four parameters <ENTER> to skip');
    repeat
      read(kbd,c);
    until c in[#13,'1','2','3','4'];
    if c<>#13 then
    begin
      writeln;
      val(c,i,e);
      write('New ',par[i].nm,'  ');
      readln(par[i].vl);
      writeln;

    end;
  until c=#13;
  clrscr;
  writeln; writeln('Current parameters :');
  for i:=1 to 4 do writeln(par[i].nm,'  ',par[i].vl);
    fiN:=par[1].vl;
    psiK:=par[2].vl;
    psiCa:=par[3].vl;
    Rnot:=par[4].vl;
end;

begin                                          { begin main program }
  clrscr;
  windowoff;
  config;
  repeat
    gotoxy(59,1);
    coltextin(15);
    write(' ',date,'  ',time,' ');
    coltextoff;

{ write main menu line }

    gotoxy(7,25); coltextin(15);
    write
      ('<N>ew file <R>ead <P>rocess <F>ile <S>how <L>ist <H>elp <Q>uit');
    coltextoff;

{ make selection }

    repeat
      read(kbd,ch);
      ch:=upcase(ch);
    until ch in['Q','G','L','W','M','A','D','C','T','N','R','P','F','S','H',#13];

    case ch of
      'G':config;
      'A':add;
      'D':del;
      'C':change;
      'M':combine;
      'W':refsample;
      'T':hidemenu;
      'N':input(0);  {new set of samples}
      'R':readdata;
      'P':analyse;
```

```
      'Q',#13:halt;
      'S':begin
            makewindow(1,1,20,4,black,yellow,' NO. OF SAMPLE');
            write('# = ');
            readln(ii);
            windowoff;
            printdta(ii);
          end;
      'H':help;
      'L':begin clrscr;report; end;
      'F':  repeat
              ff;
            until ch='Q';
    end;
  until false;
end.
```

8.2. PASCAL program for iterative calculation of the parameters for in situ production of ^{36}Cl

```
{ ELDn by Lal, 1989; ELDm by Conversi, 1950 }
{ program iteratively calculates production parameters accounting for negative muon capture }
{ data for all samples is in the form of an array at the beginning of the text }
{ array 'n' includes data for neutron stopping rate }
{ arrays 'k' and 'c' are for spallation on K and Ca }
{ if more samples are available, the above arrays can be expanded }
{ and nmax, kmax, and cmax changed to respective number of samples}
{ if desired, the value of fn can also be changed }
{ output is sent to a printer }

{$C+}
const  sigma35=44e-24;                  { thermal neutron absorption cross section for 35Cl }
       sigmaCl=33.443e-24;              { thermal neutron absorption cross section for Cl }
       lambda=2.3e-6;                   { decay constant for 36Cl }
       R0=1e-14;                        { radiogenic 36Cl }
       Im=1.6E5;          { muon stopping rate at depth 0, sea level, high latitudes }
                          { in muons/kg/yr, Rossi, 1952 }
       fd=0.83;           { after Charalambus, 1971 }
       nmax=7;            { # of samples for neutron stopping rate estimation }
       kmax=4;            { # of samples for estimation of production rate from 39K }
       cmax=2;            { # of samples for estimation of production rate from 40Ca }
       fin:real=1e6;      { initial value for thermal neutron stopping rate, n/kg/yr }
       psiK:real=2760;    { initial value for production rate from 39K, N36/kg-rock/yr }
       psiCa:real=710;    { initial value for production rate from 40Ca, N36/kg-rock/yr }
       fn:real=0.005;     { probability of production of 36Cl by muon capture by 40Ca }

       { the following arrays are formatted as follows: }
       { sigmaN, 36Cl, NCl, ELDn, t, K, Ca, ELDm, fc }

       n:array[1..nmax] of array[1..9] of real =
           {187-bulk}  ((5.14, 473e-15, 2.205e21, 14.54,   9740, 5.44, 0.21, 3.80, 0.00144),
           {187-q    }  (5.14, 493e-15, 2.120e21, 14.54,  9740, 3.61, 0.14, 3.80, 0.00096),
           {387-q    }  (5.33, 342e-15, 1.713e21, 14.16,  12510, 0.37, 0.26, 3.74, 0.00177),
           {787-bulk}   (5.34, 594e-15, 2.714e21, 11.06,  17780, 5.43, 0.49, 3.27, 0.00337),
           {787-q    }  (5.34, 344e-15, 2.290e21, 11.06,  17780, 0.54, 0.25, 3.27, 0.00171),
           {9353     }  (6.38, 244e-15, 1.590e21, 3.35, 14400, 0.86,12, 1.76, 0.07094),
           {9354     }  (6.76, 226e-15, 1.890e21, 3.35,  14400, 0.78,11.75, 1.76, 0.06693));

       k:array[1..kmax] of array[1..9] of real =
           {187-bulk}  ((5.14, 473e-15, 2.205e21, 14.54,  9740, 5.44, 0.21, 3.80, 0.00144),
           {187-m    }  (5.14, 616e-15, 2.205e21, 14.54,  9740, 7.80, 0.16, 3.80, 0.00110),
           {387-m    }  (5.33, 856e-15, 2.409e21, 14.16, 12510, 8.78, 0.22, 3.74, 0.00152),
           {787-bulk}   (5.34, 594e-15, 2.714e21, 11.06, 17780, 5.43, 0.49, 3.27, 0.00337));

       c:array[1..cmax] of array[1..9] of real=
           {9353     }  ((6.38, 244e-15, 1.590e21, 3.35,  14400, 0.86,12, 1.76, 0.07094),
           {9354     }  (6.76, 226e-15, 1.890e21, 3.35,  14400, 0.78,11.75, 1.76, 0.06693));

var xk,yk,xc,yc:real;      { values of x and y for K and Ca; x,y are later used in linear regression }
                           { to obtain slopes; the slopes are equal to production rates from K, Ca }
    xm,ym:real;            { x,y values for muon component; for future use only }
    xn,yn,f :array[1..7] of real;     { x,y for neutron stopping rate }
    sfin,spsica,spsik,sfn:real;       { sum of values of neutron, K, Ca, used to calculate means }
    ch:char;                          { dummy selection variable }
    i,j,jj,kk:integer;                { dummy counting variable }
    memo:real;                        { test variable to check if the iteration converged }
    query: boolean;                   { dummy selection variable }

begin
    writeln(lst,'Production parameters for given muon capture probability fn=',fn:5:3);
```

```
    writeln(lst);
    query:=false;
    kk:=0;
    repeat
        kk:=kk+1;
        sfin:=0.0;
        j:=0;
        for i:=1 to nmax do     {solve production equation for neutron stopping rate, fin }
        begin
            xn[i]:=sigma35*0.75*n[i,3]/n[i,1];
            yn[i]:=(((n[i,2]-R0)*n[i,3]*lambda/(1-exp(-lambda*n[i,5]))
                    -fn*n[i,8]*Im*n[i,9]*fd)/n[i,4])-psiK*n[i,6]-psiCa*n[i,7];
            fin:=yn[i]/xn[i];
            if fin>0 then begin sfin:=sfin+fin; j:=j+1; end;
        end;
        fin:=sfin/j;
        if fin=memo then query:=true;
        if query then
        begin
            for i:=1 to nmax do
            writeln(lst,'xn=',xn[i]:7:6,'    yn=',yn[i]:7:0,'    fin=',yn[i]/xn[i]:7:0);
        end;
        if query then   writeln(lst,'  fin=',fin:7:0);

        spsik:=0.0;
        j:=0;
        for i:=1 to kmax do     { solve for production rate from 39K, psiK }
        begin
            xk:=k[i,6];
            yk:=(k[i,2]-R0)*k[i,3]*lambda/(1-exp(-lambda*k[i,5]))/k[i,4]
                -fn*Im*k[i,9]*fd*k[i,8]/k[i,4]
                -psiCa*k[i,7]-fin*sigma35*0.75*k[i,3]/k[i,1];
            psik:=round(yk/xk);
            if query then
            writeln(lst,'xk=',xk:7:2,'    yk=',yk:7:0,'    psik=',psik:7:0);
            if psik>0 then begin spsik:=spsik+psik; j:=j+1; end;
        end;
        psik:=spsik/j;
        if query then writeln(lst,'  psik=',psik:7:0);

        spsica:=0.0;
        j:=0;
        for i:=1 to cmax do     { solve for production rate from 40Ca, psiCa }
        begin
        xc:=c[i,7];
        yc:=(c[i,2]-R0)*c[i,3]*lambda/(1-exp(-lambda*c[i,5]))/c[i,4]
            -fn*Im*c[i,9]*fd*c[i,8]/c[i,4]
            -psiK*c[i,6]-fin*sigma35*0.75*c[i,3]/c[i,1];
        psica:=yc/xc;
        if query then writeln(lst,'xc=',xc:7:2,'    yc=',yc:7:0,'    psiCa=',psiCa:7:0);
        if psica>0 then begin spsica:=spsica+psica; j:=j+1; end;
    end;
    psica:=spsica/j;
    if query then writeln(lst,'  psiCa=',psica:7:0);

    memo:=fin;
until (query=true) or (kk>100);          { repeat until converges or 100 iterations are made }
writeln(lst,kk,' iterations');
writeln(lst);
end.
```

8.3. PASCAL program for calculation of Cl concentration from raw ion selective electrode method data

```
{ Calculate total Cl content using data obtained      }
{ from Ion Selective Electrode method                 }
{ Input parameters are:   mass of standards           }
{                         potential of standards      }
{                         mass of final solutions     }
{                         concentration of standards  }
{                                                     }
{                         similarly for samples       }

const  std_l_mass: real=0.2;          { low standard initial mass }
       std_h_mass: real=0.2;          { high standard initial mass }
       std_l_sln_mass: real=2.0;      { low standard final solution mass }
       std_h_sln_mass: real=2.0;      { high standard final solution mass }
       std_l_pot: real=112;           { low standard potential }
       std_h_pot: real=53;            { high standard potential }
       std_l_conc: real=50;           { low standard concentration }
       std_h_conc: real=500;          { high standard concentration }

       sample_mass: real=0.2;         { sample initial mass }
       sample_sln_mass: real=2.0;     { sample final solution mass }
       sample_pot: real=100;          { sample potential }
       sample_conc: real=100;         { sample concentration }

var std_l_conc_cor, std_h_conc_cor:real;
   slope:real;

begin
   repeat
   write('Mass of low standard (0 to quit): ');readln(std_l_mass);
   if std_l_mass=0 then exit;
   write('Mass of high standard: ');readln(std_h_mass);
   write('Mass of solution of low standard: ');readln(std_l_sln_mass);
   write('Mass of solution of high standard: ');readln(std_h_sln_mass);
   write('Potential of low standard:');readln(std_l_pot);
   write('Potential of high standard:');readln(std_h_pot);
   write('Concentration of low standard:');readln(std_l_conc);
      std_l_conc_cor:=std_l_conc*std_l_mass/0.2*2.0/std_l_sln_mass;
   write('Concentration of high standard:');readln(std_h_conc);
      std_h_conc_cor:=std_h_conc*std_h_mass/0.2*2.0/std_h_sln_mass;
      slope:=1/(1/ln(10)*(ln(std_h_conc_cor/std_l_conc_cor))/(std_l_pot-std_h_pot));
      repeat
         write('Mass of sample (0 to quit):');readln(sample_mass);
```

```
            if sample_mass=0 then exit;
            write('Mass of solution of sample:');readln(sample_sln_mass);
            write('Potential of sample:');readln(sample_pot);
               sample_conc:= exp((sample_pot-std_1_pot)*
                             ln(std_h_conc_cor-std_1_conc_cor)/
                             (std_h_pot-std_1_pot)+ln(std_1_conc_cor));
               sample_conc:=sample_conc*sample_mass/0.2*2/sample_sln_mass;
            writeln('Slope of the standard line is ',slope:3:1);
            writeln('Sample concentration is ',sample_conc,' ppm');
         until sample_mass=0;
      until std_1_mass=0;
end.
```

8.4. *Description of sampling sites*

Samples were collected and site locations described by Fred M. Phillips (FMP), Stuart S. Smith (SSS) and myself (no initials). The notes are edited for clarity, but in most cases original style was preserved. Units of length were converted to metric units. Arrows mark sample sites.

8.4.1. White Mountains – Chiatovitch Creek

C–87–3 (later designated as **C–187–3**)
Chiatovitch Creek, White Mountains, 30 m E of C–387–1. Moderately weathered, fine to medium–grained granodiorite (SSS).

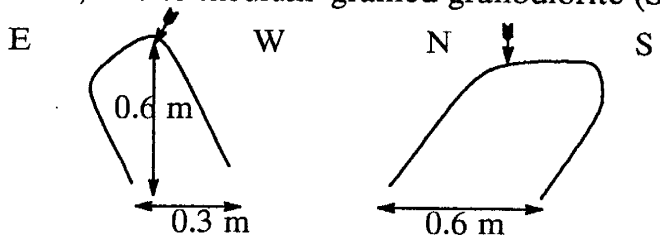

C–387–1
Chiatovitch Creek, White Mountains, Dorn's C–3 area, terminal complex, elevation 3600 m. Strongly to moderately weathered, medium–grained diorite. Largest boulder on ridge (SSS).

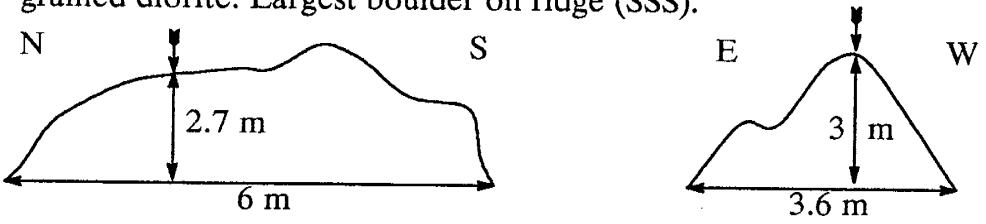

Sample from flat area on top

C–787–1
Chiatovitch Creek, White Mountains, probable maximal terminal moraine at steep drop off in valley. Weakly to moderately weathered, medium–grained diorite (monzonite) (SSS).

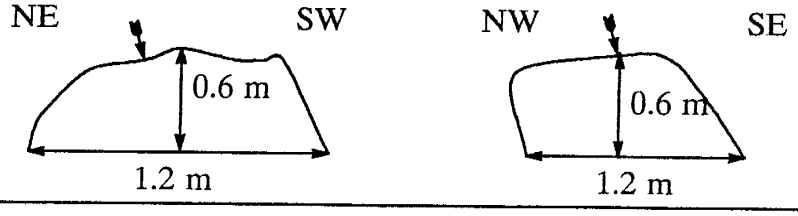

8.4.2. Hawaii – Mauna Kea

MK–MAKO–12
From older "Makanakan" flow, close to hawaiite (?) flow, covering it. In "reentrant" (FMP).

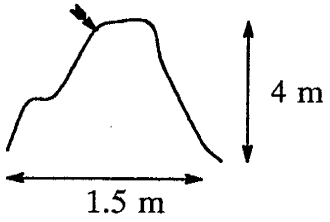

MK–MAKY–16
From crest of outermost "Younger" Makanakan end moraine on top of hawaiite lava flow (FMP).

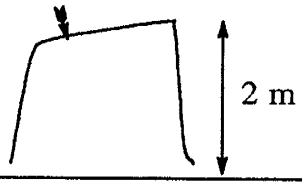

Large (2 m) high boulder
Good geometry – dense rock

MK–W–5
From top of rounded, very solid flow, interior boulder. Boulder surface smoothed by eolian erosion. Should be an excellent sample (FMP).

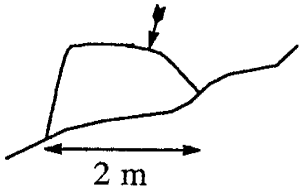

Large (2 m) high boulder
Good geometry – dense rock

MK–MAKT–29
From about 50 m NE of Cal Tech 7 mm observatory (the aluminum dome) almost on the top of Mauna Kea. Glacially polished sample. Should date the final deglaciation of MK. Good geometry, good quality (FMP).

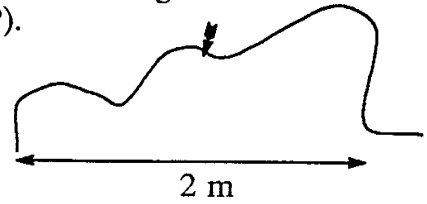

8.4.3. Sierra Nevada – Bloody Canyon (BC), Sawmill Canyon (SC)

BC–88–1
NW part of Bloody Canyon, on Tahoe crest, to the SW of Debbie's Tahoe 87 samples. The moraine crest here does seem to have fewer large boulders suitable for sampling than the 87 area below. May be older (FMP). Moderately weathered, medium–grained granodiorite

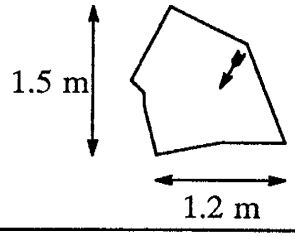

View from top, sample site marked by arrow.

The boulder is 0.8 m tall.

BC–88–5
150 m from BC–88–1 towards the canyon, the same location as Ron Dorn's samples.
Moderately weathered, medium–grained granodiorite, good surfaces.

SC–88–1
Sawmill Canyon, a hill to the S of the hill with samples BC–88–1 and 5, at much lower elevation. More than moderately weathered granodiorite.

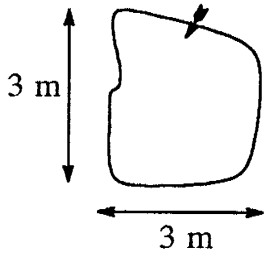

Big boulder.
View on top, sample site marked by arrow.
Many pieces are left on the boulder.

SC–88–2
100 m to the W of SC–88–1.
Moderately weathered granodiorite.

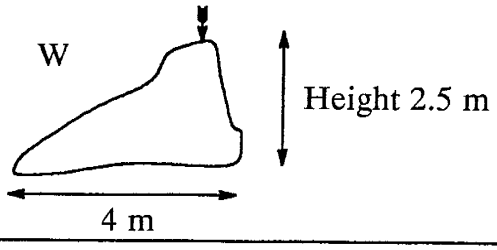

SC–88–3

500 m to the E of SC–88–2, down the hill, on S slope of the moraine. Highly weathered granodiorite, with exfoliation.

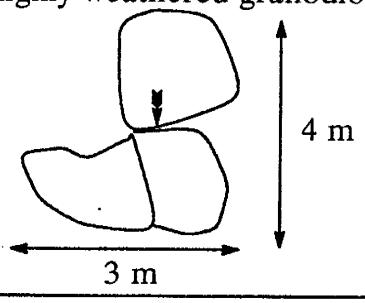

Top view on a big boulder, cracked into 3 pieces. Height 1.5 m. Smaller boulder on top of the big one was sampled. 2 pieces were taken, the bigger one is better.

BC–86–1–TI

Bloody Canyon (SSS).

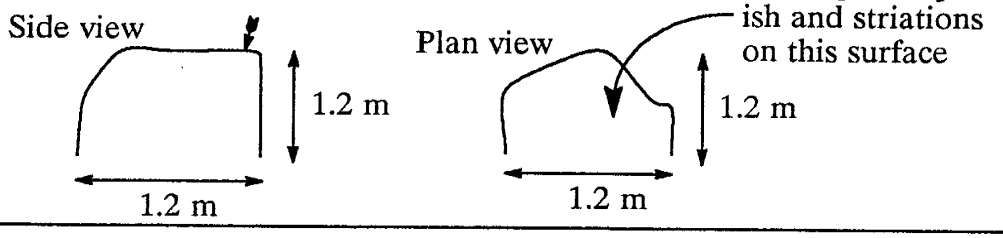

BC–86–2–TI

15 m up nose (SW).

Granodiorite, coarse grained, fractures, iron stains (SSS).

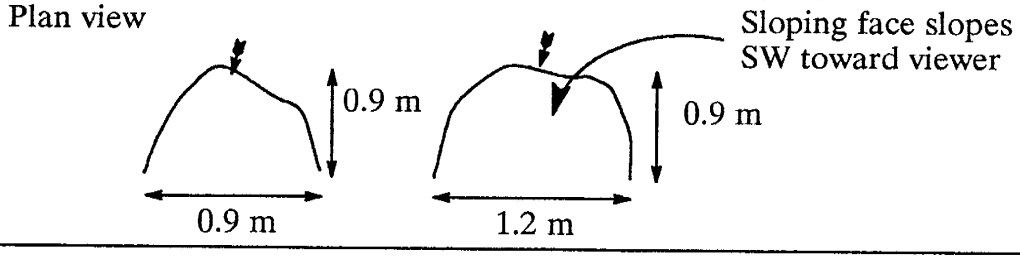

BC–86–3–TI

About 90 m SW from BC–86–2–TI.

Granodiorite, minor alteration, slightly crumbly. Boulder 0.9 m high at sampling site, 1.8 m wide, 0.9 m deep (SSS).

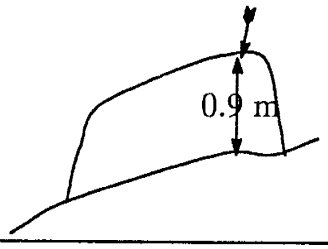

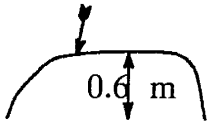

Mark top (T) of samples

BC–86–3–TI
About 90 m SW from BC–86–2–TI.
Granodiorite, minor alteration, slightly crumbly. Boulder 0.9 m high at sampling site, 1.8 m wide, 0.9 m deep (SSS).

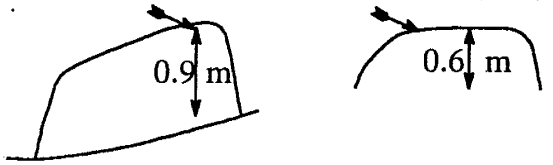

Mark top (T) of samples

BC–86–4–TI
About 6 m NW of BC–86–3 TI. All BC–86 from 1 to 4 are from ridge crest with few trees, just sage cover (SSS).
Fine–grained granodiorite, friable, some weathering? Biotite poor.

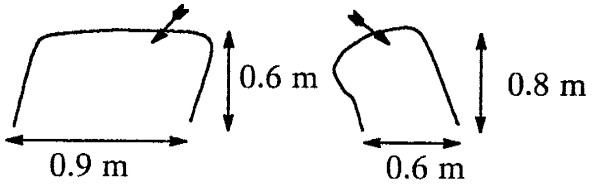

Boulder 0.8 m high, 0.9 m wide, 0.6 m deep, with glacial polish.

BC–86–5–TI
About 60 m SW of BC–86–4 TI. Taken from edge of boulder with a vertical face – FMP concern about low neutron flux (SSS).
Granodiorite, biotite–rich.

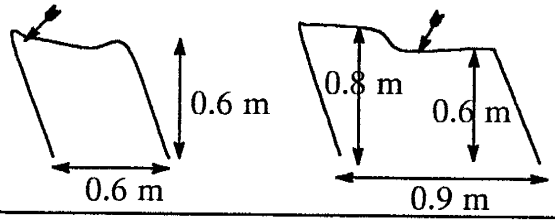

BC–86–6–TE
Tenaya moraine, about 2400 m. South of Tioga moraine just sampled. Granodiorite, fresh, massive. Next to burnt tree: evidence that 1–2 cm may have spalled off (exfoliated). Remenant polished surface raised above most of rock surface (1–2 cm). Boulder 0.7 m high, 1.5 m wide, 0.9 m deep. Site at 0.9 m (SSS).

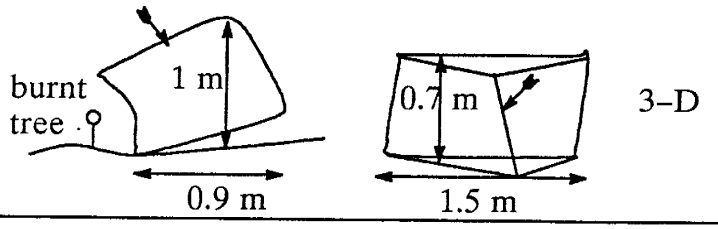

3–D

BC–86–7–TE
60 m NE of BC–86–6–TE. Granodiorite, weakly weathered. Boulder has moderate Fe staining. Sample selected for low Fe staining. Moderate forest (SSS). Boulder 1.2 m high, 0.9 m wide, 1.5 m deep.

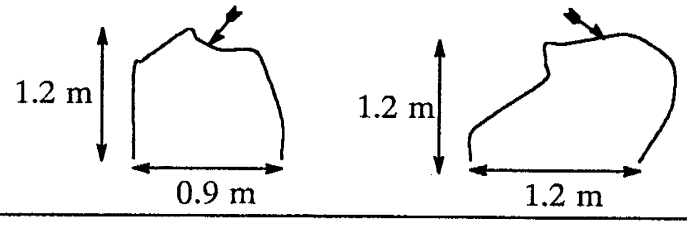

BC–86–8–TE
9 m N of BC–86–7–TE. Granodiorite, moderately weathered, medium grain size, with some coarse feldspars (1.5 cm long) (SSS). Boulder 0.9 m high, 1.2 m wide, 0.7 m deep.

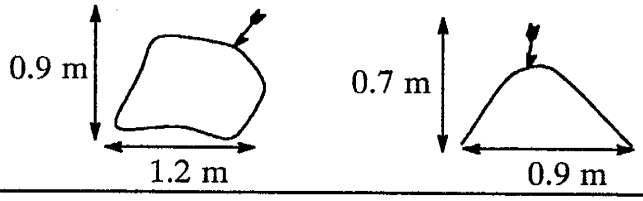

BC–86–9–TE
SW this case, top but sloping, 40 to 220°. Granodiorite, fresh, biotite–poor, some aplite and quartz veining near sample (SSS). Boulder 0.9 m high, 0.9 m wide, 0.6 m deep.

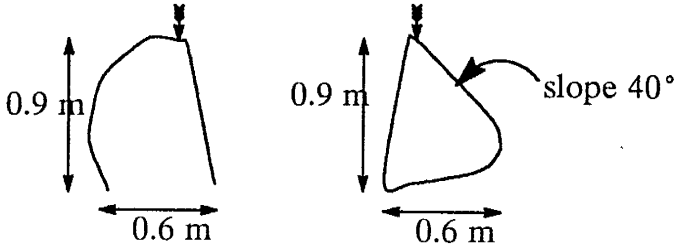

Location map of samples 7 through 10

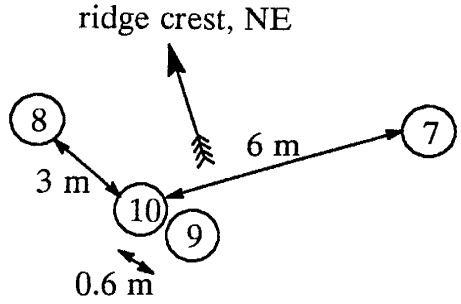

BC-86-10-TE

See diagram above for location. Sample from top of a tabular, flat boulder, near horizontal surface, "good neutron flux". Granodiorite, fresh (SSS).

Boulder 0.6 m high, 1.2 m wide, 0.9 m deep.

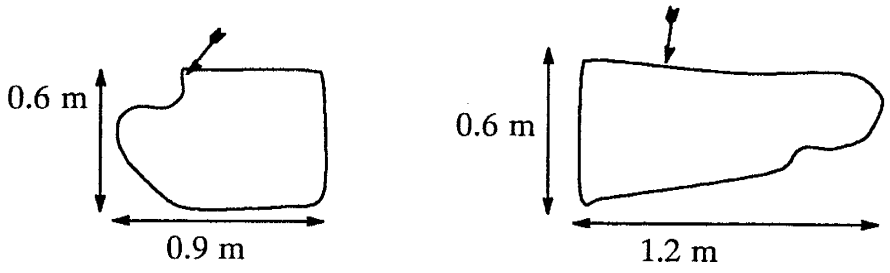

BC-86-11-TE

75 m NE of samples 7 through 11. Granite? Fine grained, pinkish. Weathering rind uniformly 4 cm thick, well developed, light gray, contrasts with pink rock. Polished surface (SSS).

Boulder 0.9 m high. Sample currently at 0.6 m. FMP thinks sample was at top once.

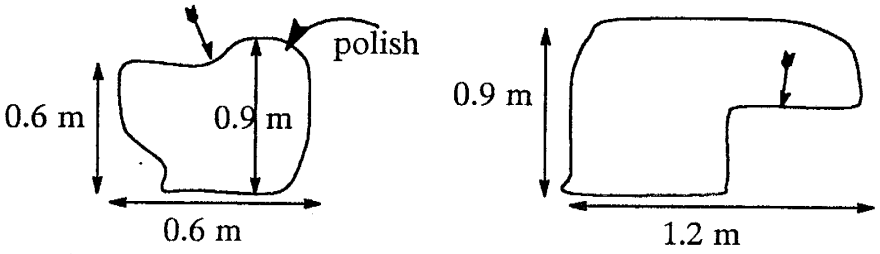

Possible soil pit, 2.4 m NE, Burke & Birkeland pit # 14 (CK).

BC-86-12-TA

Tahoe. Located at dot by TA south of Walker creek. Amphibole-rich, probably plutonic rock, moderately weathered. Very large boulder. Sample at 1.5 m high. Boulder has slumped to west, but site seems to be original top. Rock fractured up (SSS).

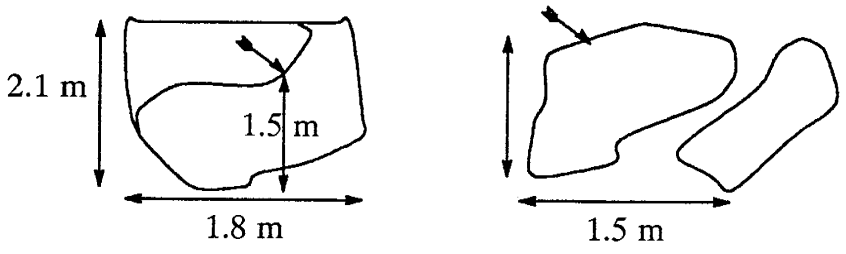

BC-86-13-TA

30 m to S of # 12. Granite, medium grained, weakly weathered. Thin pieces sampled. Boulder/site: 2.1 m high (2.7 m see drawing) from ground directly underneath sample (SSS).

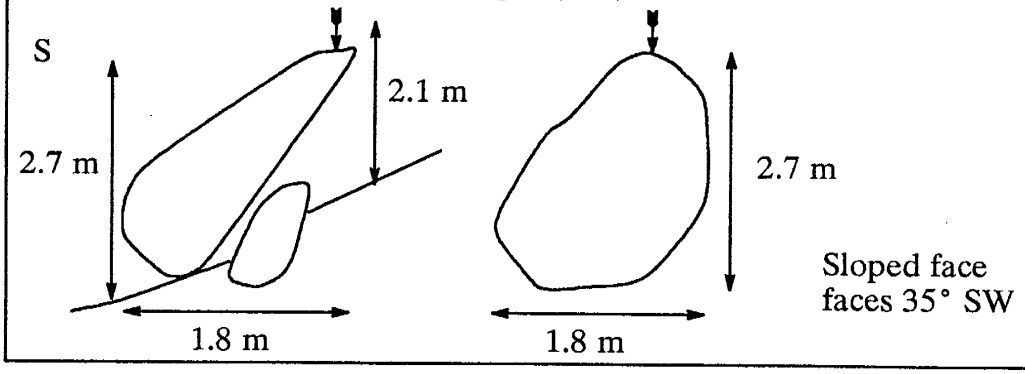

BC-86-14-TA

30 m E of # 13. Granodiorite, coarse to medium grained, fresh (SSS). Boulder 1.9 m high, 2.4 m wide, 1.8 m deep. Site at 1.8 m.

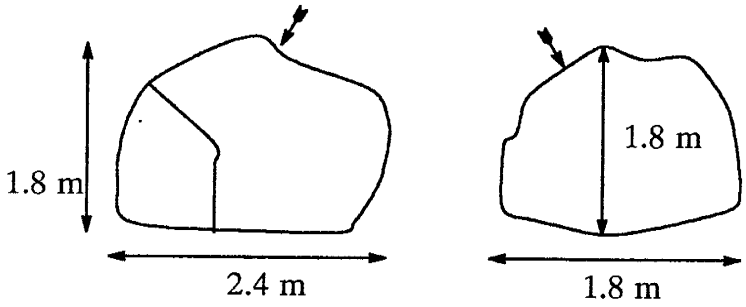

13, 14 and 15 taken S of ridge crest; exposure may not be as long.

BC-86-15-TA

150 m E of # 14, 22–30 m S (off) of ridge crest. Site at 3 m high, so even with height of ridge crest. Granodiorite, coarse to medium grained, moderately to strongly altered. Upper 4 cm of sample are weak to moderately weathered. Sampled near fracture with heavy Fe staining (SSS).

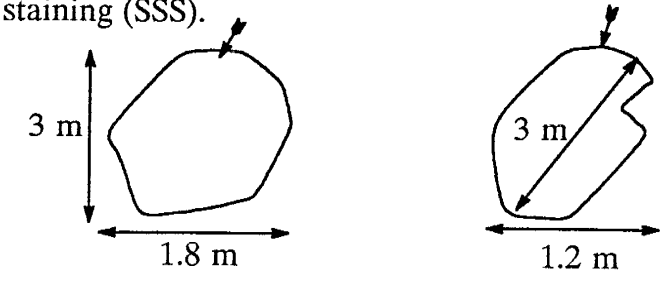

BC-86-16-TA

Located on topo. Granodiorite, coarse grained. Xenoliths on boulder surface stick out 3 cm. This much spallation/exfoliation of granodiorite may have taken place. Site 5.4–6 m high. FMP gathered sample; said it is from place where flat top begins to curve down (SSS).

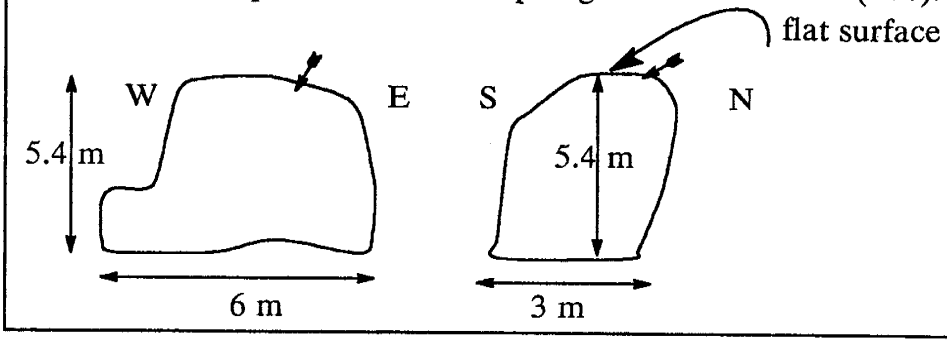

SC-86-17-MB

Mono Basin moraine in Sawmill Canyon. Southern lateral moraine. Granodiorite, coarse grained, strongly weathered, f-spars shot, strong Fe stains in spots, well jointed. Site 1.8 m high, 1.2 m wide. B+B sample pit 30 m east along crest (SSS).

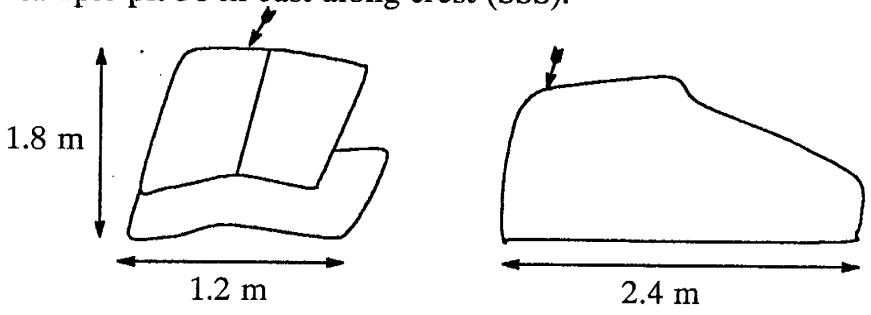

SC-86-18-MB

60 m E of # 17. Granodiorite, moderately weathered. Boulder has pegm. phase (Peg) and a 7.5 cm dike (or vein) intruding. Site 1.2 m high (SSS).

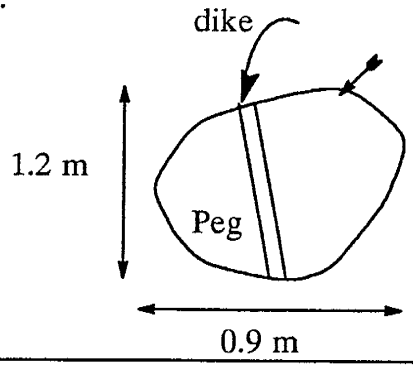

SC-86-19-MB

Marked on map. Granodiorite, moderately-well weathered. Site at 0.9 m (SSS).

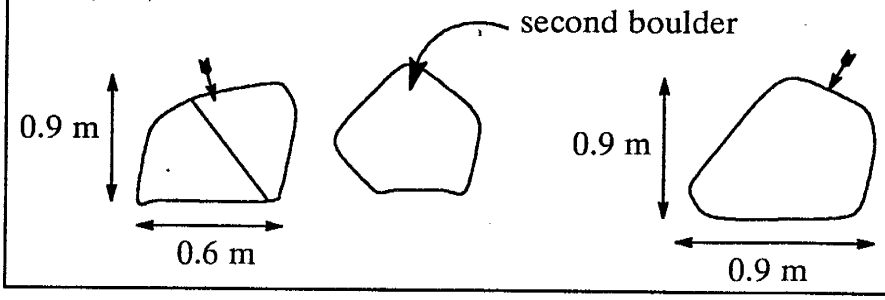

SC-86-20-MB

Granodiorite, moderately strong weathering, f-spar shot. Boulder contains xenoliths and veinlets. Site 1.6 m high (SSS).

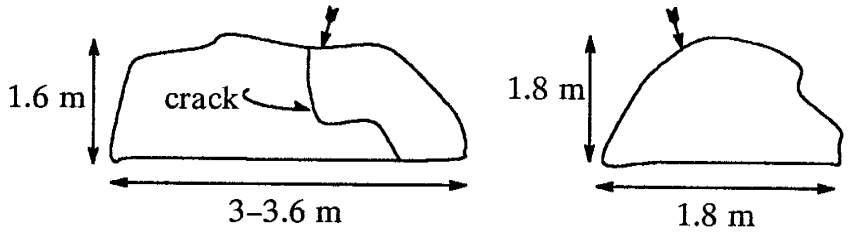

Sample has a smooth side which was exposed at crack. FMP thinks crack is not a geometry problem (timing of crack?)
Location - E of sec line.

SC-86-21-MB

60 m W of # 20. Granite, felsic ign., fine grained, rind 3-4 cm thick. Moderately weathered (SSS).

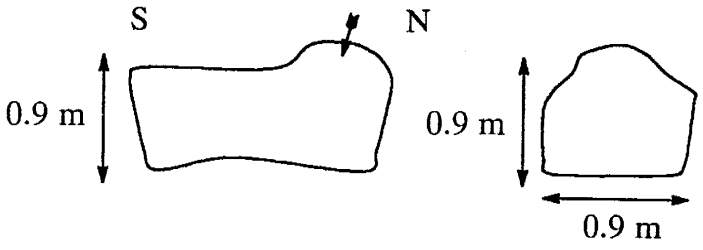

Polished surface and well developed weathering?